



Wheat Straw and Pig Manure Gasification in a Drop Tube Furnace

Tiago Miguel Martins Rio

Thesis to obtain the Master of Science Degree in

Mechanical Engineering

Supervisor: Prof. Mário Manuel Gonçalves da Costa

Examination Committee

Chairperson: Prof. Edgar Caetano Fernandes

Supervisor: Prof. Mário Manuel Gonçalves da Costa

Member of the Committee: Dr. Raquel Inês Segurado Correia Lopes da Silva

November 2019

Resumo

Devido às emissões de gases de efeito de estufa e aos consequentes danos previstos pelo aquecimento global utilizando fontes de energia fósseis, a conversão de biomassa em combustível ganhou especial atenção. A gaseificação de biomassa consegue produzir um gás de síntese de alta qualidade e subprodutos sólidos. Esta tese aborda a influência da adição de vapor de água e de dióxido de carbono na gaseificação de biomassa num reator tubular de queda livre. Partículas de estrume de porco e de palha de trigo, com dimensões entre 90 e 150 μm foram as biomassas utilizadas. A taxa de alimentação da biomassa foi fixada em 30 g/h, e o oxigénio utilizado permitiu uma razão constante de excesso de ar de 0,4. Na gaseificação de palha de trigo, a influência do rácio vapor de água/biomassa (S/B) foi analisada a 1000 °C, enquanto que na gaseificação de estrume de porco, o efeito da atmosfera de gaseificação e da temperatura foram as variáveis analisadas. A gaseificação de estrume de porco foi realizada em misturas de azoto/oxigénio, azoto/oxigénio/vapor de água e azoto/oxigénio/dióxido de carbono para diferentes temperaturas das paredes do reator entre 900 e 1200 °C. Os resultados mostram que a fuligem e o resíduo carbonoso diminuem com o aumento do rácio S/B, na gaseificação de palha de trigo. O poder calorífico do gás de síntese, a eficiência da conversão de carbono e a eficiência energética foram mais elevadas para S/B = 0,8 enquanto que para S/B = 1.7 verificou-se o maior rácio hidrogénio/monóxido de carbono. Na gaseificação de estrume de porco, a formação de resíduo carbonoso é mais baixa na mistura e azoto/oxigénio/dióxido de carbono para todas as temperaturas analisadas enquanto que para 1100 e 1200 °C a fuligem é mais reduzida na mistura azoto/oxigénio/vapor de água. Neste caso o poder calorífico do gás síntese e a eficiência energética foram mais elevadas para uma atmosfera com dióxido de carbono enquanto que a eficiência de conversão de carbono e o rácio hidrogénio/carbono foram mais elevados para uma atmosfera que continha vapor de água adicionado.

Palavras-chave

Palha de trigo, estrume de porco, reator tubular de queda livre, fuligem, resíduo carbonoso, gás de síntese.

Abstract

Due to greenhouse gas emissions and the consequent damage predicted by global warming using fossil energy sources, the conversion of biomass to fuel has gained special attention. Biomass gasification can produce a high-quality syngas and solid by-products. This thesis reports the influence of the addition of steam and carbon dioxide in a drop tube furnace (DTF). Pig manure and wheat straw particles, ranging from 90 to 150 μm were the biomass used. The biomass feeding rate was fixed at 30 g/h and oxygen was fed to the reactor at a constant excess air ratio of 0.4. In wheat straw gasification, the influence of steam/biomass (S/B) ratio at 1000 °C was analyzed while in pig manure gasification, the gasification atmosphere and temperature were the variables analyzed. Pig manure gasification was performed in mixtures of nitrogen/oxygen, nitrogen/oxygen/steam and nitrogen/oxygen/carbon dioxide for distinct DTF wall temperatures between 900 and 1200 °C. The results show that soot and char decrease, increasing the S/B ratio in wheat straw gasification. The syngas lower heating value, the carbon conversion efficiency and the cold gas efficiency were higher at S/B = 0.8, while at S/B = 1.7 the hydrogen/carbon monoxide was higher. In pig manure gasification, the quantity of char was lower in the mixture nitrogen/oxygen/carbon dioxide for all temperatures examined while for 1100 and 1200 °C the quantity of soot was lower in the mixture of nitrogen/oxygen/steam. In this case, the syngas lower heating value and the cold gas efficiency were higher for the atmosphere with carbon dioxide while the carbon conversion efficiency and the hydrogen/carbon monoxide were higher for an atmosphere with addition of steam.

Keywords

Wheat straw, pig manure, drop tube furnace, soot, char, syngas.

Acknowledgments

Firstly and foremost, I would like to thank my supervisor, Professor Mário Costa, for his support, guidance and exigency throughout the elaboration of this thesis.

I would also to thank Doctor Ana Filipa Ferreira and Ricardo Ferreira for their friendship, availability and support during the experimental work and many helpful discussions.

For the technical assistance and support on the laboratory during the measurements, and for the good times and talks, I would like to thank the technicians Manuel Pratas and Tomás Prudente.

I would also like to thank all my colleagues and friends of the Combustion Laboratory, for their amazing friendship and companion and for the relaxed conversations. In general, I wish to thank all the people I met during this journey, and who somehow contributed to the development of this dissertation.

Finally, special thanks to my parents and brother who have always supported me and gave everything they could to make these academic years easier.

Table of Contents

RESUMO	I
PALAVRAS-CHAVE	I
ABSTRACT	II
KEYWORDS	II
ACKNOWLEDGMENTS	III
TABLE OF CONTENTS	V
NOMENCLATURE	VII
LIST OF FIGURES	IX
LIST OF TABLES	X
I. INTRODUCTION	1
I.1 MOTIVATION	1
I.2 BIOMASS	3
I.3 GASIFICATION	4
<i>I.3.1 Stages of gasification</i>	<i>4</i>
I.3.1.1 Drying	6
I.3.1.2 Pyrolysis.....	6
I.3.1.3 Partial oxidation or combustion reduction	6
I.3.1.4 Reduction.....	7
<i>I.3.2 Products.....</i>	<i>7</i>
I.3.2.1 Syngas.....	7
I.3.2.2 Char	8
I.3.2.3 Tar	9
I.3.2.4 Soot	11
<i>I.3.3 Types of gasifier</i>	<i>12</i>
I.3.3.1 Moving bed or fixed bed type gasifier	12
I.3.3.2 Fluidized-bed gasifier	13
I.3.3.3 Entrained-flow reactor.....	14
<i>I.3.4 Performance Indicators</i>	<i>16</i>
<i>I.3.5 Previous studies</i>	<i>17</i>
I.3.5.1 Influence of CO ₂ addition	22
I.3.5.2 Influence of steam addition	23
I.3.5.3 Effect of other operating parameters.....	26
I.4 OBJECTIVES	27
I.5 THESIS OUTLINE.....	27
II. MATERIAL AND METHODS	28
II.1 FUEL PREPARATION AND CHARACTERIZATION	28

II.2	EXPERIMENTAL SETUP	29
II.2.1	<i>Solid Particles collection</i>	31
II.2.2	<i>Particle Morphology and Chemical Species</i>	33
II.2.3	<i>Gas collection and composition</i>	34
II.2.4	<i>Test Conditions</i>	34
II.2.5	<i>Procedure</i>	36
III.	RESULTS AND DISCUSSION.....	37
III.1	EFFECT OF S/B RATIO ON WS GASIFICATION	37
III.1.1	<i>Solid Particles</i>	37
III.1.2	<i>Composition and quality of the producer gas</i>	46
III.2	EFFECT OF GASIFICATION ATMOSPHERE AND TEMPERATURE ON PMAN GASIFICATION.....	47
III.2.1	<i>Solid Particles</i>	47
III.2.2	<i>Composition and quality of the producer gas</i>	54
IV.	CLOSURE	57
IV.1	CONCLUSIONS	57
IV.2	FUTURE WORK	57
V.	REFERENCES	59
VI.	APPENDIX	62
VI.1	APPENDIX A – PARTICULATE MATTER IN THE IMPACTOR	62
VI.2	APPENDIX B - PARTICULATE MATTER IN CYCLONE FOR PIG MANURE GASIFICATION.....	64

Nomenclature

Acronyms

BFB	Bubbling fluidized bed gasifier
CCE	Carbon conversion efficiency
CGE	Cold gas efficiency
CFB	Circulating fluidized bed gasifier
DLPI	Dekati low pressure impactor
DTF	Drop tube furnace
EDS	Energy dispersive x-ray spectroscopy
EFR	Entrained flow reactor
GC-FID	Gas chromatography- flame ionization detector
GC- MS	Gas chromatography- mass spectroscopy
GHC	Greenhouse gases
GY	Gas yield
HCS	Hynoki cypress sawdust
HHV	High heating value
LHV	Low heating value
PAHs	Polycyclic aromatic hydrocarbons
PM	Particulate matter
PMan	Pig manure
SEM	Scanning electron microscope
TCD	Thermal conductivity detector
WS	Wheat straw

Symbols

Roman characters

A/B	Air/biomass ratio
d_p	Particle diameter
F	Biomass/gasification agent
FA	Fuel/air ratio
F_{rg}	Relative biomass/air ratio
H/C	Hydrogen/carbon ratio
\dot{m}	Mass flow rate
OC	Oxygen concentration
O/C	Oxygen/carbon ratio
S/B	Steam/biomass ratio
S/C	Steam/carbon ratio
t	Particle residence time
$T_{amb.}$	Ambient temperature
T_r	Reactor temperature
V	Volume
\dot{V}	Volume flow rate
x_{carbon}	Carbon mole fraction of products
y_{carbon}	Carbon mass fraction from ultimate analysis

Greek characters

λ	Excess air coefficient
-----------	------------------------

List of Figures

FIGURE I-1 - GROSS FINAL ENERGY CONSUMPTION GLOBALLY IN 2016 [2].....	1
FIGURE I-2 - GROSS FINAL ENERGY CONSUMPTION OF ENERGY SOURCES IN 2016 [2].....	2
FIGURE I-3 - BIOMASS CARBON LIFE CYCLE [7].	3
FIGURE I-4 - END USE APPLICATIONS OF SYNGAS [12].....	8
FIGURE I-5 - SEM IMAGE OF CHAR FROM GASIFICATION OF DEALCOHOLIZED MARC OF GRAPE [15].	9
FIGURE I-6 - POTENTIAL DEPOSITION OF SOOT PARTICLES ON RESPIRATORY SYSTEM ACCORDING TO ITS SIZE IN μM [7].	12
FIGURE I-7 - SCHEMATIC OF DIFFERENT TYPES OF MOVING BED TYPE GASIFIERS: DOWNDRAFT (A), UPDRAFT (B), AND CROSSDRAFT (C) [1].	13
FIGURE I-8 – SCHEMATIC OF CONFIGURATIONS OF FLUIDIZED-BED GASIFIER: BFB (A) AND CFB (B) [9].	14
FIGURE I-9 - SCHEMATIC OF TYPES OF EFRS: TOP-FED DOWNFLOW (A) AND SIDE-FED (B) [1].	15
FIGURE I-10 - GAS COMPOSITION FOR AN ATMOSPHERE WITH CO_2 , USING BEECH SAWDUST, FROM BILLAUD ET AL. [26].	22
FIGURE I-11 - EFFECT OF TEMPERATURE ON THE COMPOSITION OF THE PRODUCER GAS IN ATMOSPHERES WITH STEAM DURING BIOMASS GASIFICATION.	25
FIGURE I-12 - EFFECT OF TEMPERATURE ON SOOT AND CHAR FORMATION IN ATMOSPHERES WITH STEAM DURING BIOMASS GASIFICATION.	26
FIGURE II-1 - SCHEMATIC OF THE EXPERIMENTAL SETUP.	30
FIGURE II-2 - DEKATI CYCLONE [35].	31
FIGURE II-3 - DEKATI CASCADE IMPACTOR (A) AND THE PARTICLE COLLECTING MECHANISM (B) [35].	32
FIGURE II-4 - SCANNING ELECTRON MICROSCOPE (SEM).	33
FIGURE III-1 - INFLUENCE OF S/B RATIO ON THE PMS COLLECTED IN THE CYCLONE AND THIRTEEN-STAGE CASCADE IMPACTOR.	37
FIGURE III-2 - EFFECT OF THE S/B RATIO ON THE FORMATION OF SOOT AND CHAR PARTICLES (A), AND ON THE CHAR, SOOT AND VOLATILES YIELDS (B).	39
FIGURE III-3 – EFFECT OF S/B RATIO ON THE SYNGAS COMPOSITION (A), AND ON GASIFICATION PERFORMANCE PARAMETERS: LHV (B), CCE AND CGE (C) AND H_2/CO RATIO (C).	46
FIGURE III-4 - INFLUENCE OF THE GASIFICATION ATMOSPHERE AND TEMPERATURE ON THE PMS COLLECTED IN THE CYCLONE (A) AND IMPACTOR (B).	47
FIGURE III-5 - ORGANIC (A) AND ASH CONTENT (B) OF THE PMS COLLECTED IN THE CYCLONE FOR ALL CONDITIONS ANALYZED.	48
FIGURE III-6 – AMOUNT OF CHAR (A) AND SOOT (B) OBTAINED IN THE GASIFICATION OF PMAN AT DIFFERENT GASIFICATION ATMOSPHERES AND TEMPERATURES.	50
FIGURE III-7 – EFFECT OF TEMPERATURE AND GASIFICATION ATMOSPHERE ON CO , CO_2 , H_2 AND CH_4 YIELD FOR PMAN GASIFICATION	54
FIGURE III-8 – EFFECT OF TEMPERATURE AND GASIFICATION ATMOSPHERE ON GASIFICATION PERFORMANCE INDICATORS: LHV (A), CGE (B), CCE (C) AND H_2/CO (D).	55

List of Tables

TABLE I-1 - REACTIONS OCCURRING IN GASIFICATION [3,10].	5
TABLE I-2 - TAR COMPOUNDS CLASSIFICATION ACCORDING TO CHEMICAL COMPOSITION, SOLUBILITY, AND CONDENSABILITY [16].	10
TABLE I-3 - TAR LIMITS IN GAS PRODUCED FOR VARIOUS APPLICATIONS [10].	11
TABLE I-4 – COMPARISON OF KEY FEATURES OF DTFs AND EFRs [5,18,22-33].	16
TABLE I-5 - MOST RELEVANT EXPERIMENTAL STUDIES ON BIOMASS GASIFICATION IN EFRs AND DTFs.	18
TABLE II-1 - WS AND PMAN THERMOCHEMICAL PROPERTIES.	28
TABLE II-2 - AERODYNAMIC DIAMETER FOR EACH STAGE OF IMPACTOR [35].	32
TABLE II-3 - EXPERIMENTAL SCHEDULE FOR THE STUDY OF THE EFFECT OF THE S/B IN WS GASIFICATION....	35
TABLE II-4 - EXPERIMENTAL SCHEDULE FOR THE STUDY OF THREE GASIFICATION ATMOSPHERES FOR PMAN GASIFICATION.	35
TABLE III-1 - SEM IMAGES, EDS AND BURNOUT ANALYSIS FOR THE PM COLLECTED IN THE CYCLONES FOR THE DIFFERENT S/B RATIOS (Tr = 1000 °C).	40
TABLE III-2 - SEM IMAGE AND EDS ANALYSIS FOR WS GASIFICATION, FOR SOME OF THE STAGES OF THE IMPACTOR (Tr = 1000° C, S/B = 0.8).	43
TABLE III-3 - SEM IMAGES, EDS ANALYSIS AND BURNOUT EXPERIMENTS FOR THE PMS COLLECTED IN THE CYCLONE FOR THE PMAN GASIFICATION (N ₂ /O ₂ /CO ₂).	51
TABLE III-4 - SEM IMAGE AND EDS ANALYSIS FOR PMAN GASIFICATION, FOR TWO STAGES OF IMPACTOR (Tr = 1000 °C, N ₂ /O ₂ /H ₂ O).	53
TABLE VI-1 - SEM IMAGES AND EDS ANALYSIS FOR WS GASIFICATION, FOR THE REMAINING STAGES OF THIRTEEN STAGE IMPACTOR (Tr = 1000 °C, S/B = 0.8).	62
TABLE VI-2 - SEM IMAGES, EDS ANALYSIS AND BURNOUT FOR PMS COLLECTED IN CYCLONE FOR PMAN GASIFICATION (N ₂ /O ₂).	64
TABLE VI-3 - SEM IMAGES, EDS ANALYSIS AND BURNOUT FOR PMS COLLECTED IN CYCLONE FOR PMAN GASIFICATION (N ₂ /O ₂ /CO ₂).	66

I. Introduction

I.1 Motivation

Over the last few years, world energy consumption has been increasing. Currently, the main source of primary energy is the fossil fuel energy, but it is facing some problems. One of the problems is the climate change associated to the greenhouse gases (GHG) emissions using fossil fuels, and another problem is the shortage of this energy source as the world energy demand increases. Therefore, to mitigate these problems it is necessary to explore renewable energy sources. Biomass is a type of renewable energy source and is abundant and well spread throughout the world, being the fourth largest energy resource available. However, within this large amount of biomass, only 5% is potentially useful for producing energy, and even so, it may be responsible for about 26% of global energy consumption [1].

Nowadays, among all sources of renewable energy, biomass is the largest renewable energy source, accounting for 13% of the world's energy consumption, as illustrated in Figure I-1 [2].

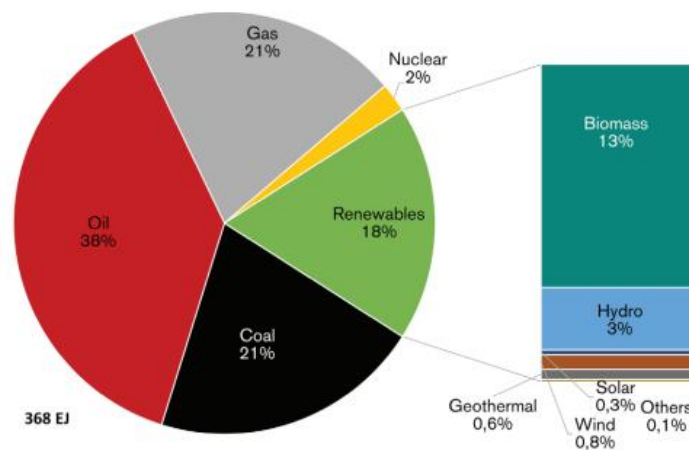


Figure I-1 - Gross final energy consumption globally in 2016 [2].

The use of biomass as an energy source varies widely, depending essentially on socioeconomic and geographical conditions. In Africa, due to the high use of traditional biomass resources, there is a greater consumption of renewable energy than any other source of energy, unlike what happens in Asia, for instance, where coal plays the most important role in the energy mix, as illustrated in Figure I-2 [2].

Over the years, various biomass conversion processes have been developed, such as biological and thermal processes. Pyrolysis, combustion and gasification are three examples of thermal conversion processes that differ mainly by their maturity level [3]. Biomass gasification seems to be the conversion process with more potential for energy generation or biofuel synthesis, using the syngas produced [4].

In addition to the syngas produced during the biomass gasification, ash, carbonaceous solid residues such as char and soot particles, and tars, a condensable product, are also generated [5]. If, on the one

hand, the formation of soot and tars should be minimized because they are undesirable products, on the other hand, the char can be used as a soil amendment or as an additive for cement plants. The ash can also be used for use in cement kilns, for the manufacture of bricks with special characteristics or lightweight wall board [3].

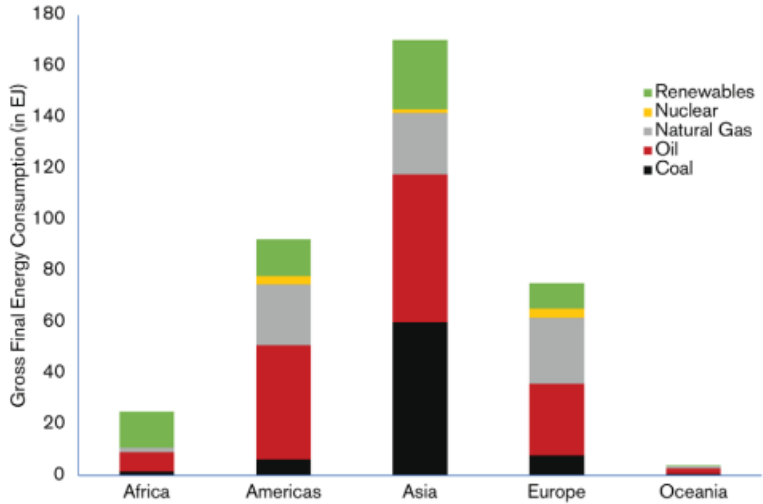


Figure I-2 - Gross final energy consumption of energy sources in 2016 [2].

I.2 Biomass

Biomass is a biological material, that is derived from living species like plants, crop residues, animals etc., which stores chemical energy in form of carbohydrates through photosynthesis process by combining solar energy and carbon dioxide [6]. It is considered a “carbon neutral fuel” since its burning does not add to the Earth’s carbon dioxide inventory, and this is illustrated in Figure I-3. Biomass is an abundant, widespread renewable energy source and does not take millions of years to develop as in the case fossil fuels [1].

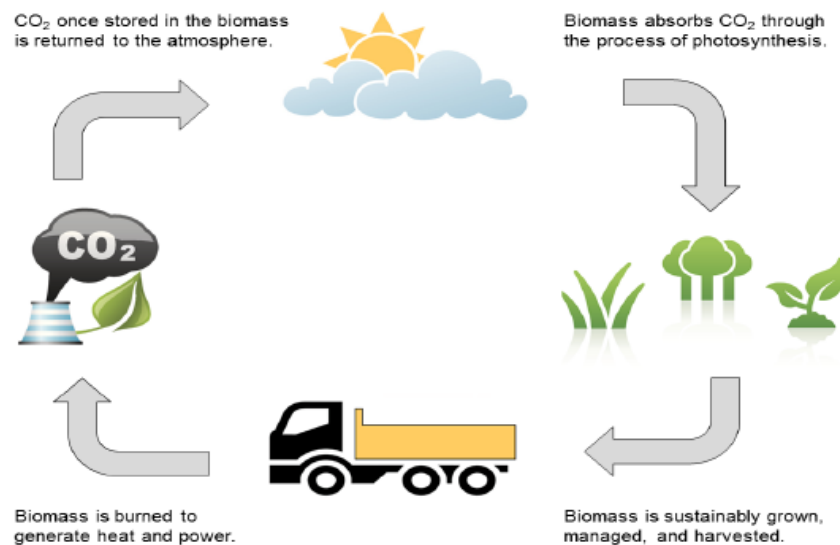


Figure I-3 - Biomass carbon life cycle [7].

Cellulose, hemicellulose and lignin are the three major polymers that compose the cell walls and other constituents of a biomass. Cellulose is a long chain polymer with a large molecular weight and a high degree of polymerization. It is the primary structural component of cell walls in biomass. Hemicellulose is a group of carbohydrates with a lower degree of polymerization and its chain structure is branched. Lignin is an integral part of the secondary cell walls of plants, being also a complex highly branched polymer of phenylpropane. It is the agent responsible for cellulose fibers cementation [1].

In general, there are two types of biomass, the non-woody and the woody biomass. The non-woody is often categorized as waste and presents a low content of lignin. Some examples of non-woody biomass are paddy husks, straw, grasses, crop stubble, trash, cotton gin trash, palm oil waste, sugarcane bagasse and animal paunch waste [8].

In contrast with fossil fuels, biomass has a high moisture content. In order to improve the efficiency of any biomass conversion process, it is necessary to resort to pre-treatments such as size reduction, drying or densification [8].

I.3 Gasification

Gasification is a complex thermochemical process that converts fossil or nonfossil fuels (solid or liquid), into useful convenient gaseous fuels or chemical feedstock. Gasification takes place in a reactor called gasifier, at high temperatures (700 – 1500 °C) in the presence of a gasifying agent such as oxygen under sub-stoichiometric conditions, air, carbon dioxide, steam or a mixture of these. The resulting gas, called producer gas or synthesis gas, is mainly composed of the following combustible gases: carbon monoxide (CO), hydrogen (H₂), methane (CH₄) and carbon dioxide (CO₂). It has a useful heating value, and it is easier to clean, transport and burn efficiently than the original feedstock [1,3,6,8,9].

I.3.1 Stages of gasification

A typical biomass gasification occurs through a sequence of complex, often overlapping, thermochemical reactions. Sansaniwal et al. [6] identified the following steps in the gasification process:

- Drying;
- Pyrolysis;
- Partial Oxidation or Combustion;
- Reduction.

Table I-1 reports the most important thermochemical reactions to be considered in the gasification process and the heat of reactions for a temperature of 25 °C.

Table I-1 - Reactions occurring in gasification [3,10].

Physical process and chemical process	Reaction	Chemical gasification process	
$\text{Biomass}_{\text{H}_2\text{O}} \rightarrow \text{Biomass}_{\text{dry}} + \text{H}_2\text{O} (\text{g})$	R1	Drying	
$\text{Biomass}_{\text{dry}} \rightarrow \text{Char} + \text{Tar} + \text{Gas}$	R2	Devolatilization/Pyrolysis	
$\text{C} + 0.5\text{O}_2 \rightarrow \text{CO} - 111 \text{ kJ/mol}$	R3 (partial oxidation)	Heterogeneous reactions	
$\text{C} + \text{O}_2 \rightarrow \text{CO}_2 - 394 \text{ kJ/mol}$	R4 (complete oxidation)		
$\text{C} + \text{H}_2\text{O}(\text{g}) \rightarrow \text{CO} + \text{H}_2 + 131 \text{ kJ/mol}$	R5 (water/gas)		
$\text{C} + \text{CO}_2 \rightarrow 2\text{CO} + 172 \text{ kJ/mol}$	R6 (Boudouard)		
$\text{C} + 2\text{H}_2 \rightarrow \text{CH}_4 - 74,8 \text{ kJ/mol}$	R7 (hydrogasification)		
$\text{Tar} + \text{O}_2 \rightarrow \text{CO} + \text{CO}_2 + \text{CH}_4 + \text{H}_2 + \text{soot}$	R8		Homogeneous reactions
$\text{Tar} + \text{CO}_2 \rightarrow \text{CO} + \text{H}_2\text{O}$	R9 (tar reforming)		
$\text{Tar} + \text{CO} \rightarrow \text{CO}_2 + \text{H}_2 + \text{CH}_4$	R10 (tar cracking)		
$\text{CO} + \text{H}_2\text{O} \leftrightarrow \text{CO}_2 + \text{H}_2 - 41,2 \text{ kJ/mol}$	R11 (water/gas shift)		
$\text{CO} + 3\text{H}_2 \leftrightarrow \text{CH}_4 + \text{H}_2\text{O} - 206 \text{ kJ/mol}$	R12 (methanation)		
$\text{CO}_2 + 4\text{H}_2 \leftrightarrow \text{CH}_4 + 2\text{H}_2\text{O} - 165 \text{ kJ/mol}$	R13		
$\text{CH}_4 + \text{H}_2\text{O} \leftrightarrow \text{CO} + 3\text{H}_2 + 206 \text{ kJ/mol}$	R14 (methane reforming)		
$\text{CH}_4 + 0.5\text{O}_2 \leftrightarrow \text{CO} + 2\text{H}_2 + 36 \text{ kJ/mol}$	R15		
$\text{H}_2 + 0.5\text{O}_2 \leftrightarrow \text{H}_2\text{O} - 242 \text{ kJ/mol}$	R16		

I.3.1.1 Drying

The moisture content of some biomass can exceed 90% [1]. Since the energy from the gasifier to vaporize water is not recoverable, the pre-treatment of raw biomass materials is necessary. To improve the end-product gas quality, a certain amount of pre-drying is necessary to remove as much moisture as possible before going to the gasifier [6]. As the biomass has inherent moisture residing within the cell structure, it is only possible to eliminate the external or surface moisture. Therefore, most gasification systems use dry biomass with a moisture content of 10% to 20%, to produce a fuel gas with an acceptable high heating value [1]. As the biomass is fed into the gasifier, water is released at around 100 °C, according to the reaction R1 (see Table I-1).

I.3.1.2 Pyrolysis

Pyrolysis occurs between 125 °C and 500 °C and is a complex process that involves the thermal breakdown of larger hydrocarbon molecules of biomass into smaller gas molecules (condensable and non-condensable) in the absence of oxygen or air. Solid charcoal, liquid tar, and gases are the products of pyrolysis, and their proportions depend on the characteristics of the biomass and the operating conditions used. During this process, at a temperature below 200 °C, while the moisture is removed, drying and reduction takes place at the same time. At 300 °C, the formation of carbonyl and carboxyl group radicals is achieved by the reduction of molecular weight of the biomass elements and CO and CO₂ are also formed. Above 300 °C, char, tar and gaseous products are formed by the decomposition of the obtained crystalline cellulose. Between 300 °C and 500 °C, methanol, acetic acid, water and acetone are formed when the lignin is decomposed. Exothermic reactions take place up to the temperature of 300 °C whereas endothermic reactions take place above 300 °C [6]. The pyrolysis of biomass is carried out according to the reaction R2 (see Table I-1).

I.3.1.3 Partial oxidation or combustion reduction

The oxidation is a very critical stage of gasification, because it decides the quality and the type of the end products. During this process, the volatile matter from biomass oxidates under exothermic chemical reactions and provides heat for drying, devolatilization and reduction reactions [7]. At this stage, heterogeneous reactions occur between the char and the oxygen (R3 and R4, partial and complete oxidation) present inside the reactor, which generates carbon dioxide, carbon monoxide and a significant amount of heat. The proportion of these gases is a function of the ash content, the oxygen availability and the temperature. Water vapors are also formed by the combination of hydrogen and oxygen (R16) [6].

I.3.1.4 Reduction

After oxidation, a reduction zone is created within the reactors. Since the oxygen inserted into the reactor is only a fraction of the stoichiometric oxygen required for complete oxidation and it still reacts in the oxidation reactions, a reducing environment is generated. Here, the char particles behave as reducing agents for the remaining gaseous substances [9]. Thus, along the gasifier, the chemical reactions that occur associated with oxidation and reduction, are a combination of homogeneous and heterogeneous reactions, in other words, reactions between gases and between gases and solids, as shown in the Table I-1. In a reactor, the char may react with oxygen, with hydrogen, steam and carbon dioxide. Generally, the rate of gasification is faster with oxygen followed by steam, carbon dioxide and hydrogen last (R3-R7) [1].

I.3.2 Products

During gasification, the fuel is converted into a gas called producer gas or syngas, however not all fuel is converted. The rest of the products are carbonaceous solid residues (char and soot particles) and condensable products (tars).

I.3.2.1 Syngas

Syngas is a mixture of gases composed mainly of CO, CO₂, H₂ and CH₄. Besides the syngas generated by biomass gasification, the syngas can be obtained from hydrocarbons such as coal and petroleum coke. The syngas produced from biomass is sometimes referred as bio syngas. The syngas obtained in gasification has small amounts of impurities such as tars, nitrogen based compounds (NH₃, HCN, etc.), sulphur based compounds (H₂S, COS, etc.), hydrogen halides (HCl, HF, etc.) and trace metals (Na, K, etc.) [11]. Depending on the final application of the syngas, these impurities can only be present below tolerable limits. Cyclone, fabric or other barrier filter, electrostatic filter and solvent scrubber are four ways to reduce dust and particles from the syngas [1]. The main end-use downstream applications of the syngas are chemicals, liquid fuels, power and gaseous fuels as illustrated in Figure I-4 [12].

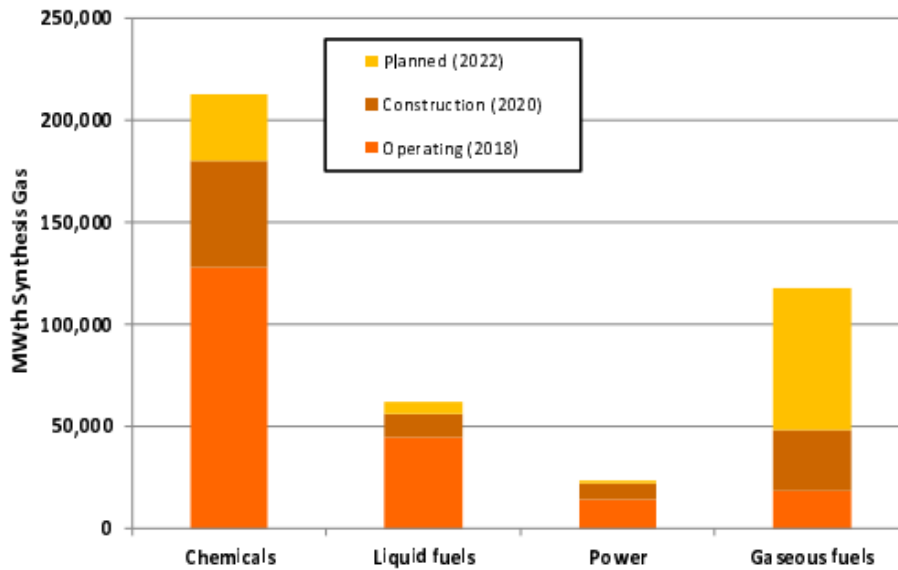


Figure I-4 - End use applications of syngas [12].

I.3.2.2 Char

Char from biomass gasification is a very heterogeneous material that presents properties dependent on the initial feedstock, the gasification technology and the operating conditions. These types of chars are stable materials with high carbon content, high porosity and consequently low density [13]. In general, the char obtained from biomass gasification consists mainly of carbon (50 - 80%), but it is not only the fixed carbon of biomass. In addition to fixed carbon, char contains some volatiles and very little inorganic ash [1]. The initial feedstock that provides the char, strongly influences its properties. For example, chars formed from slurry (chicken, swine, bovine) have usually high ash contents (up to 43.8%) [13]. Benedetti et al.[14], investigated the properties of chars collected from six different biomass gasifiers and concluded that char is similar to activated carbon. Char derived from biomass gasification had similar characteristics to activated carbon such as mechanisms of formation, carbon content and porosity. When compared to the raw biomass, due to its properties, the chars have more advantages in the transport, storage, milling, densification and feeding. Furthermore, char has a higher energy density due to their lower H/C and O/C ratios. Char presents a high heating value (HHV) between 10 MJ/kg and 33 MJ/kg, thus being attractive sources to produce clean energy. The char particles, once pulverized, can be added to the coal for later co-firing in existing industrial plants [13].

Lapuerta et al. [15] analyzed the influence of some gasifier operating conditions on the char properties produced such as, the relative biomass/air ratio (F_{rg}), temperature and steam content of the gasifying agent. The gasification was carried out in a small-scale drop-tube pilot plant, using dealcoholized marc of grape as fuel. The use of high values of F_{rg} resulted in the decrease of the bulk density that can be explained by the release of volatile matter and the conversion of a fraction of the remaining char by heterogeneous reactions, and in the increase of the carbon content because of the lower fuel

conversion. Increasing the Frg, it was also observed the presence of large quantities of volatile matter in the char, which may possibly be related to the condensation and adsorption of tars. The presence of polycyclic aromatic hydrocarbons (PAHs), toxic compounds, invalidates its use in soil amendment applications. For a high temperature air-gasification, it was observed a more opened pore structure in the char (Figure I-5) than from steam gasification. The char produced at high temperatures, due to the open pore structure and its inorganic composition can be used as catalyst support for tar removal applications.

In short, despite the problems that the composition of the ashes present in the char may cause, the char can have many applications. Domestic charcoal, activated carbon, fertilizer or soil conditioner, manure treatment, feed-additives or tar reforming catalyst are some examples of applications for char [15].

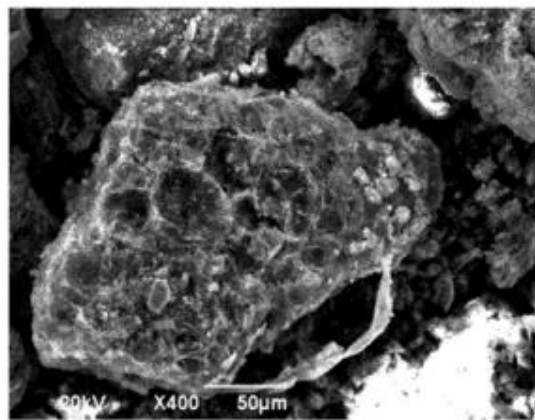


Figure I-5 - SEM image of char from gasification of dealcoholized marc of grape [15].

I.3.2.3 Tar

Tars are defined as a complex mixture of organic compounds generated during the devolatilization phase, presenting high boiling points, including aromatic and heteroaromatic species as well as PAHs [5] or in a more succinct way, tars are defined as the set of hydrocarbons with higher molecular weight than benzene [10]. The chemical composition of tars formed in biomass gasification depends on several factors such as reaction temperature, type of gasifier, type of feedstock, the gasifying agent used, the use of catalysts and the method of tar sampling and analysis [1,3]. Hernández et al. [5] investigated the influence of relative fuel/air (FA) ratio, operating temperature, and composition of air and steam in the gasifying agent on the production of tars in gasification of dealcoholized marc of grape. In this study, it was observed the non-linear tar production increase with the decrease of the excess air coefficient (λ). Using pure air or pure steam, it was checked that the amount of tars produced was reduced with temperature increase.

For tar classification, there are two paths of classifying it, tar water solubility that refers to process conditions, and tar condensation that refers to physical tar properties. With this classification it is

possible to group the different types of tars into five classes (see Table I-2) [16]. According to the conditions inside the reactor, Milne et al [17] classified tar in four groups: primary, secondary, alkyl-tertiary and tertiary condensates.

Primary tar is formed by decomposition of biomass material in the course of pyrolysis. The secondary tar is the result, due to the increase in temperature above 500 °C, of the rearrangement of the previous tar. Tar alkyl tertiary compounds contain methyl derivatives of aromatic compounds, whereas the four group generate PAHs series without substituent atoms.

Table I-2 - Tar compounds classification according to chemical composition, solubility, and condensability [16].

Tar class	Class name	Property	Representative compounds
1	GC-undetectable tar	Very heavy tars compounds that cannot be detected with a GC-FID or GC-MS equipped with a non-polar capillary column.	Determined by subtracting the gas chromatography-detectable tar fraction from the total gravimetric tar.
2	Heterocyclic	Tars containing heteroatoms; highly water-soluble compounds.	Pyridine, phenol, cresols, quinoline, isoquinoline, dibenzophenol.
3	Light aromatic (1 ring)	Usually light hydrocarbons with single ring; do not pose a problem regarding condensability and solubility.	Toluene, ethylbenzene, xylenes, styrene.
4	Light PAHs compounds (2-3 rings)	2 and 3 rings compounds; condense at low temperature even at very low concentration.	Indene, naphthalene, methylnaphthalene, biphenyl, acenaphthalene, fluorene, phenanthrene, anthracene.
5	Heavy PAHs compounds (4-7 rings)	Compound larger than 3 rings, these components condense at high- temperatures at low concentrations.	Fluoranthene, pyrene, chrysene, perylene, coronene.

Tar remains in the gaseous phase, condensing in colder sections of the gasifier. If this happens in ducts, heat exchangers or filters, it will cause deposition and blocking, reducing the process efficiency, increasing emissions and, hence increasing operating costs. The amount of tar present in the producer

gas determines its usefulness, that is, in which application it can be used. The table I-3 shows the tar limits in the producer gas for various applications [10].

Table I-3 - Tar limits in gas produced for various applications [10].

Application	Tar (mg/Nm ³)
Direct combustion	No specified limit
Internal combustion engine	< 100
Gas turbine	< 5.0
Synthesis of methanol	< 0.1
Compressors	50–500
Fuel Cells	< 1.0

I.3.2.4 Soot

The term soot is given to small spherical particles formed when carbonaceous fuels are burned under local reducing conditions and are constituted mainly of carbon. The spherical particles diameter varies from 10-50 nm and, mainly by agglomeration, the soot size increases up to 200 nm particle diameter. The production of soot depends substantially on the fuel composition and is an unwelcome by-product in many practical combustion systems [18].

Smaller soot particles, because of its size, have the capability to penetrate easily into the respiratory tracts and hence, may cause lung malfunction and premature death, thus it is a danger to the human and animal health. The potential deposition of particles based on their size on the human respiratory system is illustrated in Figure I-6. Soot particles, if released into the air, cause greenhouse effect by heating the atmosphere, due to its capacity to absorb radiation. Furthermore, soot causes many problems in the industry, such as, can affect the turbine durability and integrity, lowering the performance, can form dark exhaust plumes, may agglomerate on the walls and reduces the carbon conversion efficiency since carbon is lost from the furnace without adding any value [19].

According to Neves et al. [20], PAHs are the precursors of the soot particles in a secondary pyrolysis process. PAHs are the main constituents of the tar obtained in a primary pyrolysis process. At high temperature, these hydrocarbon molecules are susceptible to undergo both cracking and polymerization processes, promoting the soot formation (R8, see Table I-1)

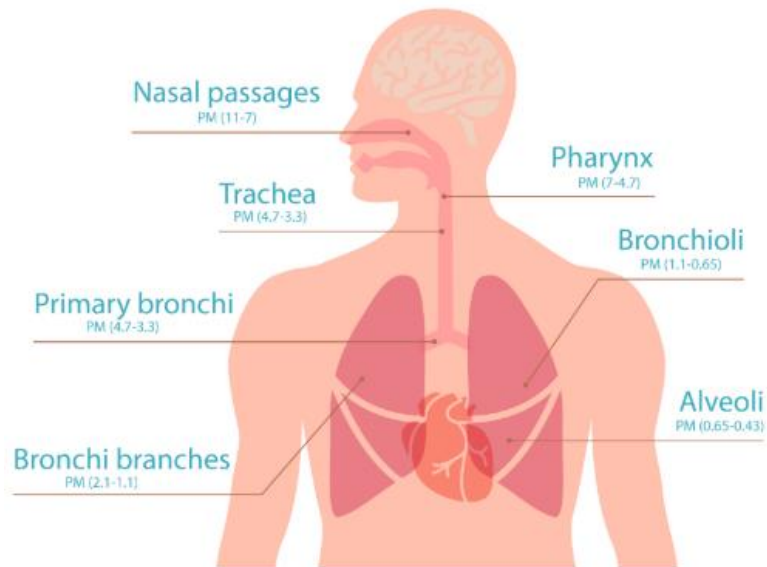


Figure I-6 - Potential deposition of soot particles on respiratory system according to its size in μm [7].

I.3.3 Types of gasifier

There are different types of biomass gasifiers. These types are available in various sizes and design and are classified primarily based on their gas-solid contacting mode and gasification atmosphere. Therefore, gasifiers are divided into three principal types: fixed or moving bed, fluidized bed and entrained flow.

I.3.3.1 Moving bed or fixed bed type gasifier

Moving bed gasifier is the simplest type of gasifier. It can be built inexpensively in small sizes, consisting of a cylindrical vessel for fuel and gasifying agents, fuel feeding unit, ash collection unit and gas exit. As its name indicates, the fuel moves down in the gasifier as a plug [1]. In this gasifier, it is difficult to reach uniform distribution of fuel, temperature and gas composition across the cross-section of the gasifier because the mixing and the heat transfer are weak [1]. These types of gasifiers are used at moderate pressure conditions of 25-30 atm, and it is used for small-scale heat and power generation applications [6]. According to the way of interaction of the gasifying agent with the biomass, the moving bed type gasifiers are classified as downdraft, updraft and crossdraft gasifiers, schematically represented in Figure I-7.

In downdraft gasifiers, air enters at a certain height below the top and interacts with the solid biomass fuel in the downward direction which results in the movement of the product gas in the co-current direction and leaves through a bed of hot ash. Since all the decomposition products pass through the high temperature and oxidation zone, the tar produced is low because of the thermal cracking and hence

the quality of fuel gas is better. Air from a set of nozzles flows downward and interacts with pyrolyzed char particles, creating a combustion zone at about 1200 °C to 1400 °C. Then the gases flow downward further and gasify the char particles in the zone of char gasification. Finally, the ash and the producer gas leave the bed at the bottom [1].

In updraft gasifiers, the gasifying medium such as, air, oxygen and steam are introduced at the bottom and flows upward while biomass travels downward, so the gas and the solids are in counter current mode. The gas produced leaves the reactor by the top. As the gas passes through the fuel bed and exits the reactor at low temperature, this type of gasifier has the highest thermal efficiency [6]. These types of gasifiers are suitable for high-ash (up to 25%), high moisture (up to 60%) biomass as well for low-volatile fuels such as charcoal [1].

In crossdraft reactors, fuel is injected from the top while air is injected at high velocity through a water-cooled nozzle from the side. Unlike the two former types, the gas is produced in the horizontal direction in front of the nozzle and is released on the wall opposite to the air intake. The excess oxygen present at the outlet of the nozzle facilitates oxidation of the char, creating a high temperature zone (> 1500 °C) in a small volume with a low tar gas production [1,8]. Then, the heat generated in the oxidation is transported to the pyrolysis zone where the feedstock is pyrolyzed. This type of reactor presents a small reaction zone with low thermal capacity that allows a faster response time than the other two configurations [1].

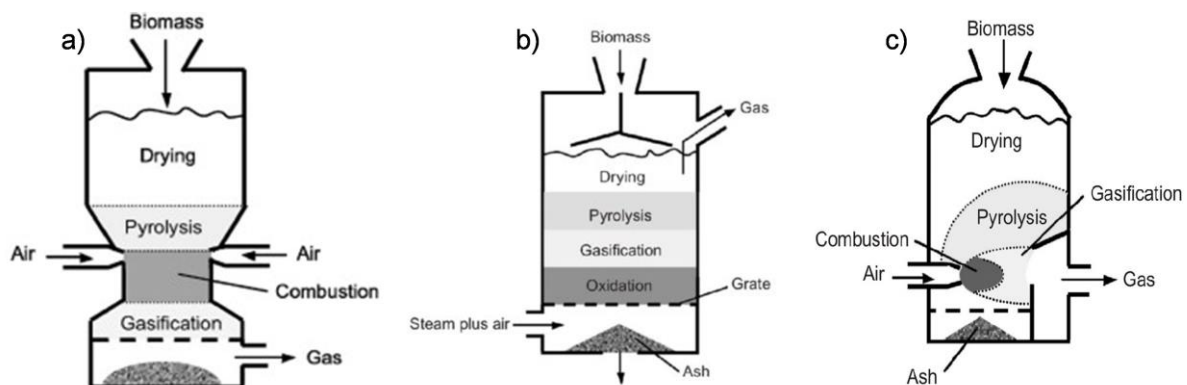


Figure I-7 - Schematic of different types of moving bed type gasifiers: downdraft (a), updraft (b), and crossdraft (c) [1].

I.3.3.2 Fluidized-bed gasifier

The fluidized bed gasifiers are characterized by the optimum mixing and temperature uniformity achieved in the gasification zone. This gasifier is made of granular particles called bed materials. These particles are maintained in a state of suspension through the passage of the gasifying agent at appropriate velocities. The fuel is fed into the reactor, interacting and mixing with bed materials at elevated temperatures (800 – 1000 °C). The high temperatures and their uniformity avoid the

agglomeration of the fuel, making this gasifier suitable for various types of fuel. This type of reactor is mainly used for large scale biomass gasification plants and the two most common configurations are bubbling fluidized bed and circulating fluidized bed, as illustrated in Figure I-8 [1,6,9].

The bubbling fluidized bed gasifier (BFB) is constituted by a vessel with a grate at the base through which the gasifier agent is introduced. Above this grate is a moving bed of fine biomass particles which are driven to a hot bed, fluidized by recirculating product gases. These gases form small bubbles that move at relatively small velocities ($< 5 \text{ m/s}$) [21].

A circulating fluidized-bed gasifier (CFB) is specifically suitable for fuels with high volatile content since this gasifier provides high residence times. This gasifier is generally constituted by a riser, a cyclone and a solid recycle device [1]. The biomass, in this type of reactor, is rapidly pyrolyzed, the tar is captured by bed material while the soot is gasified with steam [21]. Compared with the previous reactor type, this has higher fluidization velocity ($3.5 - 5.5 \text{ m/s}$) [1].

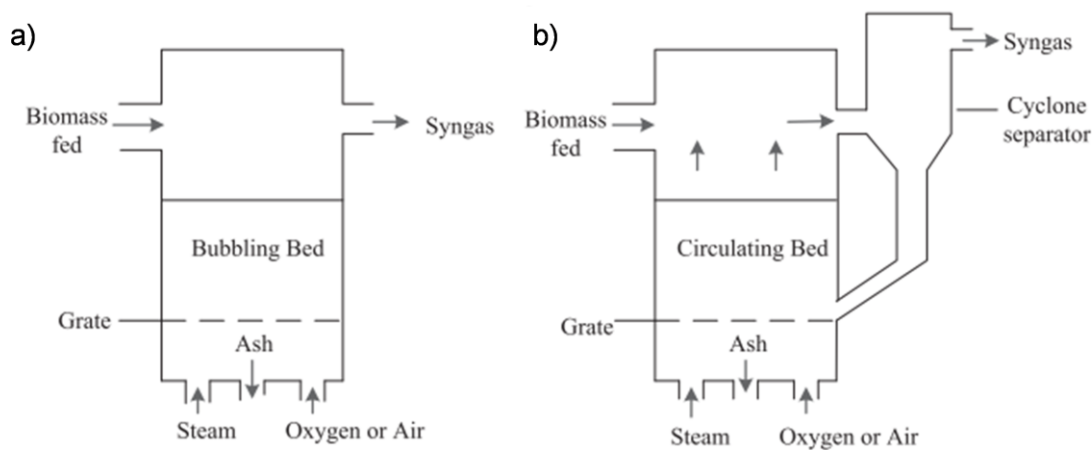


Figure I-8 – Schematic of configurations of fluidized-bed gasifier: BFB (a) and CFB (b) [9].

I.3.3.3 Entrained-flow reactor

In an entrained flow reactor (EFR), the fine fuel particles and the gasifier agent are co-currently fed at high velocities. This allows the formation of a dense cloud constituted by the gasifying agents involving the small particles as they flow through the reactor. In this type of reactor, the conversion of the solid particles is rapid, and the efficiency is high, because of the turbulent flow that is generated. The entrained flow gasifiers operate at high pressures and temperatures ($700 - 2000 \text{ }^\circ\text{C}$) and the residence time of the particles is in the order of a few seconds. Gasification reactions occur at very high rate with high carbon conversion efficiencies [3]. Due to a short residence time ($1 - 5 \text{ s}$), the solid feedstock needs to be grinded into a small particle size ($< 100 \text{ }\mu\text{m}$), in order to achieve high conversion rates [1,9]. These conversion rates can reach 100% if the gasifier is designed and handled correctly. Owing to the high temperatures that are reached inside the reactor, the producer gas is practically tar free and presents a reduced methane content. The entrained flow gasifiers can be divided into two different types: the top-fed flow and the side-fed flow, shown in Figure I-9 [1].

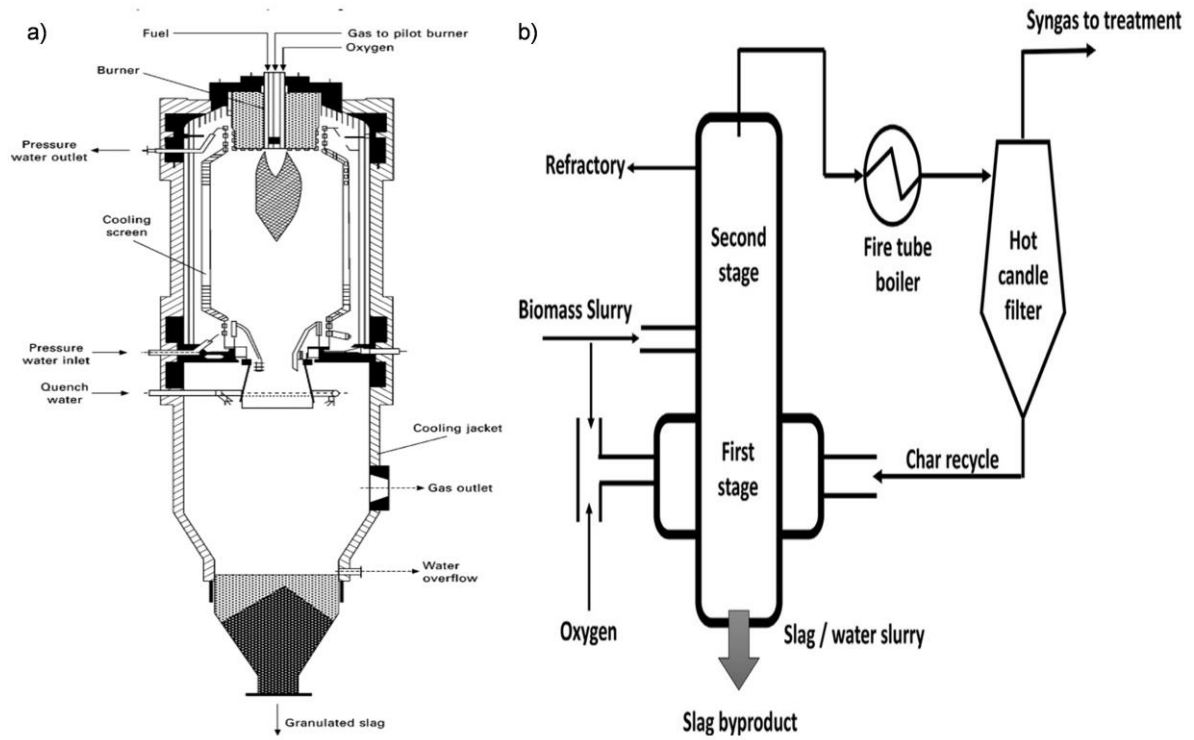


Figure I-9 - Schematic of types of EFRs: top-fed downflow (a) and side-fed (b) [1].

In order to study the biomass conversion under EFR conditions on a laboratory scale, a drop tube furnace (DTF) was developed. A DTF is a relatively simple tool that allows to reproduce some characteristics of an EFR such as the temperature, the heat flow, the residence time and the size of the particles. Although the conditions are very close of an EFR, temperatures and heating rates are slightly lower, since the mechanism of heat transfer is radiation instead of convection [22,23]. The comparison of characteristics of DTFs and EFRs are presented in Table I-4.

Table I-4 – Comparison of key features of DTFs and EFRs [5,18,22-33].

Characteristic	Equipment	
	DTF	EFR
Temperature range (°C)	700 - 1500	700 - 2000
Maximum heating rate (°C/s)	~10 ³ to 10 ⁴	~10 ⁴ to 10 ⁵
Residence time (s)	0.3 - 14	0.4 - 8
Particle size (mm)	< 1	< 1
CCE (%)	55 - 90	50 - 95
Gas LHV (MJ/kg, db)	3 - 10	7 - 9
Soot (g/kg, db)	1 - 60	1 - 50
Dominant heat transfer mechanism	Radiation	Convection

I.3.4 Performance Indicators

The ability of a gasifier to convert a solid material and its energy content into a gas is called efficiency of a gasifier. There some performance parameters to evaluate the efficiency of the gasification process and the quality of the producer gas. Villeta et al. [3] present the following:

The low heating value (LHV), that is the heat (in MJ) produced from the combustion of a Nm³ of syngas and it considers the heating values of each chemical species of the syngas.

The carbon conversion efficiency (CCE), that is defined as the ratio between the carbon leaving the gasifier in syngas and the carbon entering the gasifier:

$$CCE = \frac{Q_{syngas} \sum_i^n x_{carbon,i}}{\dot{m}_{bio} y_{carbon}} \quad (I - 1)$$

Being Q_{syngas} the syngas flow rate (in Nm³/h), x_{carbon} the carbon molar fraction of products, \dot{m}_{bio} the feeding mass rate of feedstock biomass (in kg/h) and y_{carbon} the carbon mass fraction from ultimate analysis.

The cold gas efficiency (CGE), defined as the ratio between the chemical energy leaving the reactor in syngas and chemical energy entering the reactor in biomass:

$$CGE = \frac{Q_{syngas}LHV_{syngas}}{\dot{m}_{bio}LHV_{bio}} \quad (I - 2)$$

Being LHV_{syngas} and LHV_{bio} the low heating values of syngas and biomass respectively.

The hydrogen/carbon monoxide (H₂/CO) volume ratio in syngas is another performance indicator.

I.3.5 Previous studies

A literature review is presented in this section, considering the operating conditions of EFRs and DTFs. Table I-5 shows a summary of the most relevant experimental works on biomass gasification in these types of gasifiers. The fuels and sizes, the gasifier conditions such as operating temperature, gasifying agent, residence time among others and the main results are listed on this table for each experimental study. Woody, non-woody biomass and lignite are types of biomass used and studied in the experimental studies. The main results presented focus on the influence of the gasifier conditions on the composition and quality of producer gas and on the quantity of particulate matter formed.

Table I-5 - Most relevant experimental studies on biomass gasification in EFRs and DTFs.

Reference	Fuels	Gasifier/Conditions	Main results
Zhang et al. [23] Tar destruction and soot formation in three different conversion process.	Hynoki cypress sawdust (HCS) (<100 μm)	<ul style="list-style-type: none"> • DTF • Temperatures: 600 - 1400 °C • Pyrolysis • Steam gasification (H₂O/HCS = 1.4 kg/kg, db) • Partial oxidation (O₂/HCS = 0.6 kg/kg, db) 	<ul style="list-style-type: none"> • For all experiments, the rise in operating temperature greatly decreased tar evolution; • Char yield decreased almost linearly with the increase of the temperature for the three experiments; • In comparison with rapid pyrolysis, steam gasification and partial oxidation greatly decreased soot formation; • For all experiments, the production of H₂ increased with temperature; • CO₂ formation was significantly pronounced during partial oxidation unlike pyrolysis and steam gasification, at temperatures below 1000 °C.
Hernández et al. [33] Effect of steam content in the air-steam flow	Dealcoholized marc of grape (< 500 μm)	<ul style="list-style-type: none"> • DTF • Constant biomass/gasification agent ratio (F), T = 1050 °C • Constant air/biomass ratio (A/B), T = 1050 °C: <ul style="list-style-type: none"> - steam gasification (A/B = 0) - air-steam gasification (A/B = 1.2) 	<ul style="list-style-type: none"> • For constant F: <ul style="list-style-type: none"> - An increase in the steam content caused a rise in CO, H₂ and CH₄; - There was a maximum in CGE for air-steam mixtures containing 50-70% mol steam. • For constant A/B: <ul style="list-style-type: none"> - An increase of S/B led to a rise of H₂ content and a slightly increase of CO₂ content in the product gas for steam gasification; - For air-steam gasification H₂ were more sensitive to S/B, since it increased more.

Reference	Fuels	Gasifier/Conditions	Main results
Billaud et al. [26] Influence of H ₂ O, CO ₂ and O ₂ addition on biomass gasification in EFR conditions	Beech wood (315 - 450 μm)	<ul style="list-style-type: none"> DTF Temperatures: 800 - 1400 °C Inert and oxidizing atmospheres; Steam (0.55 g/g, db), carbon dioxide (0.87 g/g, db) and oxygen (Excess air coefficient (λ): (0 – 0.61) 	<ul style="list-style-type: none"> H₂ yield decreased in CO₂ experiments and increased in H₂O experiments while CO yield decreased in CO₂ experiments at 1200 °C and 1400 °C; A high soot yield was observed at 1200 °C and 1400 °C for the three experiments; The tar yield decreased when temperature increased; Addition of H₂O or CO₂ had a significant influence on char consumption at 1200 °C and 1400 °C.
Septien et al. [22] Influence of steam on gasification of millimetric wood particles in a DTF	Beech wood (350 and 800 μm)	<ul style="list-style-type: none"> DTF Temperatures: 1000 - 1400 °C Nitrogen inert atmosphere and steam containing atmosphere Gas sampling at two different levels 	<ul style="list-style-type: none"> In both atmospheres, char yield tended to decrease as temperature increased. The total dry gas yield was higher in steam containing atmosphere. H₂ and CO₂ yields were much higher, and CO was steady or lower in steam atmosphere than in an inert atmosphere. Soot particles decreased in a wet atmosphere, but it could not be completely avoided.
Qin et al. [27] Biomass gasification behavior in an EFR: Gas product distribution and soot formation	Beech sawdust (310 μm) Pulverized wheat straw pellet (280 μm) Dried lignin	<ul style="list-style-type: none"> EFR Temperatures: 1000 - 1400 °C Residence time: 2.5 - 5 s H₂O/C (mol/mol): 0, 0.5, 1. 	<ul style="list-style-type: none"> The soot yield was reduced by a longer residence time and a larger feeder air flow, while H₂ and CO were nearly constant. High temperatures and steam addition reduced the soot yield and increased the H₂ yield. Straw, with a high potassium content, presented a lower soot yield.

Reference	Fuels	Gasifier/Conditions	Main results
<p>Qin et al. [24] High-temperature entrained flow gasification of biomass</p>	<p>Beech sawdust (280 μm) Pulverized wheat straw pellets (170 μm)</p>	<ul style="list-style-type: none"> • EFR • Temperatures: 1000, 1200, 1350 $^{\circ}\text{C}$ • Steam/carbon molar ratio (S/C): 0 - 1 • λ: 0.25 - 0.5 	<ul style="list-style-type: none"> • For experiments with and without steam, for $\lambda = 0.25$: <ul style="list-style-type: none"> - Soot started to drop down after reaching a peak value at 1200 $^{\circ}\text{C}$; - H_2 and CO yields increased, and CO_2 and C_xH_y decreased when the temperature increased. • At 1350 $^{\circ}\text{C}$, the soot yield decreased as S/C was increased. • Increasing the λ, the amount of soot decreased significantly, H_2 and CO yield decreased, and CO_2 yield increased. • Wood and straw had similar gasification behavior.
<p>Yu et al. [29] Effects of oxygen concentration (OC), excess air coefficient, and reactor temperature on the produced gas composition, gasification index and tar yield</p>	<p>Rice straw (<300 μm)</p>	<ul style="list-style-type: none"> • EFR • OC: 21 - 60% • λ: 0.15 - 0.35 • Temperatures: 800 - 1200 $^{\circ}\text{C}$ 	<ul style="list-style-type: none"> • CO_2 and H_2 increased and CO decreased when OC was increased from 21% to 50%. • The LHV of the gas was significantly increased with the increase of OC. • With the increase of λ, concentration of H_2 and CO were decreased while concentration of CO_2 was increased. • Increasing the reaction temperature, the concentrations of H_2 and CO were significantly increased while CO_2 showed a sharply decrease. • Tar yield decreased when reaction temperature, OC and λ increased.

Reference	Fuels	Gasifier/Conditions	Main results
Zhou et al. [25] The influence of reaction temperature, residence time and oxygen/biomass ratio, on the gasification	Rice husk Sawdust Camphor wood (149 - 250 μm)	<ul style="list-style-type: none"> • EFR • Temperatures: 1000 – 1400 $^{\circ}\text{C}$ • Residence time: 0.4 - 2.0 s • Oxygen/Biomass ratio: 0 - 2.0 (g/g) 	<ul style="list-style-type: none"> • CO_2 and CH_4 decreased with temperature while H_2 and CO contents increased remarkably. • As the temperature increased, the CGE also increased. • A longer residence time reduced efficiency of entire cycle and a shorter residence time resulted in incomplete gasification. • The introduction of oxygen increased the gasification and improved the CCE but reduced the LHV and the H_2/CO ratio.
Hernández et al. [31] Effect of the biomass particle size and the residence time on the syngas quality and the gasifier performance	Dealcoholized marc of grape Grapevine pruning Sawdust wastes (500 - 8000 μm)	<ul style="list-style-type: none"> • EFR • Residence time: 1.36 - 1.92 s • Temperatures: 750 - 1050 $^{\circ}\text{C}$ 	<ul style="list-style-type: none"> • The CGE, H_2/CO ratio and fuel conversion were improved by the reduction in the fuel particle size. • Increasing the space residence time, CO, H_2 and CH_4 were increased in the producer gas for all types of biomass. • CO and H_2 content were increased with an increase in both reaction temperature and space residence time.

In the following sections, the results for some experimental studies are described in more detail, mainly in gasification atmospheres with CO₂ or steam.

I.3.5.1 Influence of CO₂ addition

Billaud et al. [26] compared the influence of steam addition, carbon dioxide and the excess air coefficient on the carbon distribution in the products and on the gas species yields in a DTF. The type of biomass used in these tests was beech sawdust sieved in a size range of 315 - 450 μm with a temperature ranging from 800 °C to 1400 °C. In tests carried out with CO₂ addition, the conversion of carbon into gas reached a maximum at 1400 °C with 71% of carbon from initial biomass. Compared to pyrolysis, both the presence of steam and the presence of CO₂ caused a decrease in the amount of carbon in the tar and the soot, possibly due to the consumption of soot precursors. For the gas species yields, in CO₂ experiments, the CO₂ yield was constant between 800 °C and 1000 °C and then decreased significantly for the remaining temperatures studied. Above 1000 °C, the addition of CO₂ is notorious on CO and H₂ yields. At 1200 °C and 1400 °C, H₂ yield decreased while CO yield increased, compared to pyrolysis. The addition of CO₂ had no significant influence on light hydrocarbons yields even at high temperatures. This can be explained by the following three phenomena: char gasification, tar and soot gasification, and water-gas shift reaction. The first two cause an increase of H₂ and CO yields, however as previously mentioned, in experiments with CO₂, the H₂ yield was lower than in pyrolysis, so the third phenomenon should explain this situation. The evolution of the main gases present in the producer gas is shown in Figure I-10.

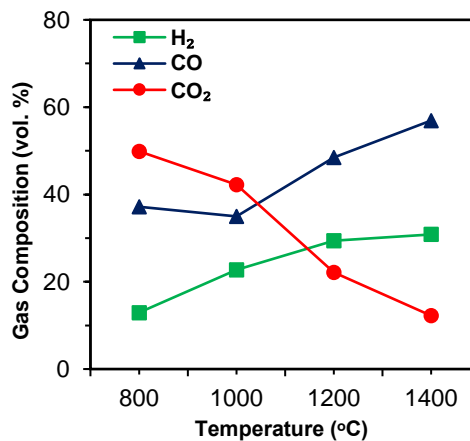


Figure I-10 - Gas composition for an atmosphere with CO₂, using beech sawdust, from Billaud et al. [26].

I.3.5.2 Influence of steam addition

Zhang et al. [23] studied steam gasification, with temperatures of 600 °C to 1400 °C, using hinoki cypress sawdust as fuel in an entrained drop tube reactor. Compared to pyrolysis, steam gasification showed a positive effect on char reduction. For the case of soot formation, a different behavior was observed. The soot formation started at 900 °C reaching a maximum at 1100 °C. Even so, compared with pyrolysis, steam addition caused a decrease in soot production. The H₂ yield was higher in steam gasification than in pyrolysis and in partial oxidation. This can be explained through steam gasification of carbon (R5) and condensable volatiles and water-gas shift reaction (R11). For the formation of CO, it initially increased from 600 °C to 800 °C and then remained constant until 1100 °C and finally increased again to the remaining temperatures. Besides reactions R3 and R5, the reactions R6 and R9 can explain this phenomenon, because they are strongly endothermic reactions, so high temperatures will promote an increase of CO. For CO₂ yield, it increased with increasing temperature up to 1100 °C and then decreased as the temperature further increased. The initial increase of CO₂ yield can be attributed to the reaction R11, whereas the reduction of CO₂ and the increase of CO can be explained by the reactions R5 and R6. Compared with pyrolysis, CH₄ formation is enhanced in steam gasification.

Hernández et al. [33], using dealcoholized marc of grape, investigated the role of the addition of steam into air in an entrained flow gasifier. First, it was studied the increase of the content of steam in air keeping the biomass/gasifying agent ratio (F) constant. Then, the effect of the steam/biomass (S/B) ratio was tested, keeping the air/biomass (A/B) ratio constant. Both tests were performed at 1050 °C. For the producer gas, in the first test, removing the effect of the N₂ dilution, the following behaviors were observed: H₂ and CH₄ increased from 7.5 to 34.4 vol.% and from 2.9 to 11.4 vol.% respectively, the CO₂ decreased from 64.4 to 22.6 vol.% and for the CO a maximum (~39 vol.%) was found for mixtures containing about 40-70% mol steam. In relation to LHV and gas yield (GY), opposite behaviors were observed. The LHV of the gas increased significantly from 1.1 MJ/kg for air gasification to 12.8 MJ/kg for steam gasification whereas the GY decreased from 3.2 to 0.5 Nm³/kg,daf for air and steam gasification respectively. This opposite behavior caused the appearance of a maximum in the CGE (> 60%) for mixtures containing 50 - 70% mol steam. For the second test, as S/B increased, it was observed an increase in H₂ and a small increase in CO₂, and a decrease in CO and in CH₄, for steam gasification. In the case of air-steam gasification, the behaviors of CO, H₂ and CH₄ were similar, but the CO₂ content slightly decreased as S/B increased. The influence of the temperature increase was also studied, either in an air gasification or in an air-steam gasification with ~ 56.5 mol% steam. Under these conditions, at elevated temperatures, H₂ and CH₄ production was higher in an air-steam gasification than in an air-gasification. For all range of temperatures tested, both the LHV and the CGE are higher when steam is added. The LHV and CGE reached a maximum of 5.7 MJ/kg and 48.7%, respectively at 1050 °C.

Septien et al. [22] studied the influence of the presence of steam in the gasification process, using as fuel, wood particles. Gasification was performed in a DTF between 1000 °C and 1400 °C with an atmosphere composed of 25 mol% steam and 75 mol% nitrogen and an inert atmosphere. In these experiments it was shown that the soot formed was much lower in a wet atmosphere than in an inert atmosphere at all temperatures studied. These results also showed that even at elevated temperatures

it is difficult to completely avoid soot, since at 1400 °C the soot represented 5 wt.% of the initial dry biomass. For char it was observed its decrease as the temperature increased for both atmospheres, but for higher temperatures the decrease was higher in wet atmosphere. In a wet atmosphere, it was also observed that the total dry gas yield was produced in higher quantity than in an inert atmosphere, especially at 1200 °C and 1400 °C. For the individual gas mass yields, H₂ and CO₂ yields were higher, CO yield is the same or lower and the CH₄ yield is higher in a wet environment, but at 1400 °C the CH₄ was not detected.

Effects of steam/carbon (S/C) molar ratio were studied by Qin et al. [24] using as fuels, wood and straw from 1000 °C to 1350 °C. For wood gasification, a soot peak at 1200 °C (58.7 g/kg) was observed using S/C ratio of 0.5. It was observed that as the S/C ratio increased from 0 to 1, at 1350 °C, the formation of soot was reduced from 39.6 g/kg fuel to 31.3 g/kg for $\lambda = 0.25$. Thus, it was possible to verify that although steam was useful for decreasing the production of soot, it was not possible to remove it completely. As the S/C ratio increased from 0 to 1, for $\lambda = 0.25$, H₂ and CO₂ yields increased from 0.53 Nm³/kg fuel to 0.65 Nm³/kg and from 0.18 Nm³/kg to 0.22 Nm³/kg, respectively, whereas CO yield decreased from 0.73 Nm³/kg to 0.67 Nm³/kg, and C_xH_y had a small increase of 0.004 Nm³/kg. For the total amount of gas yield and for the ratio H₂/CO, an increase of about 0.11 Nm³/kg and an increase from 0.7 to 1 were also observed, respectively, for the same conditions mentioned above. For straw gasification, the results obtained were very similar.

Figure I-11 illustrates the evolution of the main components of syngas with increasing temperature for the studies mentioned above. In all tests the gasification atmosphere had a percentage of steam. From the graphs it is possible to observe that, in general, the volume percentage of CO decreases for low temperatures reaching a minimum at 1000 °C or 1100 °C and increases again for high temperatures (> 1200 °C). In case of H₂, its volume percentage always increases with temperature reaching a maximum at elevated temperatures, remaining constant at high temperatures (> 1200 °C). In general, the volume percentage of CO₂ decreases slightly or does not vary significantly, depending on the type of biomass used. CH₄ is the least formed component compared to CO, H₂ and CO₂, but generally decreases with temperature, reaching up to residual amounts (practically zero) at very high temperatures.

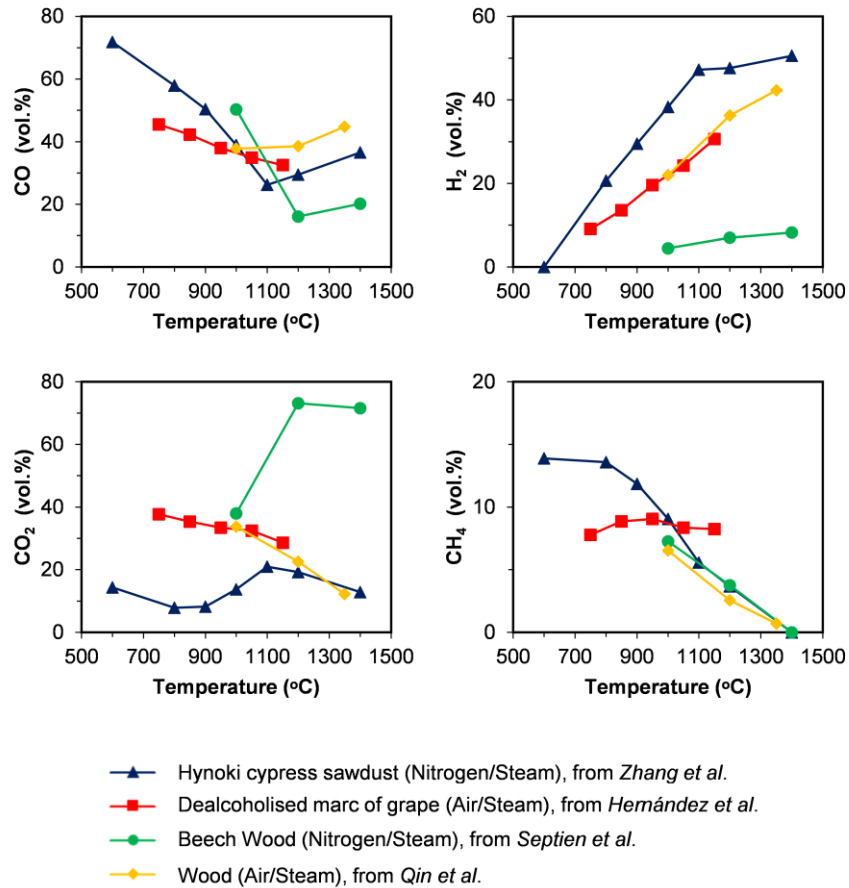


Figure I-11 - Effect of temperature on the composition of the producer gas in atmospheres with steam during biomass gasification.

The effect of temperature on soot yield and char yield in atmospheres with steam is illustrated in Figure I-12. It is possible to see that the soot yield presents a peak at 1000 °C or 1100 °C and at low temperatures is residual. The char yield decreases as temperature increases, becoming almost zero at elevated temperatures.

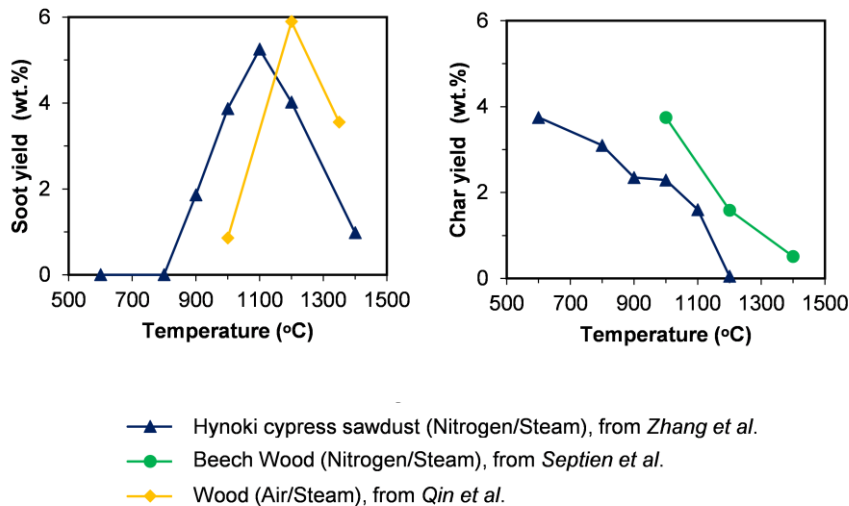


Figure I-12 - Effect of temperature on soot and char formation in atmospheres with steam during biomass gasification.

I.3.5.3 Effect of other operating parameters

There are other parameters that influence the product gas composition and the quantities of by-products generated, such as the excess air coefficient, the residence time, and the particle size.

The effect of excess air coefficient on biomass gasification was studied by Qin et al. [24,27], Yu et al. [29] and Lapuerta et al. [32]. The composition of H₂ and CO in the syngas and the soot formation were studied varying the excess air coefficient (λ). As λ increased, the volume percentage of H₂ and CO decreased. The amount of soot formed also decreased as λ increased. According to Villeta et al. [3], the higher λ , the higher oxidation rate of fuel and the consequent conversion into gas, the higher CO₂ concentration and lower hydrocarbon concentration. Typical λ values used in gasification processes range between 0.2 and 0.4.

The impact of residence time on biomass gasification was analyzed by Zhou et al. [25], using rice husk and camphor wood as fuels. The two types of biomass used presented the same behavior of the concentration of originated gases. For residence times from 0.4 s to 1.2 s, an increase in CO₂ concentration and a decrease in H₂ concentration was observed. For a residence time of 1.6 s, the concentration of CO₂ and H₂, decreased and increased, respectively, remaining almost constant at 2 s, the last residence time analyzed. The CH₄ concentration varied slightly in the residence times analyzed and was practically residual while CO concentration remained higher than the other gases.

Hernández et al. [31] investigated the influence of the particle diameter (d_p) of biomass on the gas composition and fuel conversion. It was observed that the CO, H₂ and CH₄ volume concentrations increased as the d_p reduced, while CO₂ volume concentration decreased slightly, from 8000 μm to 500 μm diameter particles. The fuel conversion increased significantly from 57.5% to 91.4% for 8000 μm and 500 μm diameter particles respectively. In general, a reduced d_p (higher particle external surface)

allows a higher quality syngas, a reduction in reactor size and residence time required to complete the cracking of the condensable and heavy fractions.

I.4 Objectives

From the literature review, it was found that there is still a lack of experimental gasification tests in drop tube reactors or similar, regarding the analysis of the formed particles. Therefore, the main objective of this work is to quantify and to characterize chemical and morphologically the resulting particulate matter from the gasification process and to analyze the composition and quality of syngas. Through the characterization of the collected particles it is possible to distinguish char and soot particles formed in different gasification atmospheres. Scanning electron microscope (SEM) imaging, energy dispersive x-ray spectroscopy (EDS) and Burnout analysis were the mechanisms used to examine the solid sampling gathered and a gas chromatograph (GC) was used to determine the syngas composition. The influence of S/B ratio, the temperature variation, the gasification atmosphere and the type of biomass used are parameters studied in this work.

In short, the objectives of this work are:

1. To study the effect of the S/B ratio on char and soot formation and on composition and quality of syngas produced at a constant temperature.
2. To examine the influence of gasification atmosphere and temperature on the resulting particulate matter and on syngas composition and quality.

I.5 Thesis outline

The last three chapters of the present thesis are described next. Chapter II describes the materials and methods used in the preparation and characterization of the studied biomass, the experimental setup, the methods used for particle collection and subsequent analysis, the test conditions and the experimental procedure. Chapter III presents the results and their discussion of the effects of the S/B ratio in wheat straw (WS) gasification and the effect of the gasification atmosphere and temperature in pig manure (PMan) gasification. Lastly, Chapter IV presents the main conclusions of this thesis and suggests some points to study in future research.

II. Material and Methods

II.1 Fuel preparation and characterization

In this work two types of biomass were used, wheat straw (WS) pellets and pig manure (PMan). These two types of raw biomass were pulverized with a 1-mm-diameter sieve using a laboratory-scale mill Retsch SM 100. The particles used in the experiments presented a size of 90 - 150 μm . This particle size was obtained by using a SS-15 Gilson Economy 203 mm Sieve Shaker. After the feedstock particles had the correct size, they were stored in sealed bags to avoid oxidation. As recommended by reference [34], before each measurement, the samples were dried in an oven at 105 °C for approximately 18h to remove the excess moisture content.

The properties of the two types of biomass residues used are present in the Table II-1, including the ash composition.

Table II-1 - WS and PMan thermochemical properties.

Parameter	WS	PMan
Proximate analysis (wt.%, as received)		
Moisture	8.0	17.8
Volatile matter	64.9	42.7
Ash	14.7	33.7
Fixed Carbon (by dif.)	12.4	5.8
Heating value (MJ/kg, as received)		
Low	13.0	9.4
Ultimate analysis (wt.%, dry ash free)		
C	41.1	49.7
H	5.3	5.4
N	0.7	5.4
S	< 0.02	1.6
O (by dif.)	52.6	37.9

II.2 Experimental setup

The experimental setup schematic, used in this work, is shown in the Figure II-1. The gasification system consists of a biomass feeder, a gas (nitrogen, oxygen and carbon dioxide) supply system, a vertical drop tube reactor, a particulate collection system and a gas sampling and analysis system.

The feed system consists of a twin-screw volumetric feed where the biomass is poured. The fuel particles are then transferred to the injector with the aid of the carrier gas. The injector is water cooled and is inserted into the vertical tube. It has a central pipe for the inlet of the biomass particles and the carrier gas and a concentric passage for the introduction of a secondary stream. The carrier gas is nitrogen (N_2) and for the secondary stream is used a mixture of nitrogen with oxygen (O_2) and steam (H_2O) or carbon dioxide (CO_2). The steam is produced on a generator controlled by dedicated software. It consists of a pressurized container at 2 bar with distilled water, a boiler and gas and water flow meters. The boiler heats up to 200 °C and the water flow meter measures up to 1200 g/h. In order to prevent steam condensation, the steam line is heated to 200 °C. The remaining gases (N_2 , O_2 and CO_2) are supplied from bottles and the flow rates are controlled by manual flow meters.

The place where the gasification takes place consists of a nonporous mullite tube with a total length of 1750 mm and an inner diameter of 40 mm placed in an electrically heated furnace. This furnace can reach a maximum temperature of 1300 °C. Along the furnace, there are three equally spaced thermocouples (type R) to monitor continuously the wall temperatures.

At the bottom of the reactor is located the particle collection system. This system is constituted by two cyclones, an in-house made cyclone and a commercial cyclone (Dekati®) and a Dekati low pressure impactor (DLPI, Dekati® Ltd.) to collect the solid particles. In order to avoid gases condensation, the impactor and the Dekati® cyclone were kept at 150 °C by two Winkler heating blankets. The introduced gases, as well as those formed during the process are transported to the gas analyzers with the aid of pumps. The gas analyzers are constituted by a paramagnetic pressure analyzer for O_2 and a non-dispersive infrared analyzer CO_2 and CO . In the gas analyzers, it is only possible to observe the volumetric concentration of O_2 , CO_2 and CO . The remaining gases (H_2 and CH_4) were analyzed with the aid of a GC after collecting the producer gas in bags.

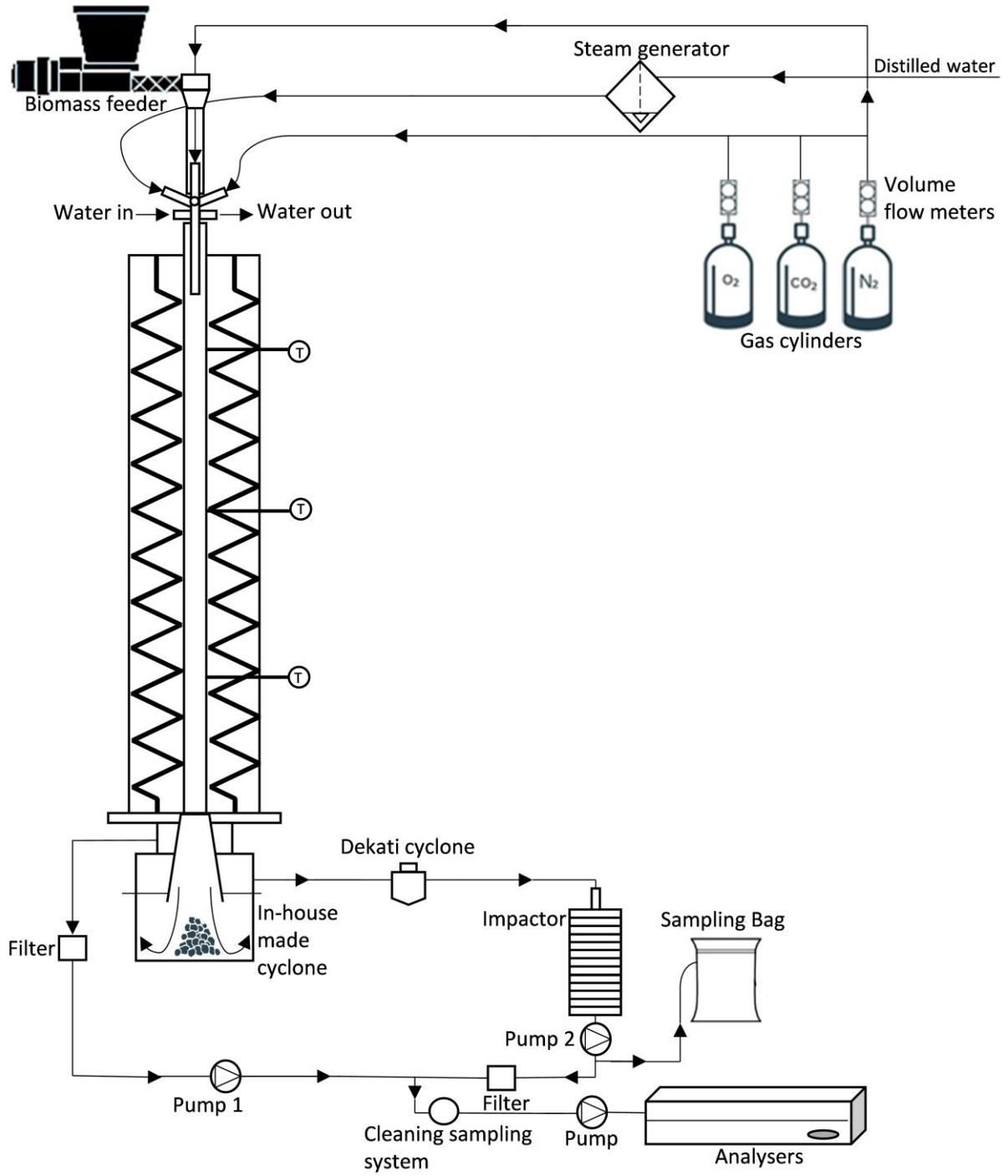


Figure II-1 - Schematic of the experimental setup.

II.2.1 Solid particles collection

At the lower end of the DTF there is a cyclone to gather the largest solid particles ($> 10 \mu\text{m}$). In addition to this, before the solid collection, the cyclone allows bypassing the solid particles system, in order to create a steady state. Then, the flow of gases and particles passes through a Dekati® cyclone, shown in the Figure II-2, that provides a cut size of $10 \mu\text{m}$. In order to achieve a cut size of $10 \mu\text{m}$, the nominal gas flow through this cyclone is about 10 L/min. Next, the flow passes through the low pressure thirteen-stage cascade impactor (DLPI, Dekati® Ltd.) where the smallest particles ($< 10 \mu\text{m}$) are collected. The impactor and its particle collecting mechanism are illustrated in the Figure II-3. The flow, at high speed passes through the nozzles of the jet plate and makes a sharp turn to flow between the plates. The particles above a certain size cannot make the sharp turn and are retained in the next filter. With the aid of a vacuum pump (115V/60 Hz IA-906 Dekati®), the nominal low pressure and gas flow through the cyclone and the impactor are kept at 100 mbar and 10 L/min.



Figure II-2 - Dekati cyclone [35].

The thirteen stages of the impactor allow the classification of particles, in thirteen groups of diameters according to the Table II-2. To determine the amount of particulate matter formed, the substrates were weighed before and after each experiment.

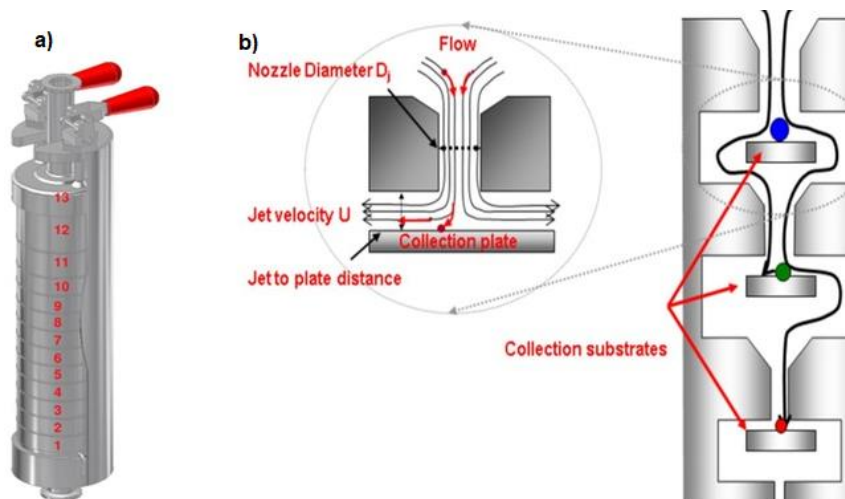


Figure II-3 - Dekati cascade impactor (a) and the particle collecting mechanism (b) [35].

Table II-2 - Aerodynamic diameter for each stage of impactor [35].

Impactor Stage	Aerodynamic Diameter (μm)
1	0.028
2	0.055
3	0.094
4	0.158
5	0.265
6	0.386
7	0.616
8	0.950
9	1.597
10	2.384
11	3.979
12	6.651
13	9.862

II.2.2 Particle morphology and Chemical Species

The particles collected at each stage of the impactor and in cyclone, after being weighed, were analyzed in a Scanning electron microscope (SEM, Hitachi S2400) available at Instituto Superior Técnico, Figure II-4). This equipment was used to evaluate the morphology and chemical composition of collected particulate matter (PM). The SEM presents an energy dispersive x-ray spectroscopy (EDS) detector, that allows to provide the ultimate composition of a small sample with a resolution of $1 \mu\text{m}^2$. For each PM sample, the chemical composition data, in terms of carbon, oxygen and ashes, was obtained from three different areas of about $50 \times 50 \mu\text{m}^2$ each.



Figure II-4 - Scanning electron microscope (SEM).

To obtain a broader view of the chemical composition of particles, burnout experiments were performed with a larger amount of PM than in the SEM, approximately 400 mg. The burnout consisted of burning particles in a muffle in order to assess the carbon and ash composition. The particles were burned using a heating ramp up to $1100 \text{ }^\circ\text{C}$, over 14 h. This temperature allows the total evaporation of the organic material (carbon) present in the samples. Based on the final sample (ashes), after burning, it was possible to conclude about the organic and inorganic content present in the particles collected in the cyclone. The burnouts were not performed with the PM collected on impactor because of the small amount collected here.

II.2.3 Gas collection and composition

The producer gas was collected at the end of the setup in SKC FlexFoil® sampling bags. Using a Clarus 500 GC available at Instituto Superior Técnico, the gas composition was measured. The GC model is equipped with a thermal conductivity detector (TCD) to measure the light gases.

II.2.4 Test conditions

The experimental work was divided into two parts. The first part (shown in Table II-3) consisted on the study of the influence of steam/biomass (S/B) ratio on wheat straw (WS) gasification. The temperature of the reactor used was set at 1000 °C and the S/B was varied from 0 (without steam addition) to 1.7. In the second part (shown in Table II-4) of the work, pig manure (PMan) was used as fuel. It was investigated the effect of three different gasification atmospheres with the temperature varying from 900 to 1200 °C. The first gasification atmosphere consisted of a mixture of nitrogen and oxygen (N₂/O₂) and the other two with the addition of carbon dioxide (N₂/O₂/CO₂) and steam (N₂/O₂/H₂O), respectively. The fuel particle residence time (t, in seconds), for the two parts, in the reactor was approximately 2-3 seconds, which was determined by the following equation:

$$t = \frac{V_{reactor} \cdot (273 + T_{amb.})}{(\dot{V}_{inletgas}) \cdot (273 + T_r)} \cdot 60 \quad (II - 1)$$

Being $V_{reactor}$ the reactor volume (in m³), $\dot{V}_{inletgas}$ the total inlet gas flow (in m³/min), T_r the reactor temperature (in °C), and $T_{amb.}$ the ambient temperature (in °C).

The excess air coefficient (λ) used in both parts of the experiments was 0.4, and is given by:

$$\lambda = \frac{\dot{V}_{O_2,used}}{\dot{V}_{O_2,stoichiometric}} \quad (II - 2)$$

The volumetric flow rate of O₂, used to obtain the appropriate λ , was calculated by the ultimate analysis on a dry basis of the two types of biomass used.

The following two tables, Table II-3 and Table II-4, summarize the test conditions used for WS and PMan gasification, respectively. In WS gasification, two tests were performed for each condition, while in pig manure gasification only one test was performed for each of the twelve conditions.

Table II-3 - Experimental schedule for the study of the effect of the S/B in WS gasification.

No.	T_r (°C)	\dot{m}_f (g/h)	\dot{m}_{steam} (g/h)	S/B (g/g)	\dot{V}_{steam} (L/min)	\dot{V}_{O_2} (L/min)	\dot{V}_{N_2} (L/min)	Total (L/min)
1	1000	30	0	0	0	0.11	9.89	10
2			15	0.5	0.54		9.35	
3			25	0.8	0.90		8.99	
4			50	1.7	1.80		8.09	

Table II-4 - Experimental schedule for the study of three gasification atmospheres for PMan gasification.

No.	T_r (°C)	\dot{m}_f (g/h)	\dot{V}_{N_2} (L/min)	\dot{V}_{O_2} (L/min)	\dot{V}_{CO_2} (L/min)	\dot{V}_{steam} (L/min)
1	900	30	10	0.11	---	---
2	1000					
3	1100					
4	1200					
5	900	30	10	0.11	0.54	---
6	1000					
7	1100					
8	1200					
9	900	30	10	0.11	---	0.54
10	1000					
11	1100					
12	1200					

II.2.5 Procedure

The experimental procedure used throughout the tests was similar in both parts and is summarized next. The first step of the experiments was turn on the gas analyzers and the cooled water of the injector and then the electrical furnace to a desired temperature. After that, the biomass feedstock, previously ground and homogenized, with the required size, was loaded into the biomass feeder system. After connecting the biomass transport tube to the injector, the nitrogen was turned on with the appropriate flow rate in order to remove all the oxygen present in the reactor. When the reactor was free of oxygen, the amount of oxygen required for the gasification conditions was added. To complete the necessary gasification atmosphere, the addition of steam or carbon dioxide was then performed. After the conditions of gasification atmosphere were stable, the biomass feeder system was turned on. To ensure the stabilization of the reactions inside the reactor, the pump 1 was used during the first five minutes, to ensure the gases reached the gas analyzers without passing through the thirteen-stage cascade impactor. After the five minutes of stabilization, the pump 1 was turned off and the pump 2 was turned on. For fifteen minutes, using the pump 2, the char and the soot particles were collected in cyclone and impactor, respectively. The CO₂ and CO volume percentages, given by the gas analyzers, were registered during this period. After fifteen minutes, the pump 2 was turned off and all flows (biomass, nitrogen, oxygen and steam or carbon dioxide) were stopped and the test was finished. Both the cyclones and the impactor were taken out and their content was weighed and then properly stored for subsequent analyses. The producer gas was collected in bags and then analyzed in the GC.

III. Results and Discussion

This chapter is divided into two subchapters. In the first subchapter is presented and discussed the results of the study of the effect of the S/B ratio on the formation of char and soot particles and on syngas composition and quality using WS as biomass. In the second subchapter, the results of PMan gasification are analyzed in three gasification atmospheres described previously at four different temperatures (see Table II-4).

III.1 Effect of S/B ratio on WS gasification

III.1.1 Solid particles

The PMs resulting from the gasification process are essentially char, soot and ash particles. In these experimental tests the obtained particles were separated into two size categories. The cyclone collected particles with a diameter larger than 10 μm while the thirteen-stage cascade impactor collected the particles with a diameter smaller than 10 μm . Figure III-1 illustrates the influence of S/B ratio on the generation of PMs in the cyclone and in the thirteen-stage cascade impactor.

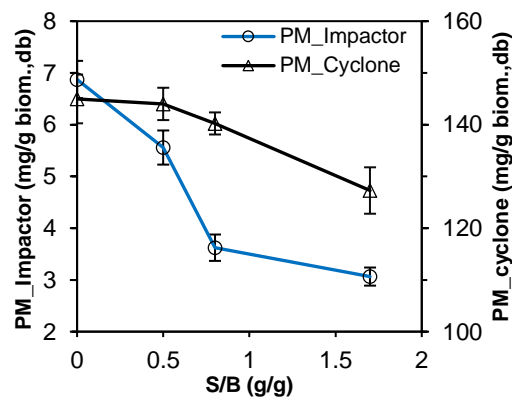


Figure III-1 - Influence of S/B ratio on the PMs collected in the cyclone and thirteen-stage cascade impactor.

In this plot it can be observed that the PM collected in the cyclone decreased from 144.97 to 127.01 mg/g, db, as the S/B ratio increased from 0 to 1.7. The same behavior was observed in the particles collected in the thirteen-stage cascade impactor, where there was a decrease from 6.87 to 3.06 mg/g, db, as the S/B ratio increased.

In order to be able to distinguish between char, soot and ash particles, SEM and EDS analysis were performed for the PMs collected in the two devices. In the EDS, for each sample, the chemical composition data was obtained from three different areas of about 50 x 50 μm^2 each. To consolidate the EDS results it was performed a burnout experiment (explained in section II.2.2), only for PMs collected in the cyclones.

The SEM, EDS and Burnout analysis for the PMs collected in the cyclones for the different S/B ratios are presented in Table III-1. For the four conditions analyzed, the particles shown in the SEM images are very similar, have irregular shapes, some pores and have about 100 μm . From the EDS analysis, these particles are constituted of about 60 wt.% of carbon, 23-27 wt.% of oxygen and 13-20 wt.% of ash, regardless of the S/B ratio used. Through the burnout analysis, it was observed that the organic content present in the PMs decreased slightly, increasing the S/B ratio, from 48 wt.% to 41 wt.%. The EDS and Burnout analysis showed a slight difference, due to measurement techniques. In the EDS analysis a small sample was used and only a small portion of it was analyzed while in the Burnout analysis a significant amount of the sample was used and analyzed. From the morphological characteristics represented in the SEM images and the chemical composition graphically presented from the EDS and Burnout analysis it is possible to state that the PM collected in the cyclone are essentially char and ashes.

SEM and EDS analysis were also performed for particles collected in all stages of the thirteen-stage cascade impactor. The Burnout analysis was not performed, due to the small number of PM in the filters and the fact that they have a substrate in their bed, thus affecting the reliability of the results. Table III-2 presents the SEM and EDS analysis for the PM collected in the thirteen-stage cascade impactor, for a S/B = 0.8, for the stages 3,5,8,9,10,12. The SEM images show, for stages 3,5,8, that the particles are substantially uniform in shape and form agglomerates of about 200 nm. In addition, the EDS analysis shows that the PMs collected at these stages have 80-90 wt.% of carbon. On other hand, in the remaining stages (9,10,12), the particles have an irregular shape, some porosity and they are constituted of about 54-63 wt.% of carbon. The stages 1,2,4,6, and 7 (see Appendix A) presented the same peculiarities as stages 3,4 and 8 and the stages 11 and 13 (see Appendix A) the same as stages 9,10 and 12. Thus, given above the mentioned characteristics of char (see section I.3.2.2) and soot (see section I.3.2.4), it can be affirmed that the PM collected at stages 1 to 8 are soot particles and those collected at stages 9 to 13 are char particles. Therefore, the PM collected in the cyclones and in the stages 9-13 of the impactor are char particles and in the remaining stages of the impactor are soot particles. For the remaining S/B ratios, the particles present in the stages of the impactor showed the same characteristics except for the amount present in them.

Figure III-2 a) illustrates the effect of the S/B ratio on the formation of soot and char particles. The char represented in this plot corresponds to the sum of the total amount of particles collected in the cyclones and in the stages of the impactor referred above, while the soot corresponds to 85 % of the sum of the particles collected in stages 1 to 8 of the thirteen-stage cascade impactor. This approach was made because the filters have some amount of ash, a contaminant, and not only pure soot particles, so it is assumed that the soot generated is constituted only by carbon.

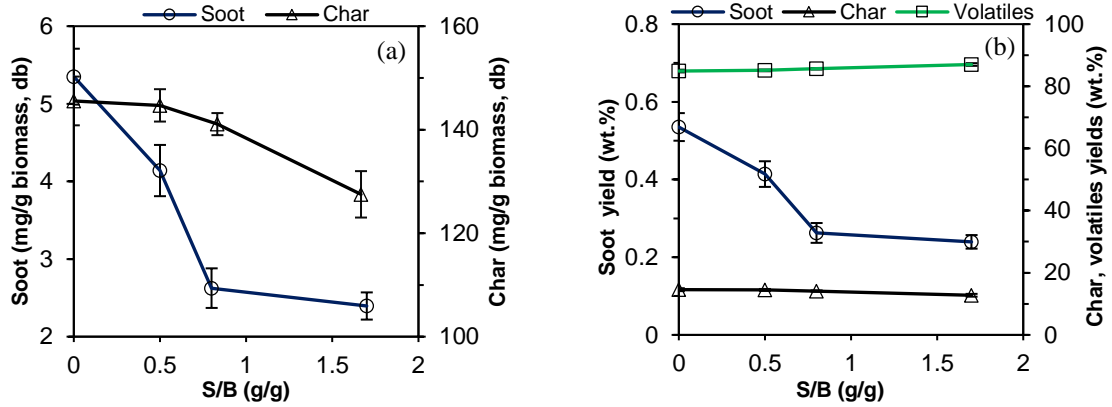


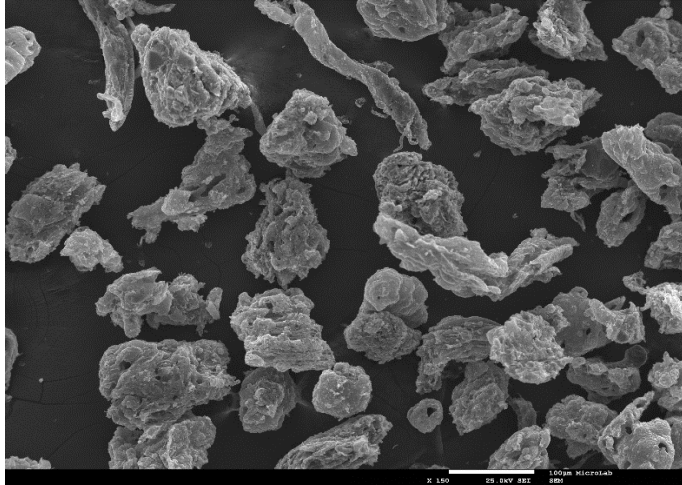
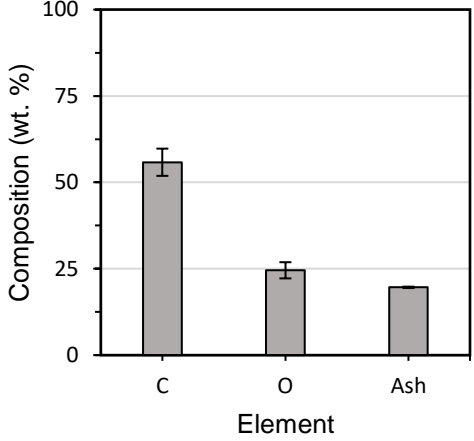
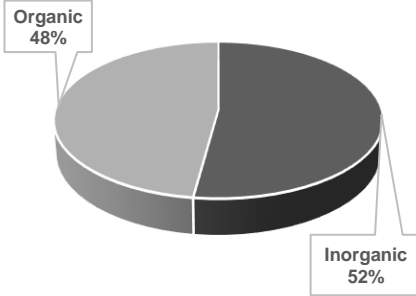
Figure III-2 - Effect of the S/B ratio on the formation of soot and char particles (a), and on the char, soot and volatiles yields (b).

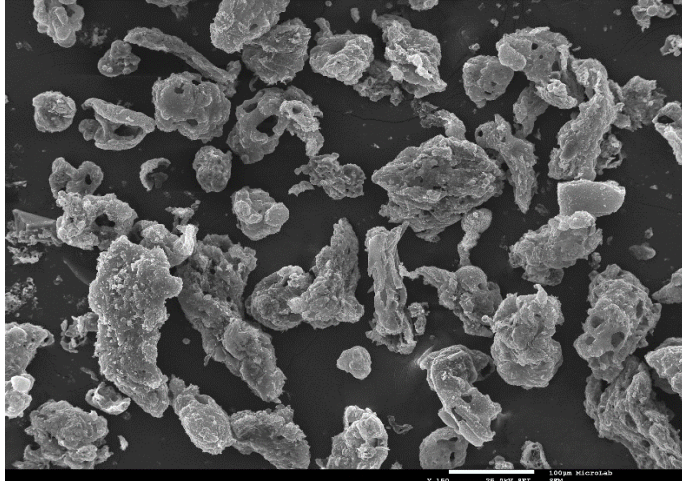
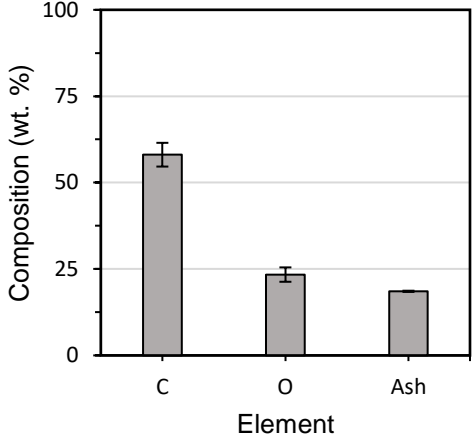
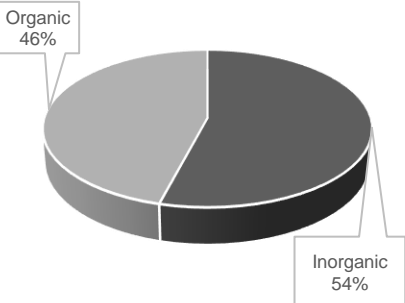
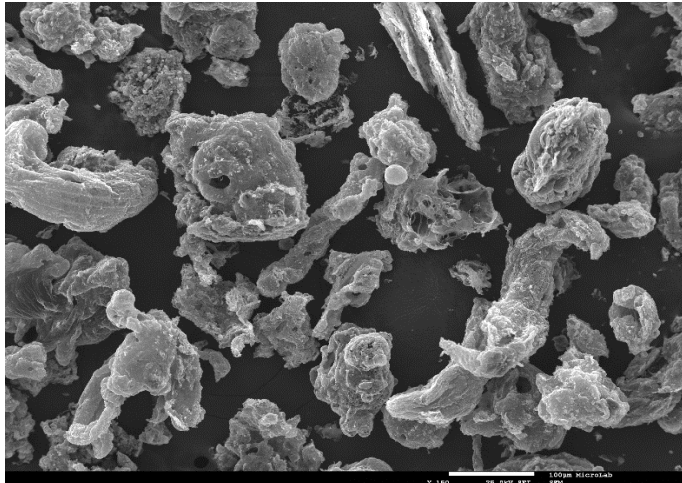
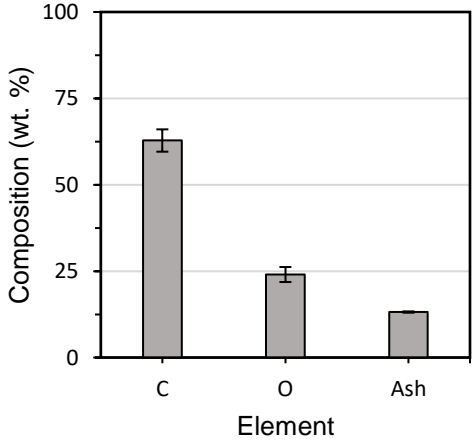
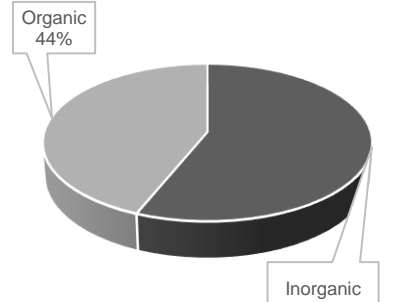
From Figure III-2 a), it can be observed that both char and soot decrease as steam is added to the gasifying environment. The amount of char particles decreased from 145.55 to 127.51 mg/g dry biomass while the collected soot particles decreased from 5.35 to 2.40 mg/g dry biomass, when the S/B ratio increased from 0 to 1.7. The Figure III-2 b) illustrates the evolution of char, soot and volatiles yields for the four conditions tested. As the S/B ratio increases, the volatiles yield increase from 84.91 to 87.01 wt.%, while char and soot yields decrease.

From these two plots, it can be concluded that increasing the S/B ratio, the quantity of PM produced decreases and the production of volatiles increases. The water/gas reaction (R5) may be the justification for this behavior, since in this reaction, the carbon reacts with the steam originating CO and H₂.

Table III-1 shows, mainly by the burnout analysis, that these conclusions are supported since the organic matter present in the unconverted material collected in the cyclones decreased, with the increase of the S/B ratio. Thus, the addition of steam facilitated the conversion of carbon present in biomass to volatiles.

Table III-1 - SEM images, EDS and Burnout analysis for the PM collected in the cyclones for the different S/B ratios (Tr = 1000 °C).

S/B (g/g)	SEM Image	EDS Analysis	Burnout Experiment														
0		 <table border="1"> <caption>EDS Analysis Data (Estimated)</caption> <thead> <tr> <th>Element</th> <th>Composition (wt. %)</th> </tr> </thead> <tbody> <tr> <td>C</td> <td>~55</td> </tr> <tr> <td>O</td> <td>~25</td> </tr> <tr> <td>Ash</td> <td>~20</td> </tr> </tbody> </table>	Element	Composition (wt. %)	C	~55	O	~25	Ash	~20	 <table border="1"> <caption>Burnout Experiment Data (Estimated)</caption> <thead> <tr> <th>Category</th> <th>Percentage</th> </tr> </thead> <tbody> <tr> <td>Organic</td> <td>48%</td> </tr> <tr> <td>Inorganic</td> <td>52%</td> </tr> </tbody> </table>	Category	Percentage	Organic	48%	Inorganic	52%
Element	Composition (wt. %)																
C	~55																
O	~25																
Ash	~20																
Category	Percentage																
Organic	48%																
Inorganic	52%																

S/B (g/g)	SEM Image	EDS Analysis	Burnout Experiment														
0.5		 <table border="1"> <caption>EDS Analysis Data (0.5 g/g S/B)</caption> <thead> <tr> <th>Element</th> <th>Composition (wt. %)</th> </tr> </thead> <tbody> <tr> <td>C</td> <td>~58</td> </tr> <tr> <td>O</td> <td>~23</td> </tr> <tr> <td>Ash</td> <td>~19</td> </tr> </tbody> </table>	Element	Composition (wt. %)	C	~58	O	~23	Ash	~19	 <table border="1"> <caption>Burnout Experiment Data (0.5 g/g S/B)</caption> <thead> <tr> <th>Category</th> <th>Percentage</th> </tr> </thead> <tbody> <tr> <td>Organic</td> <td>46%</td> </tr> <tr> <td>Inorganic</td> <td>54%</td> </tr> </tbody> </table>	Category	Percentage	Organic	46%	Inorganic	54%
Element	Composition (wt. %)																
C	~58																
O	~23																
Ash	~19																
Category	Percentage																
Organic	46%																
Inorganic	54%																
0.8		 <table border="1"> <caption>EDS Analysis Data (0.8 g/g S/B)</caption> <thead> <tr> <th>Element</th> <th>Composition (wt. %)</th> </tr> </thead> <tbody> <tr> <td>C</td> <td>~63</td> </tr> <tr> <td>O</td> <td>~23</td> </tr> <tr> <td>Ash</td> <td>~14</td> </tr> </tbody> </table>	Element	Composition (wt. %)	C	~63	O	~23	Ash	~14	 <table border="1"> <caption>Burnout Experiment Data (0.8 g/g S/B)</caption> <thead> <tr> <th>Category</th> <th>Percentage</th> </tr> </thead> <tbody> <tr> <td>Organic</td> <td>44%</td> </tr> <tr> <td>Inorganic</td> <td>56%</td> </tr> </tbody> </table>	Category	Percentage	Organic	44%	Inorganic	56%
Element	Composition (wt. %)																
C	~63																
O	~23																
Ash	~14																
Category	Percentage																
Organic	44%																
Inorganic	56%																

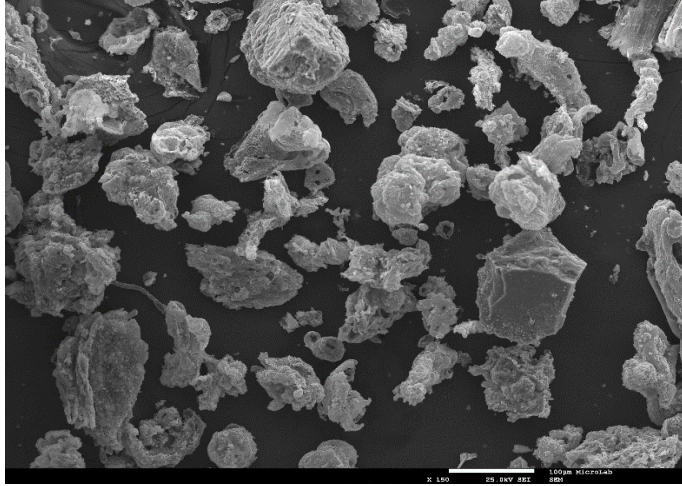
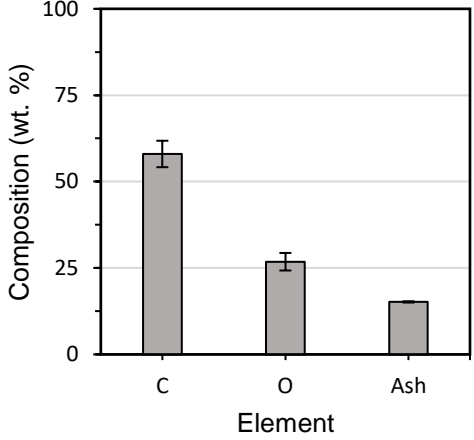
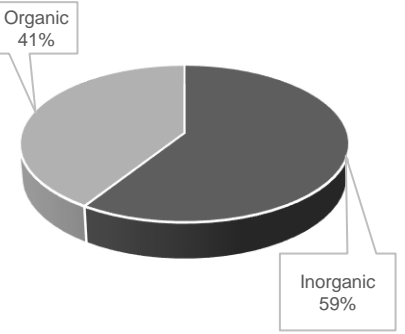
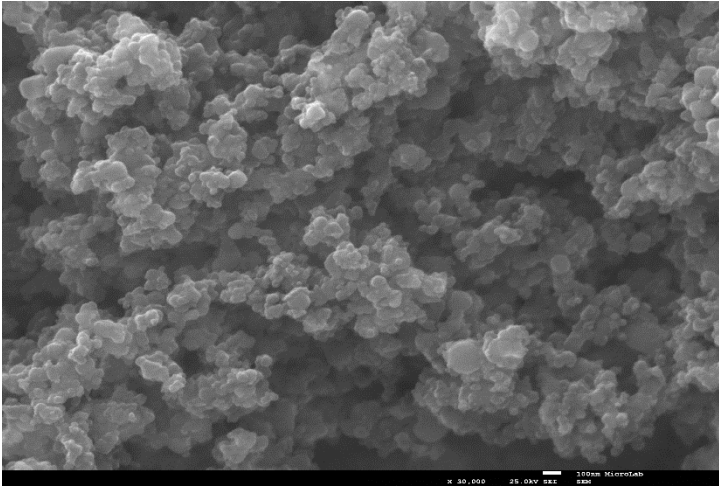
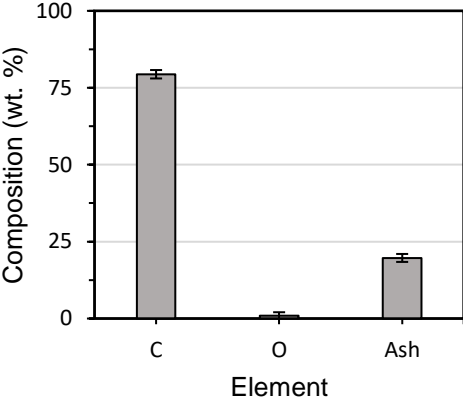
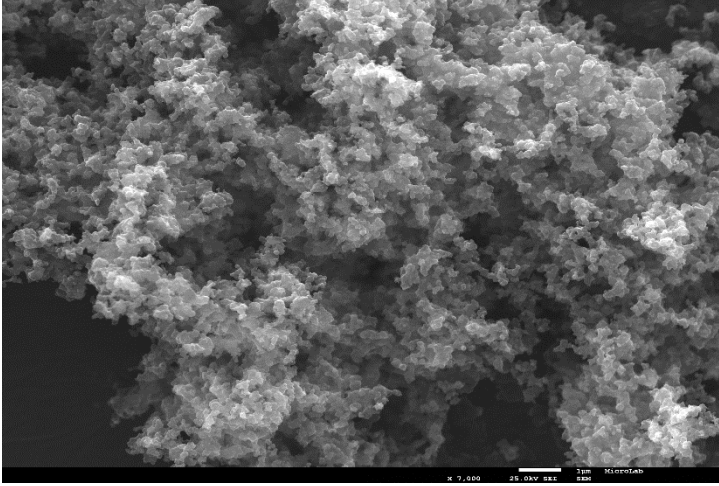
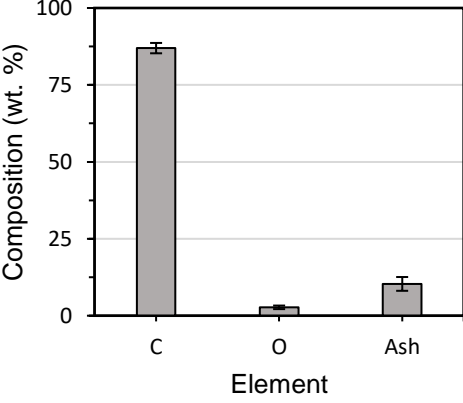
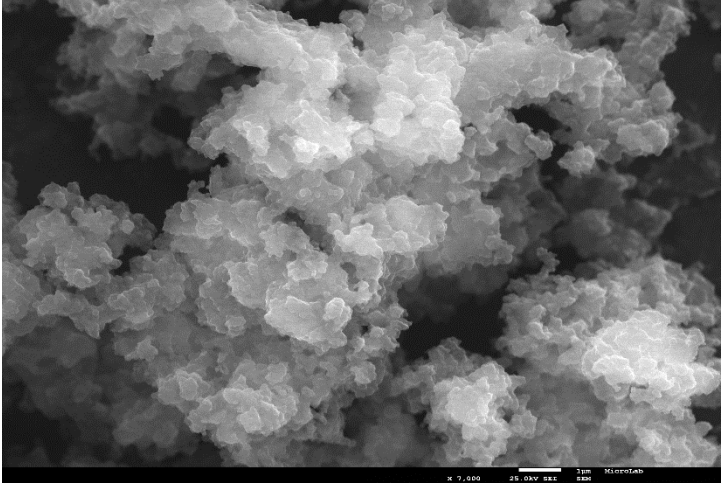
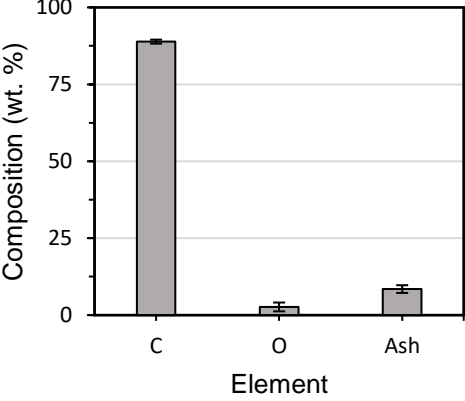
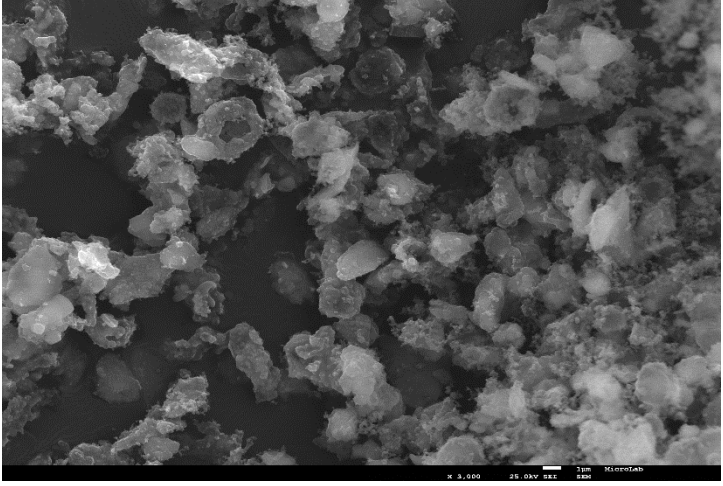
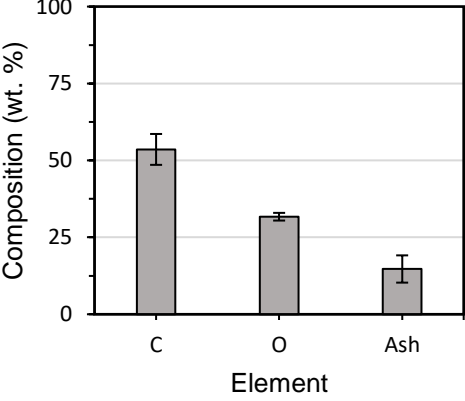
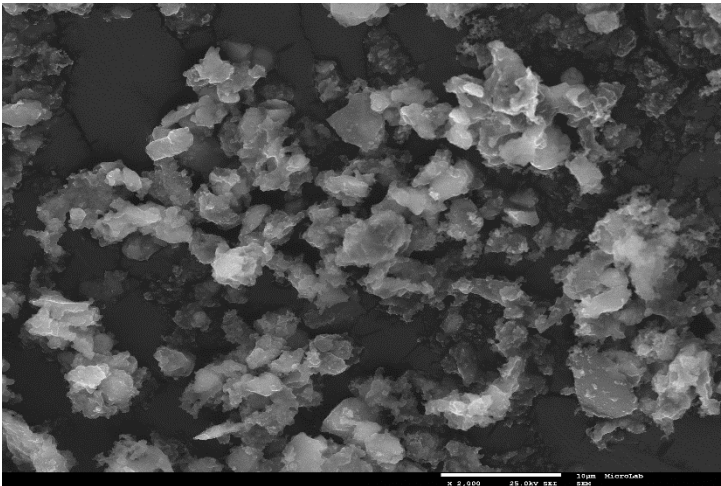
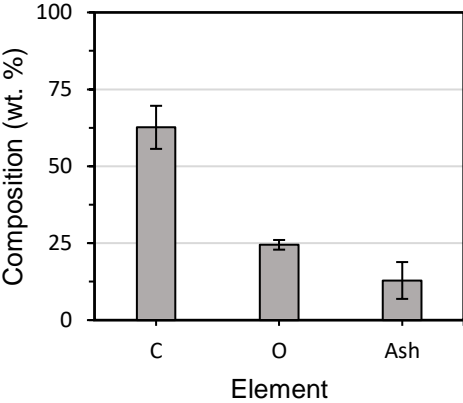
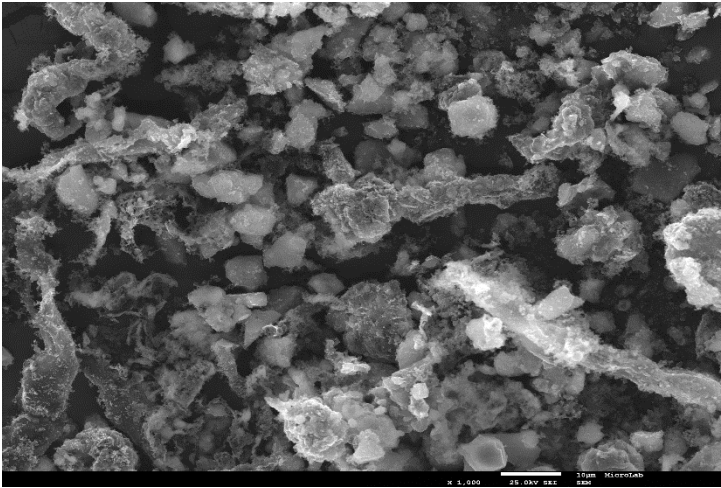
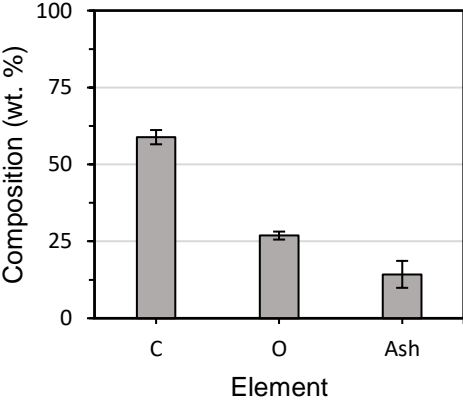
S/B (g/g)	SEM Image	EDS Analysis	Burnout Experiment														
1.7		 <table border="1"> <caption>EDS Analysis Data</caption> <thead> <tr> <th>Element</th> <th>Composition (wt. %)</th> </tr> </thead> <tbody> <tr> <td>C</td> <td>~58</td> </tr> <tr> <td>O</td> <td>~26</td> </tr> <tr> <td>Ash</td> <td>~16</td> </tr> </tbody> </table>	Element	Composition (wt. %)	C	~58	O	~26	Ash	~16	 <table border="1"> <caption>Burnout Experiment Data</caption> <thead> <tr> <th>Component</th> <th>Percentage</th> </tr> </thead> <tbody> <tr> <td>Organic</td> <td>41%</td> </tr> <tr> <td>Inorganic</td> <td>59%</td> </tr> </tbody> </table>	Component	Percentage	Organic	41%	Inorganic	59%
Element	Composition (wt. %)																
C	~58																
O	~26																
Ash	~16																
Component	Percentage																
Organic	41%																
Inorganic	59%																

Table III-2 - SEM image and EDS analysis for WS gasification, for some of the stages of the impactor (Tr = 1000° C, S/B = 0.8).

Stage	SEM Image	EDS Analysis								
3		 <table border="1"> <caption>EDS Analysis Data for Stage 3</caption> <thead> <tr> <th>Element</th> <th>Composition (wt. %)</th> </tr> </thead> <tbody> <tr> <td>C</td> <td>~78</td> </tr> <tr> <td>O</td> <td>~1</td> </tr> <tr> <td>Ash</td> <td>~21</td> </tr> </tbody> </table>	Element	Composition (wt. %)	C	~78	O	~1	Ash	~21
Element	Composition (wt. %)									
C	~78									
O	~1									
Ash	~21									
5		 <table border="1"> <caption>EDS Analysis Data for Stage 5</caption> <thead> <tr> <th>Element</th> <th>Composition (wt. %)</th> </tr> </thead> <tbody> <tr> <td>C</td> <td>~85</td> </tr> <tr> <td>O</td> <td>~2</td> </tr> <tr> <td>Ash</td> <td>~13</td> </tr> </tbody> </table>	Element	Composition (wt. %)	C	~85	O	~2	Ash	~13
Element	Composition (wt. %)									
C	~85									
O	~2									
Ash	~13									

Stage	SEM Image	EDS Analysis								
8		 <table border="1"> <caption>EDS Analysis Data for Stage 8</caption> <thead> <tr> <th>Element</th> <th>Composition (wt. %)</th> </tr> </thead> <tbody> <tr> <td>C</td> <td>~88</td> </tr> <tr> <td>O</td> <td>~3</td> </tr> <tr> <td>Ash</td> <td>~9</td> </tr> </tbody> </table>	Element	Composition (wt. %)	C	~88	O	~3	Ash	~9
Element	Composition (wt. %)									
C	~88									
O	~3									
Ash	~9									
9		 <table border="1"> <caption>EDS Analysis Data for Stage 9</caption> <thead> <tr> <th>Element</th> <th>Composition (wt. %)</th> </tr> </thead> <tbody> <tr> <td>C</td> <td>~55</td> </tr> <tr> <td>O</td> <td>~32</td> </tr> <tr> <td>Ash</td> <td>~13</td> </tr> </tbody> </table>	Element	Composition (wt. %)	C	~55	O	~32	Ash	~13
Element	Composition (wt. %)									
C	~55									
O	~32									
Ash	~13									

Stage	SEM Image	EDS Analysis								
10		 <table border="1"> <caption>EDS Analysis Data for Stage 10</caption> <thead> <tr> <th>Element</th> <th>Composition (wt. %)</th> </tr> </thead> <tbody> <tr> <td>C</td> <td>~62</td> </tr> <tr> <td>O</td> <td>25</td> </tr> <tr> <td>Ash</td> <td>~13</td> </tr> </tbody> </table>	Element	Composition (wt. %)	C	~62	O	25	Ash	~13
Element	Composition (wt. %)									
C	~62									
O	25									
Ash	~13									
12		 <table border="1"> <caption>EDS Analysis Data for Stage 12</caption> <thead> <tr> <th>Element</th> <th>Composition (wt. %)</th> </tr> </thead> <tbody> <tr> <td>C</td> <td>~58</td> </tr> <tr> <td>O</td> <td>26</td> </tr> <tr> <td>Ash</td> <td>~16</td> </tr> </tbody> </table>	Element	Composition (wt. %)	C	~58	O	26	Ash	~16
Element	Composition (wt. %)									
C	~58									
O	26									
Ash	~16									

III.1.2 Composition and quality of the producer gas

The main gas products generated during the gasification process are H₂, CO, CO₂ and CH₄. The producer gas was mainly formed by N₂ (~ 97 vol.%), as a result of the large amount of nitrogen used. Figure III-3 (a) illustrates the gas composition of the syngas as a function of the S/B ratio. The volume concentration of each gas specie was normalized, without nitrogen. Increasing the S/B ratio from 0 to 1.7 the H₂ yield increased significantly from 10.25 to 17.88 vol.%, while the CO₂ yield slightly decreased from 35.14 to 29.57 vol.%, and the CH₄ remained almost constant close to 7 vol.%. The CO yield increased slightly initially but then decreased from 52.92 to 46.10 vol.% when increasing the S/B from 0.5 to 1.7. Hernández et al. [33], in an air-steam gasification, obtained similar trends for the volume concentrations of each gas specie, varying the S/B ratio from 0.64 to 1.57. Due to the increase of steam involved in the reactions, the improvement of the steam reforming of char and methane, and the water/gas shift reaction (R11) occur, and this can explain the trends shown on the plot. The tar cracking (R10) may also contribute to these behaviors.

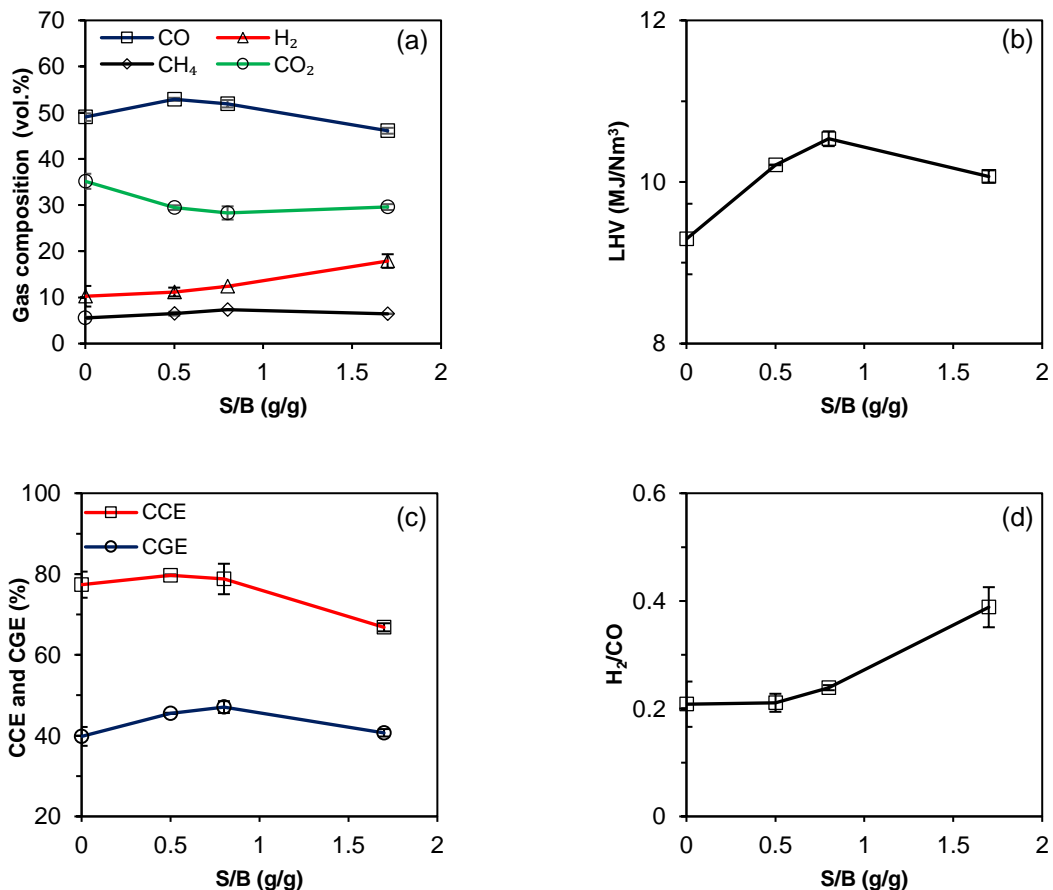


Figure III-3 – Effect of S/B ratio on the syngas composition (a), and on gasification performance parameters: LHV (b), CCE and CGE (c) and H₂/CO ratio (d).

The LHV of the syngas (Figure III-3 (b)) was estimated considering the contribution of the CO (12.63 MJ/Nm³), H₂ (10.78 MJ/Nm³) and CH₄ (35.88 MJ/Nm³) yields, by the low heating values from the company TU Wien represented in Waldheim et al. [36]. The LHV increased from 9.29 to 10.54 MJ/Nm³, when the S/B ratio increased from 0 to 0.8. For a S/B = 0.8, the LHV decreased to 10.07 MJ/Nm³, as the result of the decrease of CO and CH₄ yields, despite the increase in Hydrogen yield.

The CGE and CCE (Figure III-3 (c)) presented similar trends. The CGE increased from 39.81 to 47.06% and CCE remained close to 80% when increasing the S/B ratio from 0 to 0.8. For S/B = 0.8, the CGE and CCE decreased to 40.70 and 66.81%, respectively. These decreases can be explained by the decrease in the LHV of the syngas and the decrease in the carbon leaving the reactor through the syngas, respectively.

The H₂/CO ratio was enhanced by the increase of S/B ratio, because of the high increase in H₂ yield and the small CO yield variation.

III.2 Effect of gasification atmosphere and temperature on PMan gasification

III.2.1 Solid particles

For the PMan gasification, the PM was also collected in the cyclone and in thirteen-stage cascade impactor as in the case of WS gasification (see section III.1.1). Figure III-4 illustrates the effect of the gasification atmosphere and temperature on the PMs collected in the cyclone (a) and impactor (b).

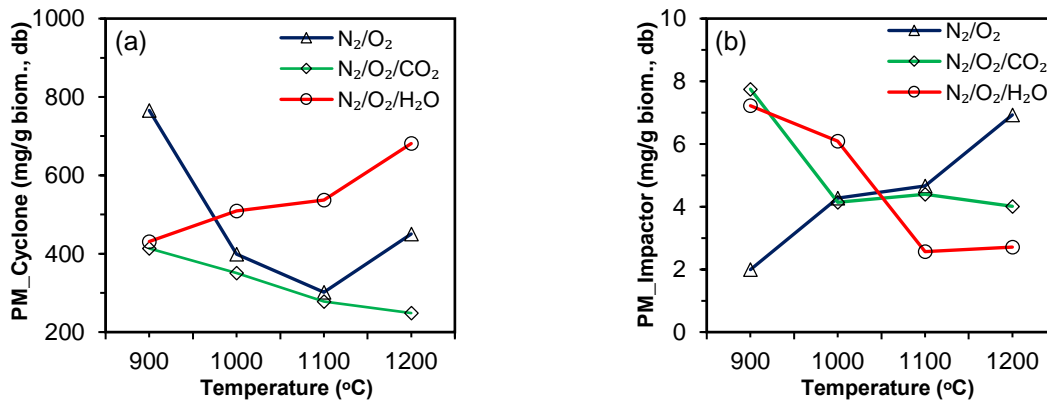


Figure III-4 - Influence of the gasification atmosphere and temperature on the PMs collected in the cyclone (a) and impactor (b).

By these plots, the quantity of PMs collected in cyclone and impactor is highly dependent of the gasification atmosphere. For the gasification with N₂/O₂, the solids collected in the cyclone have a minimum at 1100 °C, increasing at 1200 °C. However, for the smaller particles, collected in the impactor, the amount increased from 2 mg/g to 8 mg/g, approximately as the temperature increased from 900 to

1200 °C. When CO₂ was added to the atmosphere, the behavior of the number of particles generated was different. The quantity of PMs collected in the cyclone and impactor decreased, increasing the temperature, from 414.40 to 248.54 mg/g and from 7.75 to 4.01 mg/g, respectively. Moreover, at temperatures above 1000 °C, the quantity of small particles (< 10 μm) collected remained constant. On the other hand, when adding steam to the N₂/O₂ gasification atmosphere the opposite behavior was observed for the PMs collected in the cyclone. The number of particles larger than 10 μm increased from 431.17 to 681.16 mg/g, as temperature increased. The number of particles collected in the impactor decreased until 1100 °C and then remained almost constant at 1200 °C. It should be noted that during the particle collection period the number of small particles (< 10 μm) obtained is about 2 orders of magnitude lower than the larger particles (> 10 μm).

The particles are only differentiated by size. In order to characterize them as char and soot, it was necessary to perform SEM/EDS and burnout analysis. The table III-3 illustrates the SEM, EDS and burnout analysis for the PMs collected in cyclone for PMan gasification on a N₂/O₂/CO₂ atmosphere for each temperature examined. For the other two atmospheres the SEM images and results obtained by the two analysis are similar (see Appendix B).

Through the SEM images, for this gasification atmosphere, it is possible to observe porous particles with irregular shapes, being similar for the four temperatures analyzed. From the EDS analysis, a relatively low percentage of carbon, between 4 and 30 wt.%, and a high percentage of ash, between 39 and 47 wt.% were obtained, regardless the temperature studied. The burnout experiments show that the organic content present in the particles collected in cyclone was low and decreased from 16 wt.% to 5 wt.% when the temperature used during the gasification increased from 900 to 1200 °C. In this case, the EDS and the Burnout analysis also showed differences due to the quantity of particles used in each analysis.

The Figure III-5, presents the organic (a) and the ash content (b) obtained by the burnout analysis for all the gasification atmospheres and for each temperature examined.

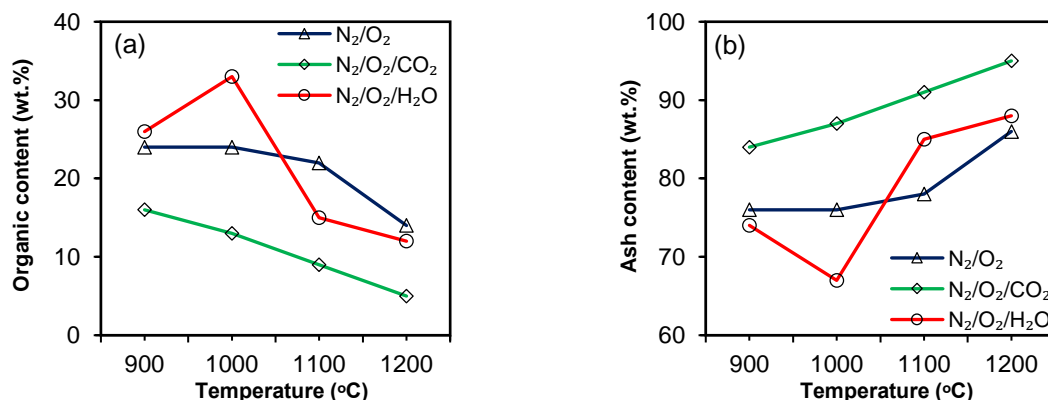


Figure III-5 - Organic (a) and ash content (b) of the PMs collected in the cyclone for all conditions analyzed.

It can be seen, in general, that the organic content present in these particles decreased as the temperature increased, with only a maximum observed at 1000 °C when steam is used with N₂ and O₂. The organic content was always lower, when CO₂ was used in the gasification atmosphere, than in the other atmospheres used. The minimum organic content obtained was 5 wt.% in an atmosphere with CO₂ at 1200 °C and the maximum was 33 wt.% when steam (H₂O) was used at 1000 °C. The behavior of the ash content in these particles is the opposite, obtaining a maximum of 95 wt.% at 1200 °C with CO₂ present in the atmosphere.

The SEM images and analysis of the data obtained by the EDS along with the burnout analysis revealed that the particles collected in cyclone are essentially char for all gasification atmospheres and for each temperature examined.

For the particles collected in thirteen-stage cascade impactor, SEM/EDS analysis were also performed. Only stages 5, 13 were analyzed for all conditions and the results for N₂/O₂/H₂O atmosphere are shown in Table III-4. For the upper stage (stage 13), the SEM image shows particles with different shapes and sizes and are dispersed. The EDS analysis shows a low carbon content, around 18 wt.%. From these characteristics, it can be assumed that these particles are mostly char. For stages 9 to 12, it was observed the same behavior, so it can be affirmed that these particles are essentially char.

For stage 5, SEM image shows a different particle morphology. The particles are small and uniform and are agglomerated. The EDS analysis presents a relatively higher content than the particles collected in the upper stages. The carbon content obtained at these stages was about 55 wt.%. The other stages, 1 to 8 show similar characteristics, so it can be assumed that the particles collected in stages 1 to 8 are essentially soot.

In short, the char particles are obtained in the cyclone and upper stages (9 to 13) of impactor, while soot is obtained in stages 1 to 8 of impactor. This separation of char and soot particles is valid for WS and PMan gasification.

The following plots, Figure III-6, show the total char (a) and soot (b) obtained. Given the alleged contamination of soot samples with ash, it is assumed that the soot particles are composed of 100% of carbon, and the remainder corresponds to the contamination. Thus, the soot obtained corresponds to 55% of the quantity of particles obtained in the appropriate stages of the impactor.

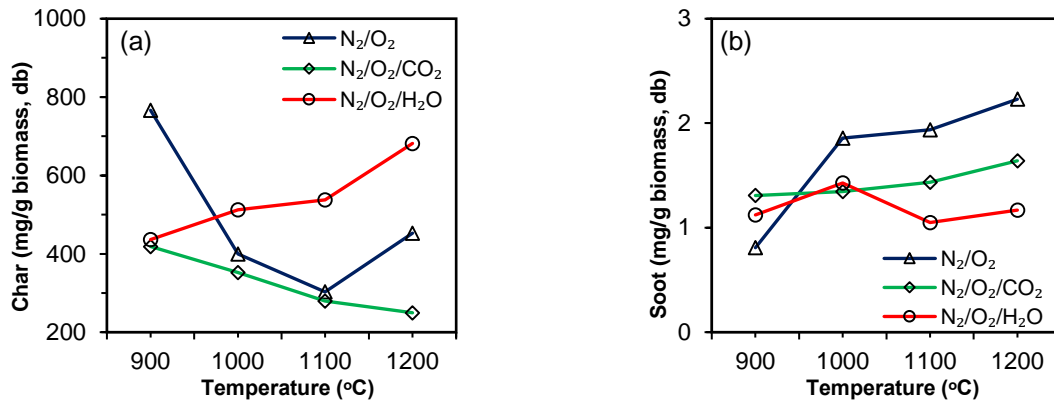
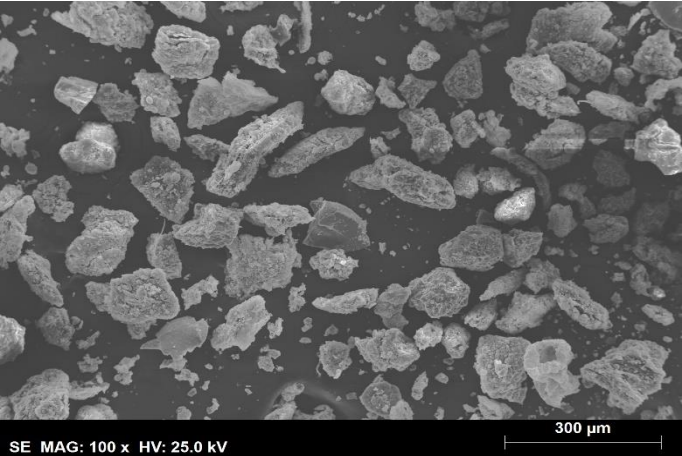
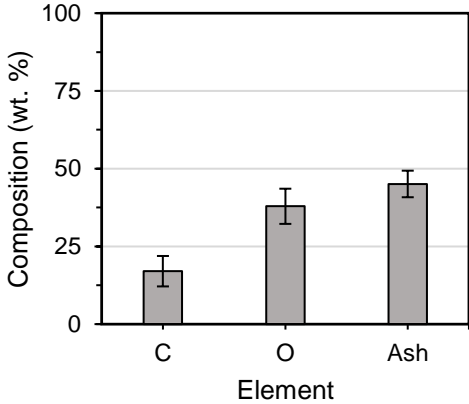
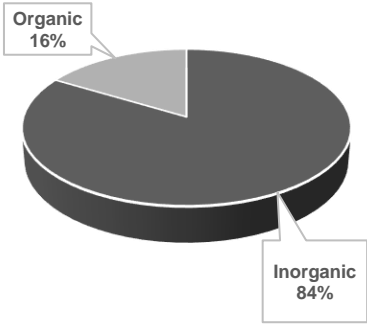
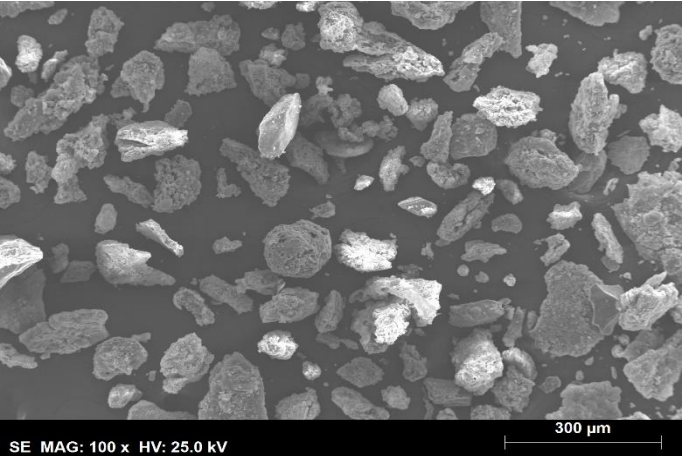
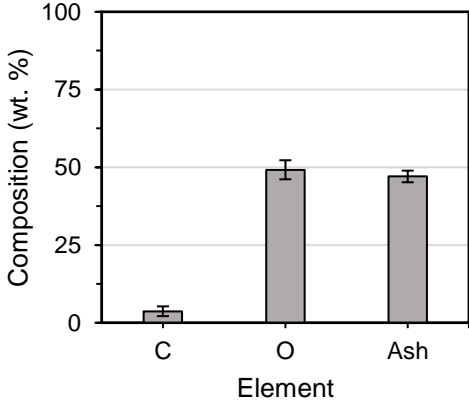
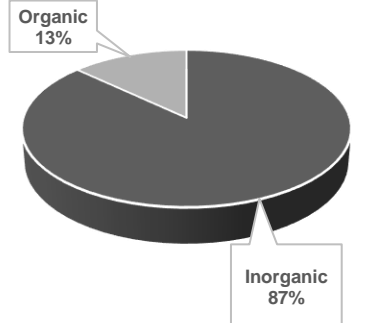


Figure III-6 – Amount of char (a) and soot (b) obtained in the gasification of PMan at different gasification atmospheres and temperatures.

From the Figure III-6 (a), the quantity of char collected mostly in cyclone depends greatly on the gasification atmosphere. The N₂/O₂/CO₂ atmosphere generated the minimal quantity of char particles at all temperatures studied, compared to other atmospheres. In this atmosphere, the amount of char particles decreased from 418.77 to 249.56 mg/g. In the case of soot particles, the N₂/O₂/H₂O atmosphere originated less soot particles at highest temperatures, 1100 and 1200 °C. Although the amount of soot generated is very small, it can be stated, by looking the Figure III-6 (b), that adding CO₂ or steam, the formation of soot particles is reduced above 1000 °C, when compared to N₂/O₂ atmosphere.

Table III-3 - SEM images, EDS analysis and burnout experiments for the PMs collected in the cyclone for the PMAN gasification (N₂/O₂/CO₂)

Tr (°C)	SEM Image	EDS Analysis	Burnout Experiment														
900		 <table border="1"> <caption>EDS Analysis Data (900°C)</caption> <thead> <tr> <th>Element</th> <th>Composition (wt. %)</th> </tr> </thead> <tbody> <tr> <td>C</td> <td>~18</td> </tr> <tr> <td>O</td> <td>~38</td> </tr> <tr> <td>Ash</td> <td>~45</td> </tr> </tbody> </table>	Element	Composition (wt. %)	C	~18	O	~38	Ash	~45	 <table border="1"> <caption>Burnout Experiment Data (900°C)</caption> <thead> <tr> <th>Component</th> <th>Percentage</th> </tr> </thead> <tbody> <tr> <td>Organic</td> <td>16%</td> </tr> <tr> <td>Inorganic</td> <td>84%</td> </tr> </tbody> </table>	Component	Percentage	Organic	16%	Inorganic	84%
Element	Composition (wt. %)																
C	~18																
O	~38																
Ash	~45																
Component	Percentage																
Organic	16%																
Inorganic	84%																
1000		 <table border="1"> <caption>EDS Analysis Data (1000°C)</caption> <thead> <tr> <th>Element</th> <th>Composition (wt. %)</th> </tr> </thead> <tbody> <tr> <td>C</td> <td>~5</td> </tr> <tr> <td>O</td> <td>~48</td> </tr> <tr> <td>Ash</td> <td>~47</td> </tr> </tbody> </table>	Element	Composition (wt. %)	C	~5	O	~48	Ash	~47	 <table border="1"> <caption>Burnout Experiment Data (1000°C)</caption> <thead> <tr> <th>Component</th> <th>Percentage</th> </tr> </thead> <tbody> <tr> <td>Organic</td> <td>13%</td> </tr> <tr> <td>Inorganic</td> <td>87%</td> </tr> </tbody> </table>	Component	Percentage	Organic	13%	Inorganic	87%
Element	Composition (wt. %)																
C	~5																
O	~48																
Ash	~47																
Component	Percentage																
Organic	13%																
Inorganic	87%																

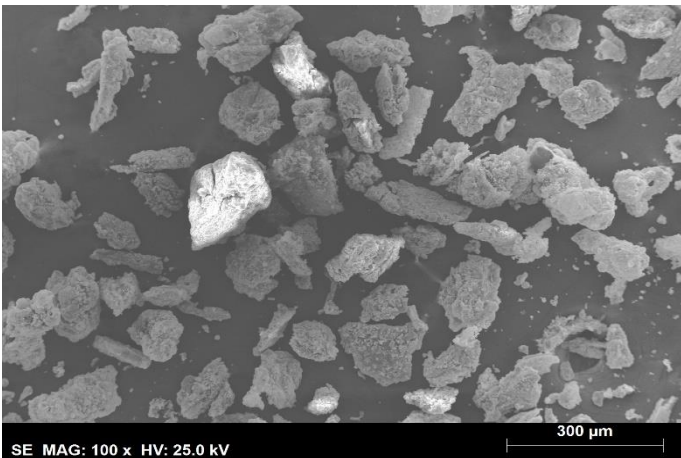
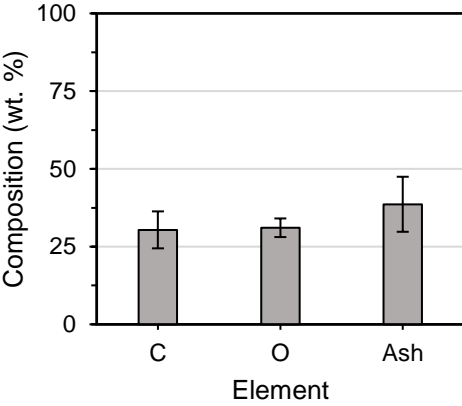
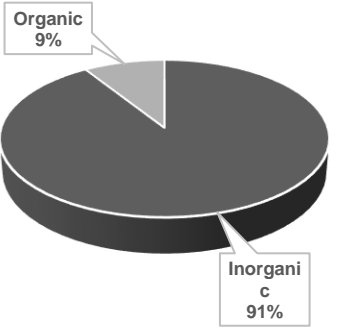
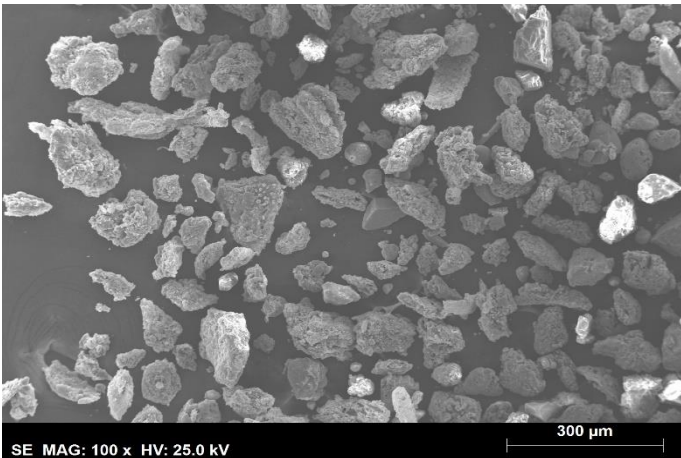
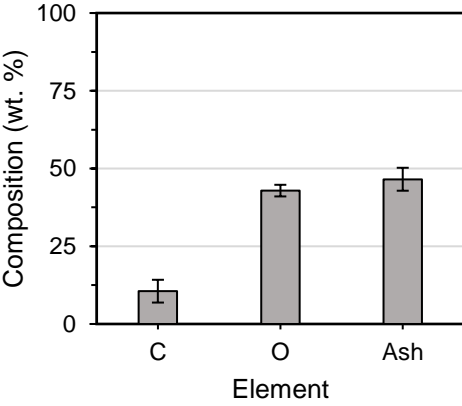
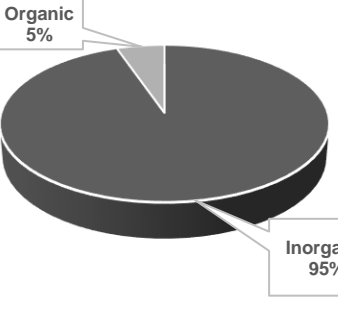
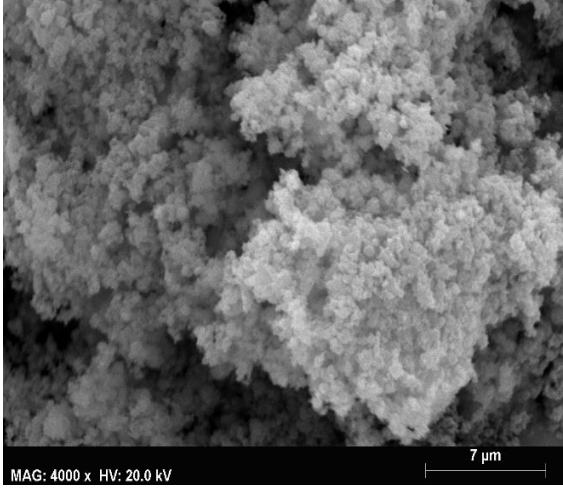
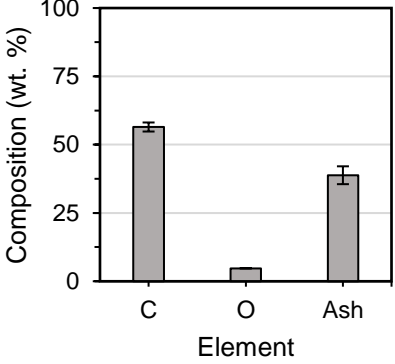
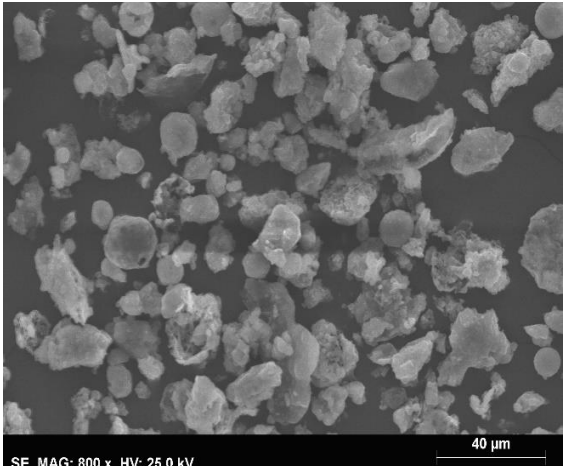
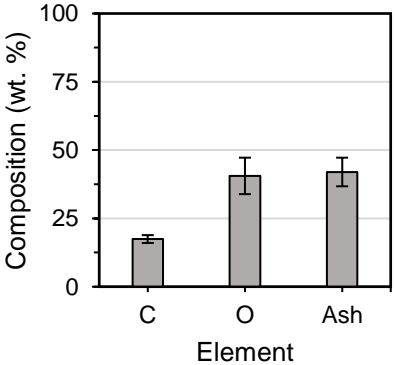
Tr (°C)	SEM Image	EDS Analysis	Burnout Experiment														
1100		 <table border="1"> <caption>EDS Analysis Data (1100°C)</caption> <thead> <tr> <th>Element</th> <th>Composition (wt. %)</th> </tr> </thead> <tbody> <tr> <td>C</td> <td>~30</td> </tr> <tr> <td>O</td> <td>~30</td> </tr> <tr> <td>Ash</td> <td>~40</td> </tr> </tbody> </table>	Element	Composition (wt. %)	C	~30	O	~30	Ash	~40	 <table border="1"> <caption>Burnout Experiment Data (1100°C)</caption> <thead> <tr> <th>Component</th> <th>Percentage</th> </tr> </thead> <tbody> <tr> <td>Organic</td> <td>9%</td> </tr> <tr> <td>Inorganic</td> <td>91%</td> </tr> </tbody> </table>	Component	Percentage	Organic	9%	Inorganic	91%
Element	Composition (wt. %)																
C	~30																
O	~30																
Ash	~40																
Component	Percentage																
Organic	9%																
Inorganic	91%																
1200		 <table border="1"> <caption>EDS Analysis Data (1200°C)</caption> <thead> <tr> <th>Element</th> <th>Composition (wt. %)</th> </tr> </thead> <tbody> <tr> <td>C</td> <td>~10</td> </tr> <tr> <td>O</td> <td>~45</td> </tr> <tr> <td>Ash</td> <td>~45</td> </tr> </tbody> </table>	Element	Composition (wt. %)	C	~10	O	~45	Ash	~45	 <table border="1"> <caption>Burnout Experiment Data (1200°C)</caption> <thead> <tr> <th>Component</th> <th>Percentage</th> </tr> </thead> <tbody> <tr> <td>Organic</td> <td>5%</td> </tr> <tr> <td>Inorganic</td> <td>95%</td> </tr> </tbody> </table>	Component	Percentage	Organic	5%	Inorganic	95%
Element	Composition (wt. %)																
C	~10																
O	~45																
Ash	~45																
Component	Percentage																
Organic	5%																
Inorganic	95%																

Table III-4 - SEM image and EDS analysis for PMan gasification, for two stages of impactor (Tr = 1000 °C, N₂/O₂/H₂O).

Stage	SEM Image	EDS Analysis								
5		 <table border="1"> <caption>EDS Analysis Data for Stage 5</caption> <thead> <tr> <th>Element</th> <th>Composition (wt. %)</th> </tr> </thead> <tbody> <tr> <td>C</td> <td>~58</td> </tr> <tr> <td>O</td> <td>~5</td> </tr> <tr> <td>Ash</td> <td>~37</td> </tr> </tbody> </table>	Element	Composition (wt. %)	C	~58	O	~5	Ash	~37
Element	Composition (wt. %)									
C	~58									
O	~5									
Ash	~37									
13		 <table border="1"> <caption>EDS Analysis Data for Stage 13</caption> <thead> <tr> <th>Element</th> <th>Composition (wt. %)</th> </tr> </thead> <tbody> <tr> <td>C</td> <td>~18</td> </tr> <tr> <td>O</td> <td>~42</td> </tr> <tr> <td>Ash</td> <td>~40</td> </tr> </tbody> </table>	Element	Composition (wt. %)	C	~18	O	~42	Ash	~40
Element	Composition (wt. %)									
C	~18									
O	~42									
Ash	~40									

III.2.2 Composition and quality of the producer gas

For PMan gasification, the producer gas was mainly formed by N_2 (~ 97%), as in the case of WS gasification. Figure III-7 illustrates the behavior of the gas species for each gasification atmosphere as a function of the operating temperature. The volume concentrations presented on the plots are normalized for a N_2 free producer gas.

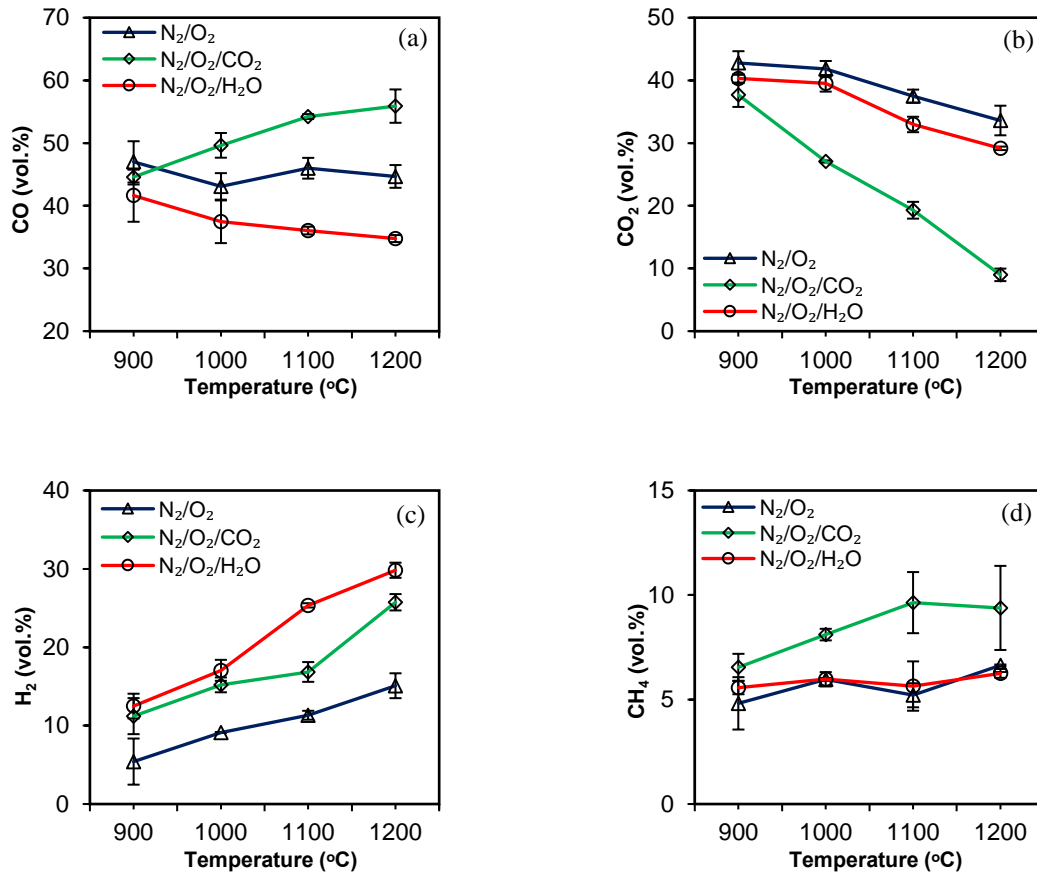


Figure III-7 – Effect of temperature and gasification atmosphere on CO, CO₂, H₂ and CH₄ yield for PMan gasification

For the temperature range examined, it was found that the CO₂ yield decreased while the H₂ yield significantly increased, between 900 and 1200 °C, for all the gasification atmospheres. However, the CO yield slightly decreased for N₂/O₂ and N₂/O₂/H₂O atmospheres and increased for the N₂/O₂/CO₂ atmosphere as the temperature increased from 900 to 1200 °C. The CH₄ yield had a small variation, but it was higher for the N₂/O₂/CO₂ atmosphere. At 1200 °C, the N₂/O₂/CO₂ atmosphere presented the highest CO yield and the smallest CO₂ yield with 55.89 and 8.98 vol.% respectively. The H₂ production was higher at 1200 °C for the N₂/O₂/H₂O atmosphere followed by N₂/O₂/CO₂ atmosphere and finally the N₂/O₂ with 29.83, 25.74 and 15.09 vol.%, respectively. Hussein et al. [37] studied the gasification of chicken manure in three gasifying media and also found similar behaviors for the gas species when increasing the temperature.

As the increase in temperature benefits the endothermic reactions, the reactions R5, R6 e R14 were promoted in these experiments. The water/gas reaction (R5, Table I-1) and methane steam reforming (R14, Table I-1) produces CO and H₂ consuming H₂O and CH₄ and the boudouard reaction (R6, Table I-1) consumes CO₂ producing CO. These endothermic reactions may explain the decrease in the CO₂ yield and the increase in H₂ yield. The water/gas shift reaction (R11, Table I-1) can explain the small variation of the CO yield, on N₂/O₂ and N₂/O₂/H₂O atmospheres, because it is slightly exothermic and occurs easily, and produces H₂ and CO₂ consuming CO and H₂O. The addition of CO₂ should promote the boudouard reaction, which results in higher CO production. The addition of steam should promote the water/gas reaction and the methane steam reforming reaction, but the water/gas shift reaction also occurs. This justifies the low CO yield variation and the larger amount of H₂ produced when compared to the other gasification atmospheres (N₂/O₂ and N₂/O₂/CO₂).

To predict the best condition that produces a high-quality syngas, the LHV, the CGE, the CCE and the H₂/CO were examined. Figure III-8 illustrates the influence of the temperature and gasification atmosphere on these performance parameters.

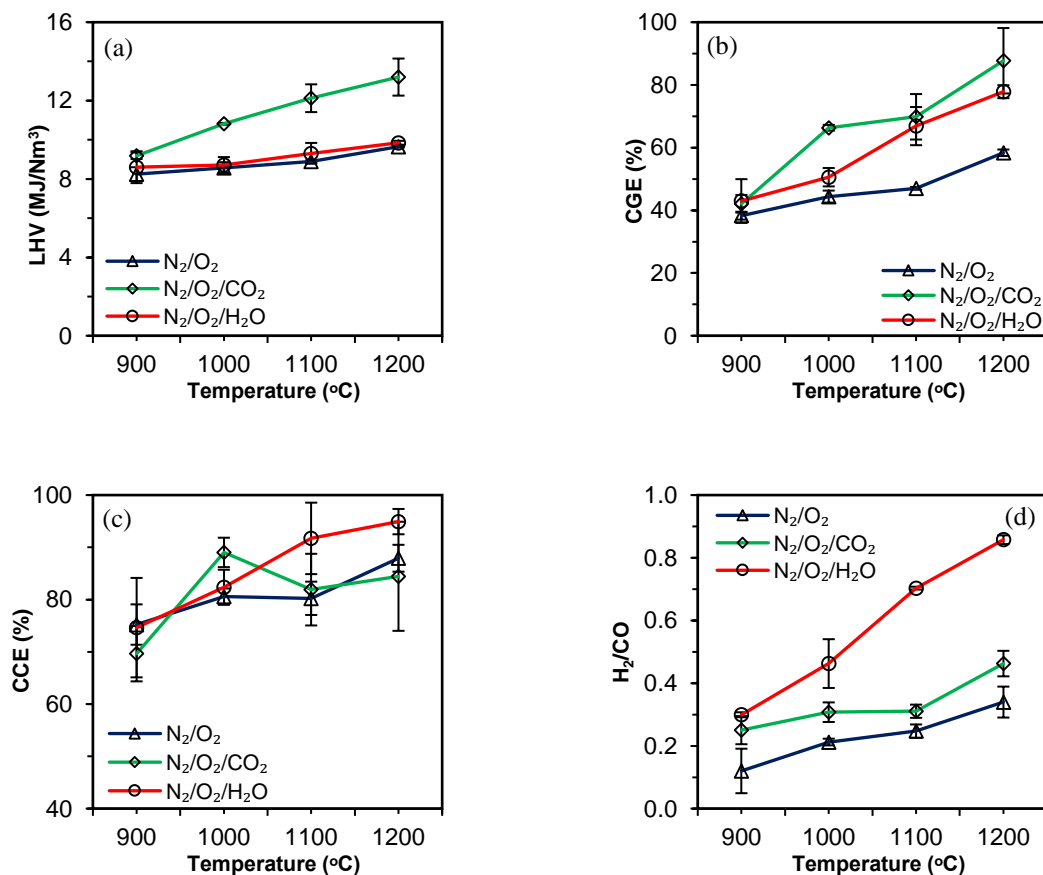


Figure III-8 – Effect of temperature and gasification atmosphere on gasification performance indicators: LHV (a), CGE (b), CCE (c) and H₂/CO (d).

The LHV (Figure III-8 (a)), increased for an operating temperature between 900 and 1200 °C for the three gasification atmospheres, but it is more pronounced in the atmosphere with CO₂. In this atmosphere, the LHV increased from 9.19 to 13.20 MJ/Nm³. This result can be attributed to the fact that

CO yield and CH₄ yield are more pronounced in this atmosphere than in the others. In N₂/O₂ and N₂/O₂/H₂O atmospheres the LHV slightly increased from about 8.60 to 9.85 MJ/Nm³.

As the temperature increased from 900 to 1200 °C, CGE (Figure III-8 (b)) also increased for all gasification atmospheres examined. At 900 °C, the CGE was about 40%, similar for the three atmospheres while for higher temperatures the values were different. At 1200 °C, the CGE was higher for the atmosphere with CO₂, followed by the atmosphere with steam and finally for the N₂/O₂ atmosphere with 87.71, 77.84 and 58.37% respectively. This tendency could be explained by the increase of the LHV for the N₂/O₂/CO₂ atmosphere and by the increase in the syngas yield for the N₂/O₂/H₂O that is higher than in N₂/O₂ atmosphere.

In general, the CCE (Figure III-8 (c)), increased with temperature for all the gasification atmospheres. At 1200 °C, the CCE was higher for the N₂/O₂/H₂O atmosphere with 94.92% because the syngas yield was more pronounced in this atmosphere. At 900 °C, the CCE was identical for the N₂/O₂ and N₂/O₂/H₂O, about 75% and slightly lower for the N₂/O₂/CO₂ atmosphere, about 69.65%.

Due to the high increase in the H₂ yield and a small variation of the CO yield for the three gasification atmospheres, the H₂/CO ratio was enhanced, increasing the temperature from 900 to 1200 °C. At 1200 °C, for instance, the H₂/CO ratio was maximum for the N₂/O₂/H₂O atmosphere, because of high H₂ yield and a small CO yield, reaching 0.86.

IV. Closure

IV.1 Conclusions

In the present work, two types of biomass were used. The effect of S/B ratio was studied in wheat straw gasification while the influence of temperature and gasification atmosphere were analyzed in the gasification of pig manure.

In wheat straw gasification, varying the S/B ratio at a constant temperature, it can be concluded that higher S/B ratio (up to the maximum analyzed), less char and soot are formed. Thus, increasing the steam content in the gasification atmosphere reduces the number of solid particles formed and increases the quantity of volatiles formed. The percentage of carbon present in the originated char particles (see their burnout analysis) also reduces increasing the S/B ratio, i.e., the conversion of carbon present in the biomass is increased with the increase of steam in the gasification atmosphere. Since soot is an undesirable product, WS gasification at S/B = 1.7 can be a good solution to decrease its production. Results for the syngas composition and quality indicate that higher S/B ratios result in higher H₂ yield and higher H₂/CO while the LHV, CCE and CGE present a maximum value at S/B = 0.8.

In the case of pig manure gasification, it is concluded that the number of solid particles formed depends significantly on the gasification atmosphere used. If the objective of gasification is to generate the smallest amount of char particles, it can be concluded that the atmosphere with CO₂ at 1200 °C is the best. In order to reduce the quantity of soot formed (an undesirable product), an atmosphere with steam at high temperatures should be used, although the amount of soot is always reduced in all cases. However, further tests are required for each condition to verify this trend. The syngas composition obtained in the gasification of pig manure showed that the CO and CH₄ yields are higher for a gasification atmosphere with CO₂ while the CO₂ and H₂ yields are higher for an N₂/O₂ atmosphere and for an atmosphere with steam, respectively. The LHV and the CGE were higher for the atmosphere with CO₂ addition, while the CCE and the H₂/CO were higher for the atmosphere with steam addition, at 1200 °C.

IV.2 Future work

In this master thesis, the impact of various operating conditions on biomass gasification in a drop tube reactor was studied. The variation of the S/B ratio at a constant temperature, the influence of steam or carbon dioxide addition to a gasification atmosphere at different temperatures and the use of two types of biomass from different sources were the parameters studied throughout this work.

For future work, it would be interesting to study the influence of other operating parameters, such as, the biomass particle size, the residence time or the impregnation of biomass with inorganics. These parameters may affect the amount and size of the resulting solid particles as well their composition and the syngas composition and quality. Another product obtained in the gasification process is tar, a black and viscous fluid, undesirable for downstream applications. It would be interesting to study its formation and composition in different gasification atmospheres with different types of biomass. The gas produced

during the gasification process is also important to examine as there are several downstream applications. To improve the quality of the gas obtained, further investigation on syngas cleaning technologies would also be interesting.

V. References

- [1] P. Basu, *Biomass gasification and pyrolysis: Practical design and theory*, 1st ed., Elsevier Inc., 2010.
- [2] WBA global bioenergy statistics, World Bioenergy Association, 2018.
- [3] M. La Villetta, M. Costa, and N. Massarotti, Modelling approaches to biomass gasification: A review with emphasis on the stoichiometric method, *Renew. Sustain. Energy Rev.*, vol. 74, no. February, pp. 71–88, 2017.
- [4] V. S. Sikarwar, M. Zhao, P. S. Fennell, N. Shah, and E. J. Anthony, Progress in biofuel production from gasification, *Prog. Energy Combust. Sci.*, vol. 61, pp. 189–248, 2017.
- [5] J. J. Hernández, R. Ballesteros, and G. Aranda, Characterisation of tars from biomass gasification: Effect of the operating conditions, *Energy*, vol. 50, pp. 333–342, 2013.
- [6] S. K. Sansaniwal, K. Pal, M. A. Rosen, and S. K. Tyagi, Recent advances in the development of biomass gasification technology: A comprehensive review, *Renew. Sustain. Energy Rev.*, vol. 72, no. December 2015, pp. 363–384, 2017.
- [7] V. Lopes, *Particulate matter from biomass combustion in a Drop Tube Furnace*. Master Thesis in Mechanical Engineering, Instituto Superior Técnico, 2016.
- [8] E. R. Widjaya, G. Chen, L. Bowtell, and C. Hills, Gasification of non-woody biomass: A literature review, *Renew. Sustain. Energy Rev.*, vol. 89, no. September 2016, pp. 184–193, 2018.
- [9] S. De, A. K. Agarwal, V. S. Moholkar, B. Thallada, *Coal and Biomass Gasification*, 2018.
- [10] M. Lucia, V. Rios, A. M. González, E. Eduardo, S. Lora, and O. Agustin, Biomass and Bioenergy Reduction of tar generated during biomass gasification : A review, *Biomass and Bioenergy*, vol. 108, no. November 2017, pp. 345–370, 2018.
- [11] N. Abdoulmoumine, S. Adhikari, A. Kulkarni, and S. Chattanathan, A review on biomass gasification syngas cleanup, *Appl. Energy*, vol. 155, pp. 294–307, 2015.
- [12] C. Higman, *Syngas Database: 2018 Update*, 2018.
- [13] B. Khiari, M. Jeguirim, L. Limousy, and S. Bennici, Biomass derived chars for energy applications, *Renew. Sustain. Energy Rev.*, vol. 108, no. November 2018, pp. 253–273, 2019.
- [14] V. Benedetti, F. Patuzzi, and M. Baratieri, Characterization of char from biomass gasification and its similarities with activated carbon in adsorption applications, *Appl. Energy*, no. August, pp. 1–8, 2017.
- [15] J. J. Hernández, M. Lapuerta, and E. Monedero, Characterisation of residual char from biomass gasification: effect of the gasifier operating conditions, *J. Clean. Prod.*, vol. 138, pp. 83–93, 2016.

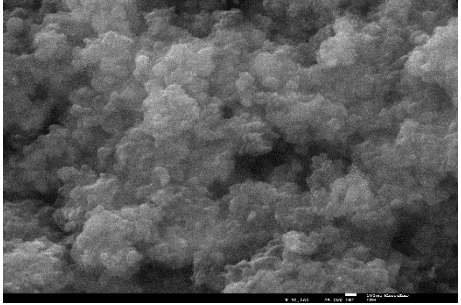
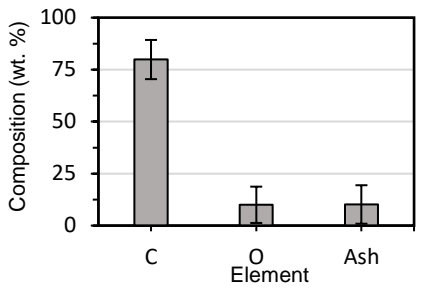
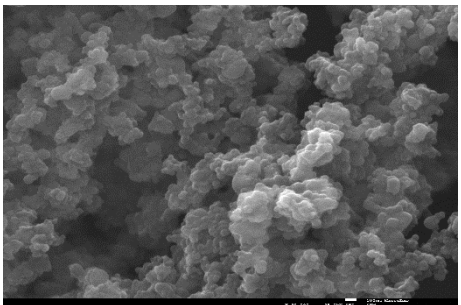
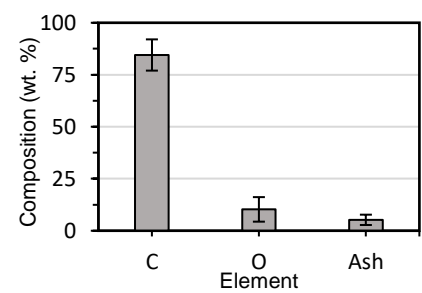
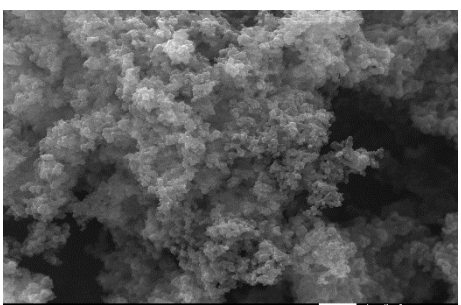
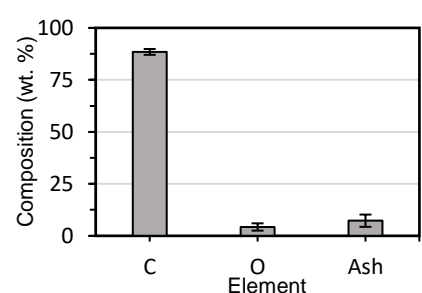
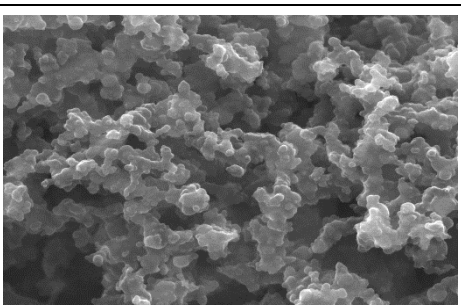
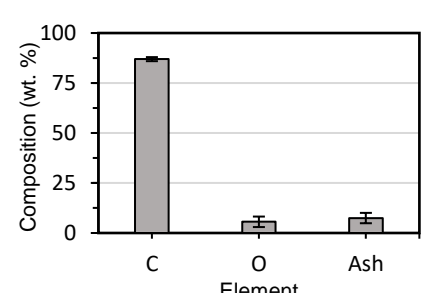
- [16] S. Anis and Z. A. Zainal, Tar reduction in biomass producer gas via mechanical, catalytic and thermal methods: A review, *Renew. Sustain. Energy Rev.*, vol. 15, no. 5, pp. 2355–2377, 2011.
- [17] T.A. Milne and R. J. Evans, Biomass gasifier "tars": their nature, formation, and conversion; Report NREL/TP-570-25357; National Renewable Energy Laboratory (NREL): Golden, CO, 1998, Golden Color. Natl. Renew. Energy Lab., no. November, p. v, 1998.
- [18] B. R. Stanmore, J. F. Brilhac, and P. Gilot, The oxidation of soot: A review of experiments, mechanisms and models, *Carbon N. Y.*, vol. 39, no. 15, pp. 2247–2268, 2001.
- [19] V. Kurian, Asphaltene gasification : Soot formation and metal distribution, 2016.
- [20] D. Neves, H. Thunman, A. Matos, L. Tarelho, and A. Gómez-Barea, Characterization and prediction of biomass pyrolysis products, *Prog. Energy Combust. Sci.*, vol. 37, no. 5, pp. 611–630, 2011.
- [21] N. A. Samiran, M. N. M. Jaafar, J. H. Ng, S. S. Lam, and C. T. Chong, Progress in biomass gasification technique - With focus on Malaysian palm biomass for syngas production, *Renew. Sustain. Energy Rev.*, vol. 62, pp. 1047–1062, 2016.
- [22] S. Septien, S. Valin, M. Peyrot, B. Spindler, and S. Salvador, Influence of steam on gasification of millimetric wood particles in a drop tube reactor : Experiments and modelling, *Fuel*, vol. 103, pp. 1080–1089, 2013.
- [23] Y. Zhang, S. Kajitani, M. Ashizawa, and Y. Oki, Tar destruction and coke formation during rapid pyrolysis and gasification of biomass in a drop-tube furnace, *Fuel*, vol. 89, no. 2, pp. 302–309, 2010.
- [24] K. Qin, W. Lin, P. A. Jensen, and A. D. Jensen, High-temperature entrained flow gasification of biomass, *Fuel*, vol. 93, pp. 589–600, 2012.
- [25] J. Zhou, Q. Chen, H. Zhao, X. Cao, Q. Mei, Z. Luo, K. Cen, Biomass-oxygen gasification in a high-temperature entrained-flow gasifier, *Biotechnol. Adv.*, vol. 27, no. 5, pp. 606–611, 2009.
- [26] J. Billaud, S. Valin, M. Peyrot, and S. Salvador, Influence of H₂O, CO₂ and O₂ addition on biomass gasification in entrained flow reactor conditions: Experiments and modelling, *Fuel*, vol. 166, no. November, pp. 166–178, 2016.
- [27] K. Qin, P. A. Jensen, W. Lin, and A. D. Jensen, Biomass gasification behavior in an entrained flow reactor: Gas product distribution and soot formation, *Energy and Fuels*, vol. 26, no. 9, pp. 5992–6002, 2012.
- [28] T. Ogi, M. Nakanishi, Y. Fukuda, and K. Matsumoto, Gasification of oil palm residues (empty fruit bunch) in an entrained-flow gasifier, *Fuel*, vol. 104, pp. 28–35, 2013.
- [29] H. Yu, Z. Li, X. Yang, L. Jiang, Z. Zhang, and D. Chen, Experimental research on oxygen-

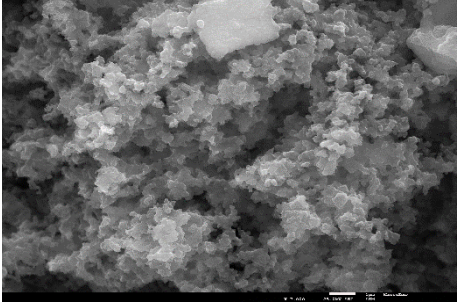
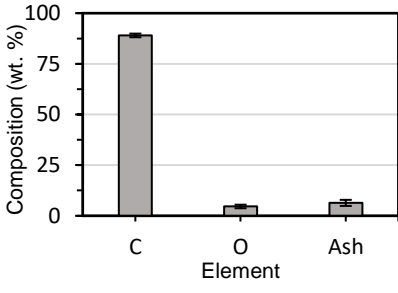
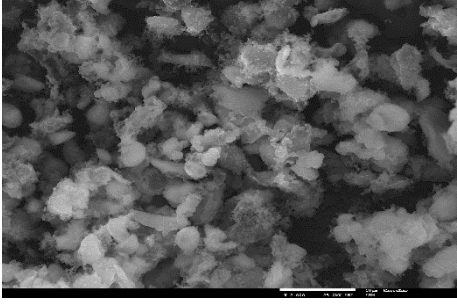
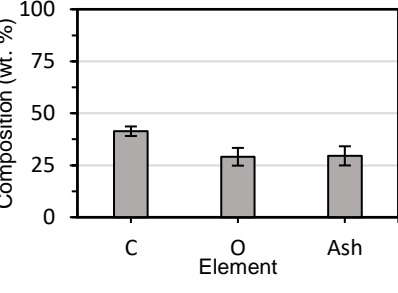
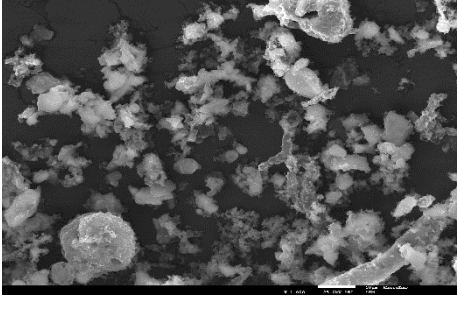
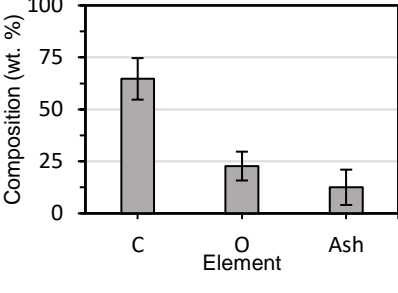
- enriched gasification of straw in an entrained-flow gasifier, *J. Renew. Sustain. Energy*, vol. 5, no. 5, pp. 1–13, 2013.
- [30] F. Weiland, H. Wiinikka, H. Hedman, J. Wennebro, E. Pettersson, and R. Gebart, Influence of process parameters on the performance of an oxygen blown entrained flow biomass gasifier, *Fuel*, vol. 153, pp. 510–519, 2015.
- [31] J. J. Hernández, G. Aranda-Almansa, and A. Bula, Gasification of biomass wastes in an entrained flow gasifier: Effect of the particle size and the residence time, *Fuel Process. Technol.*, vol. 91, no. 6, pp. 681–692, 2010.
- [32] M. Lapuerta, J. J. Hernández, A. Pazo, and J. López, Gasification and co-gasification of biomass wastes: Effect of the biomass origin and the gasifier operating conditions, *Fuel Process. Technol.*, vol. 89, pp. 828–837, 2008.
- [33] J. J. Hernández, G. Aranda, J. Barba, and J. M. Mendoza, Effect of steam content in the air-steam flow on biomass entrained flow gasification, *Fuel Process. Technol.*, vol. 99, pp. 43–55, 2012.
- [34] J. G. Brammer and A. V. Bridgwater, The influence of feedstock drying on the performance and economics of a biomass gasifier - Engine CHP system, *Biomass and Bioenergy*, vol. 22, no. 4, pp. 271–281, 2002.
- [35] Dekati Low Pressure Impactor user manual ver. 3.4, 2007.
- [36] L. Waldheim, T. Nilsson, Heating value of gases from biomass gasification, *IEA Bioenergy Agreement*, 2001.
- [37] M. S. Hussein, K. G. Burra, R. S. Amano, and A. K. Gupta, Temperature and gasifying media effects on chicken manure pyrolysis and gasification, *Fuel*, vol. 202, pp. 36–45, 2017.

VI. Appendix

VI.1 Appendix A – Particulate Matter in the Impactor

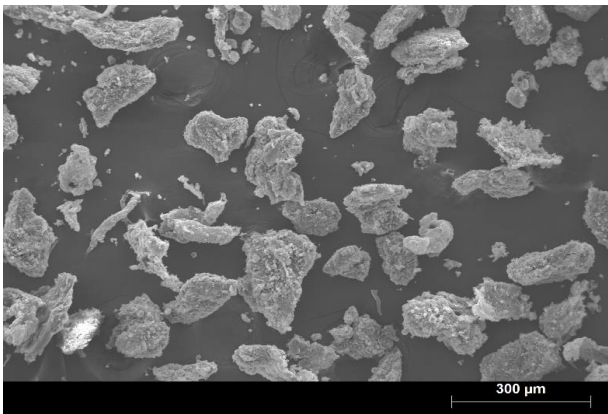
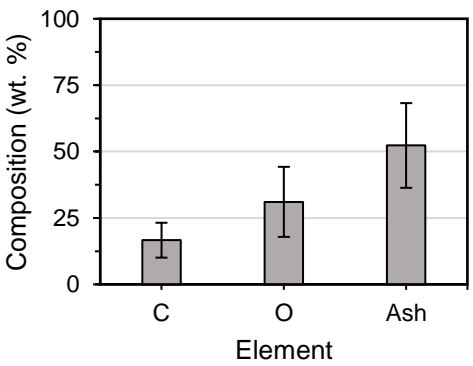
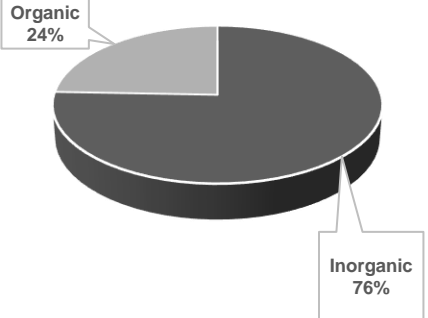
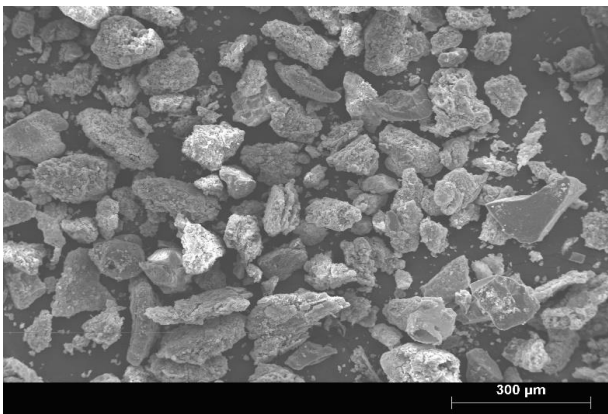
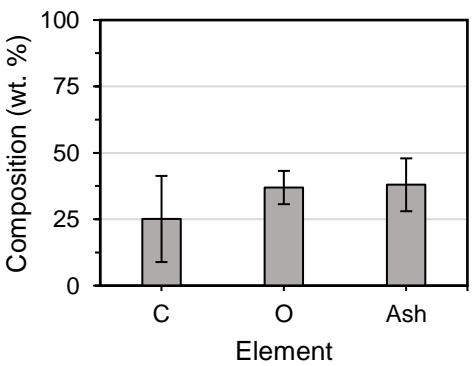
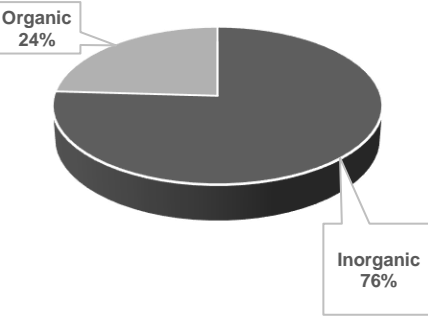
Table VI-1 - SEM images and EDS analysis for WS gasification, for the remaining stages of thirteen stage impactor (Tr = 1000 °C, S/B = 0.8).

Stage	SEM Image	EDS Analysis
1		 Composition (wt. %) vs Element (C, O, Ash)
2		 Composition (wt. %) vs Element (C, O, Ash)
4		 Composition (wt. %) vs Element (C, O, Ash)
6		 Composition (wt. %) vs Element (C, O, Ash)

Stage	SEM Image	EDS Analysis								
7		 <table border="1"> <caption>EDS Analysis Data for Stage 7</caption> <thead> <tr> <th>Element</th> <th>Composition (wt. %)</th> </tr> </thead> <tbody> <tr> <td>C</td> <td>~90</td> </tr> <tr> <td>O</td> <td>~5</td> </tr> <tr> <td>Ash</td> <td>~5</td> </tr> </tbody> </table>	Element	Composition (wt. %)	C	~90	O	~5	Ash	~5
Element	Composition (wt. %)									
C	~90									
O	~5									
Ash	~5									
11		 <table border="1"> <caption>EDS Analysis Data for Stage 11</caption> <thead> <tr> <th>Element</th> <th>Composition (wt. %)</th> </tr> </thead> <tbody> <tr> <td>C</td> <td>~40</td> </tr> <tr> <td>O</td> <td>~28</td> </tr> <tr> <td>Ash</td> <td>~28</td> </tr> </tbody> </table>	Element	Composition (wt. %)	C	~40	O	~28	Ash	~28
Element	Composition (wt. %)									
C	~40									
O	~28									
Ash	~28									
13		 <table border="1"> <caption>EDS Analysis Data for Stage 13</caption> <thead> <tr> <th>Element</th> <th>Composition (wt. %)</th> </tr> </thead> <tbody> <tr> <td>C</td> <td>~65</td> </tr> <tr> <td>O</td> <td>~22</td> </tr> <tr> <td>Ash</td> <td>~12</td> </tr> </tbody> </table>	Element	Composition (wt. %)	C	~65	O	~22	Ash	~12
Element	Composition (wt. %)									
C	~65									
O	~22									
Ash	~12									

VI.2 Appendix B - Particulate Matter in cyclone for Pig Manure gasification

Table VI-2 - SEM images, EDS analysis and Burnout for PMs collected in cyclone for PMAN gasification (N₂/O₂).

Tr (°C)	SEM Image	EDS Analysis	Burnout Experiment														
900		 <table border="1"> <caption>EDS Analysis Data (900°C)</caption> <thead> <tr> <th>Element</th> <th>Composition (wt. %)</th> </tr> </thead> <tbody> <tr> <td>C</td> <td>~18</td> </tr> <tr> <td>O</td> <td>~32</td> </tr> <tr> <td>Ash</td> <td>~50</td> </tr> </tbody> </table>	Element	Composition (wt. %)	C	~18	O	~32	Ash	~50	 <table border="1"> <caption>Burnout Experiment Data (900°C)</caption> <thead> <tr> <th>Component</th> <th>Percentage</th> </tr> </thead> <tbody> <tr> <td>Organic</td> <td>24%</td> </tr> <tr> <td>Inorganic</td> <td>76%</td> </tr> </tbody> </table>	Component	Percentage	Organic	24%	Inorganic	76%
Element	Composition (wt. %)																
C	~18																
O	~32																
Ash	~50																
Component	Percentage																
Organic	24%																
Inorganic	76%																
1000		 <table border="1"> <caption>EDS Analysis Data (1000°C)</caption> <thead> <tr> <th>Element</th> <th>Composition (wt. %)</th> </tr> </thead> <tbody> <tr> <td>C</td> <td>~25</td> </tr> <tr> <td>O</td> <td>~38</td> </tr> <tr> <td>Ash</td> <td>~37</td> </tr> </tbody> </table>	Element	Composition (wt. %)	C	~25	O	~38	Ash	~37	 <table border="1"> <caption>Burnout Experiment Data (1000°C)</caption> <thead> <tr> <th>Component</th> <th>Percentage</th> </tr> </thead> <tbody> <tr> <td>Organic</td> <td>24%</td> </tr> <tr> <td>Inorganic</td> <td>76%</td> </tr> </tbody> </table>	Component	Percentage	Organic	24%	Inorganic	76%
Element	Composition (wt. %)																
C	~25																
O	~38																
Ash	~37																
Component	Percentage																
Organic	24%																
Inorganic	76%																

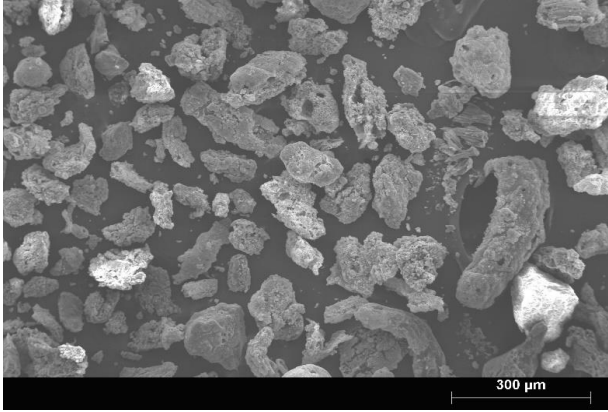
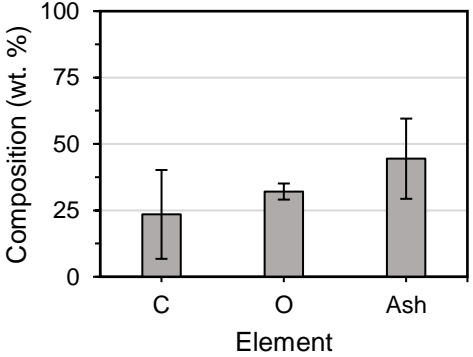
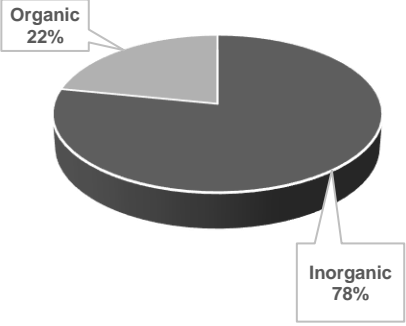
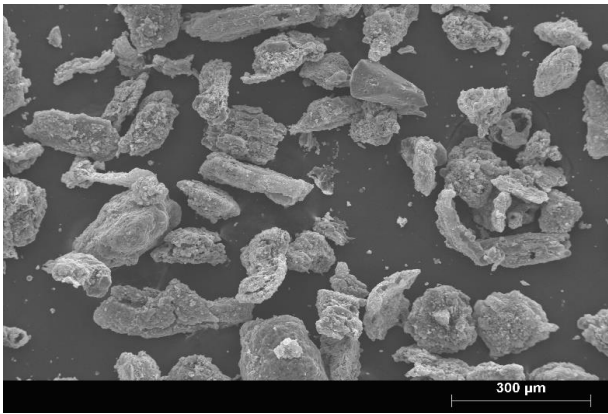
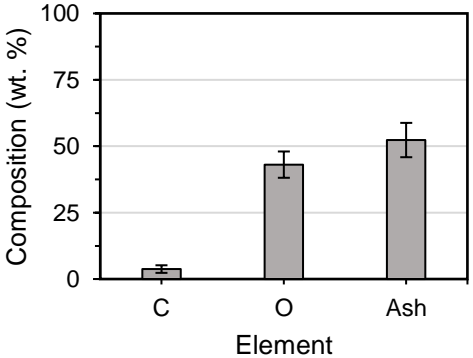
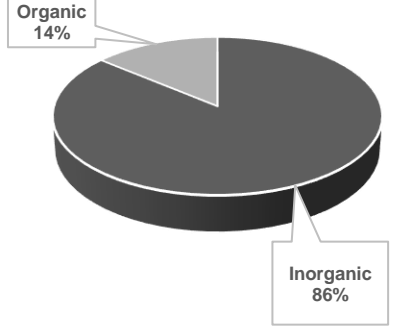
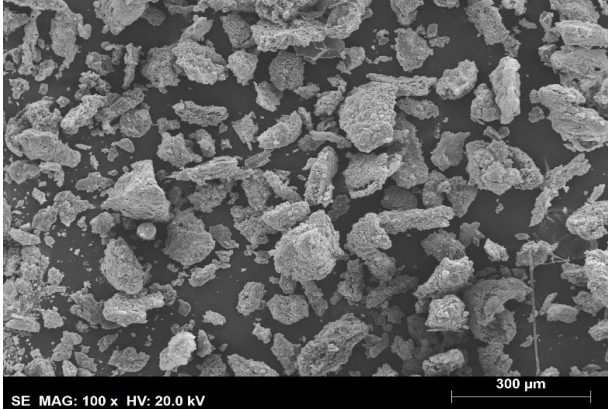
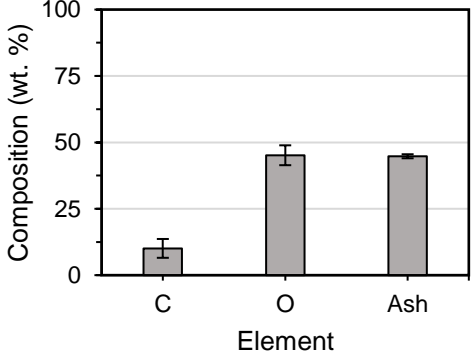
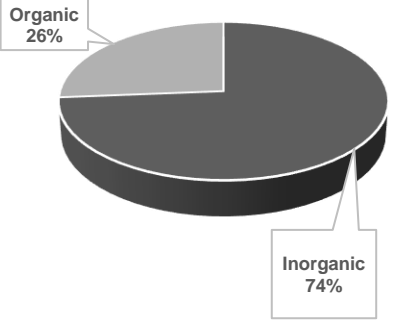

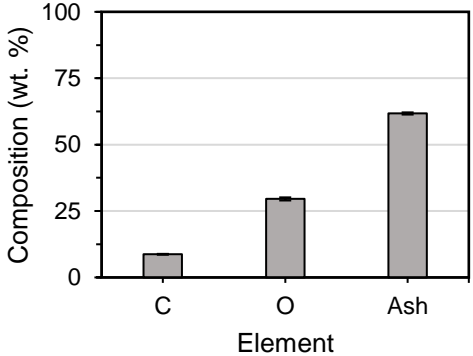
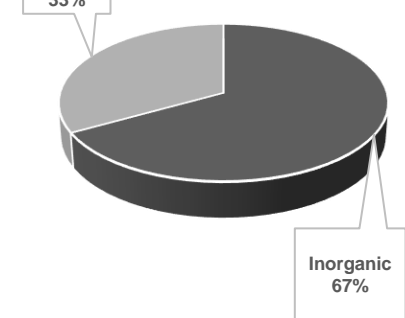
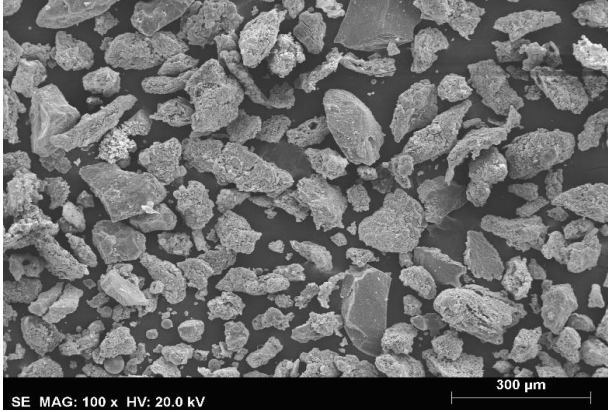
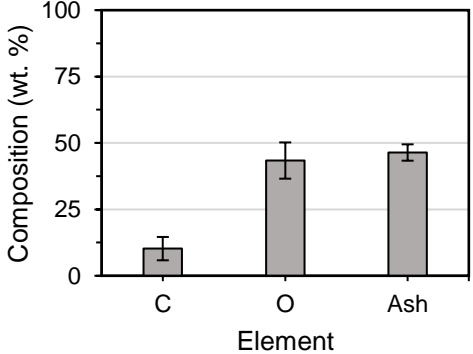
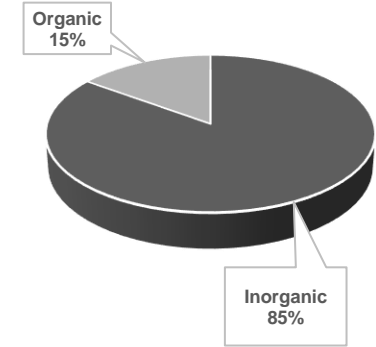
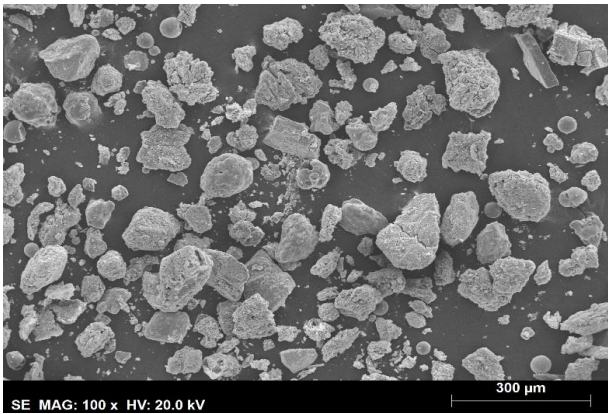
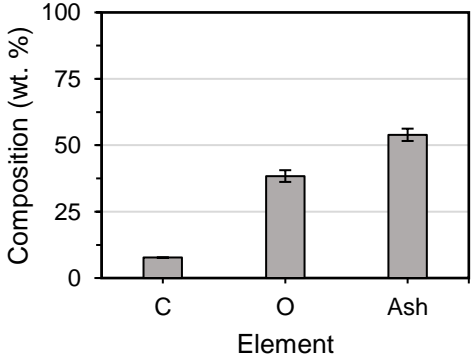
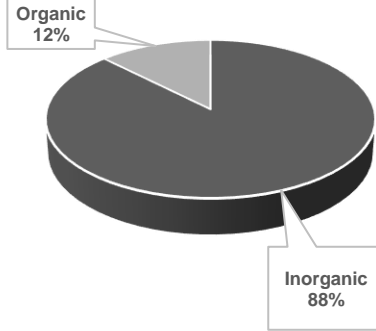
Tr (°C)	SEM Image	EDS Analysis	Burnout Experiment														
1100		 <table border="1"> <caption>EDS Analysis Data (1100°C)</caption> <thead> <tr> <th>Element</th> <th>Composition (wt. %)</th> </tr> </thead> <tbody> <tr> <td>C</td> <td>~23</td> </tr> <tr> <td>O</td> <td>~32</td> </tr> <tr> <td>Ash</td> <td>~45</td> </tr> </tbody> </table>	Element	Composition (wt. %)	C	~23	O	~32	Ash	~45	 <table border="1"> <caption>Burnout Experiment Data (1100°C)</caption> <thead> <tr> <th>Component</th> <th>Percentage</th> </tr> </thead> <tbody> <tr> <td>Organic</td> <td>22%</td> </tr> <tr> <td>Inorganic</td> <td>78%</td> </tr> </tbody> </table>	Component	Percentage	Organic	22%	Inorganic	78%
Element	Composition (wt. %)																
C	~23																
O	~32																
Ash	~45																
Component	Percentage																
Organic	22%																
Inorganic	78%																
1200		 <table border="1"> <caption>EDS Analysis Data (1200°C)</caption> <thead> <tr> <th>Element</th> <th>Composition (wt. %)</th> </tr> </thead> <tbody> <tr> <td>C</td> <td>~3</td> </tr> <tr> <td>O</td> <td>~43</td> </tr> <tr> <td>Ash</td> <td>~54</td> </tr> </tbody> </table>	Element	Composition (wt. %)	C	~3	O	~43	Ash	~54	 <table border="1"> <caption>Burnout Experiment Data (1200°C)</caption> <thead> <tr> <th>Component</th> <th>Percentage</th> </tr> </thead> <tbody> <tr> <td>Organic</td> <td>14%</td> </tr> <tr> <td>Inorganic</td> <td>86%</td> </tr> </tbody> </table>	Component	Percentage	Organic	14%	Inorganic	86%
Element	Composition (wt. %)																
C	~3																
O	~43																
Ash	~54																
Component	Percentage																
Organic	14%																
Inorganic	86%																

Table VI-3 - SEM images, EDS analysis and Burnout for PMs collected in cyclone for PMAN gasification (N₂/O₂/CO₂).

Tr (°C)	SEM Image	EDS Analysis	Burnout Experiment														
900		 <table border="1"> <caption>EDS Analysis Data (900°C)</caption> <thead> <tr> <th>Element</th> <th>Composition (wt. %)</th> </tr> </thead> <tbody> <tr> <td>C</td> <td>~10</td> </tr> <tr> <td>O</td> <td>~45</td> </tr> <tr> <td>Ash</td> <td>~45</td> </tr> </tbody> </table>	Element	Composition (wt. %)	C	~10	O	~45	Ash	~45	 <table border="1"> <caption>Burnout Experiment Data (900°C)</caption> <thead> <tr> <th>Component</th> <th>Percentage</th> </tr> </thead> <tbody> <tr> <td>Organic</td> <td>26%</td> </tr> <tr> <td>Inorganic</td> <td>74%</td> </tr> </tbody> </table>	Component	Percentage	Organic	26%	Inorganic	74%
Element	Composition (wt. %)																
C	~10																
O	~45																
Ash	~45																
Component	Percentage																
Organic	26%																
Inorganic	74%																
1000		 <table border="1"> <caption>EDS Analysis Data (1000°C)</caption> <thead> <tr> <th>Element</th> <th>Composition (wt. %)</th> </tr> </thead> <tbody> <tr> <td>C</td> <td>~10</td> </tr> <tr> <td>O</td> <td>~30</td> </tr> <tr> <td>Ash</td> <td>~60</td> </tr> </tbody> </table>	Element	Composition (wt. %)	C	~10	O	~30	Ash	~60	 <table border="1"> <caption>Burnout Experiment Data (1000°C)</caption> <thead> <tr> <th>Component</th> <th>Percentage</th> </tr> </thead> <tbody> <tr> <td>Organic</td> <td>33%</td> </tr> <tr> <td>Inorganic</td> <td>67%</td> </tr> </tbody> </table>	Component	Percentage	Organic	33%	Inorganic	67%
Element	Composition (wt. %)																
C	~10																
O	~30																
Ash	~60																
Component	Percentage																
Organic	33%																
Inorganic	67%																

Tr (°C)	SEM Image	EDS Analysis	Burnout Experiment														
1100		 <table border="1"> <caption>EDS Analysis Data (1100°C)</caption> <thead> <tr> <th>Element</th> <th>Composition (wt. %)</th> </tr> </thead> <tbody> <tr> <td>C</td> <td>~10</td> </tr> <tr> <td>O</td> <td>~45</td> </tr> <tr> <td>Ash</td> <td>~45</td> </tr> </tbody> </table>	Element	Composition (wt. %)	C	~10	O	~45	Ash	~45	 <table border="1"> <caption>Burnout Experiment Data (1100°C)</caption> <thead> <tr> <th>Component</th> <th>Percentage</th> </tr> </thead> <tbody> <tr> <td>Organic</td> <td>15%</td> </tr> <tr> <td>Inorganic</td> <td>85%</td> </tr> </tbody> </table>	Component	Percentage	Organic	15%	Inorganic	85%
Element	Composition (wt. %)																
C	~10																
O	~45																
Ash	~45																
Component	Percentage																
Organic	15%																
Inorganic	85%																
1200		 <table border="1"> <caption>EDS Analysis Data (1200°C)</caption> <thead> <tr> <th>Element</th> <th>Composition (wt. %)</th> </tr> </thead> <tbody> <tr> <td>C</td> <td>~8</td> </tr> <tr> <td>O</td> <td>~40</td> </tr> <tr> <td>Ash</td> <td>~52</td> </tr> </tbody> </table>	Element	Composition (wt. %)	C	~8	O	~40	Ash	~52	 <table border="1"> <caption>Burnout Experiment Data (1200°C)</caption> <thead> <tr> <th>Component</th> <th>Percentage</th> </tr> </thead> <tbody> <tr> <td>Organic</td> <td>12%</td> </tr> <tr> <td>Inorganic</td> <td>88%</td> </tr> </tbody> </table>	Component	Percentage	Organic	12%	Inorganic	88%
Element	Composition (wt. %)																
C	~8																
O	~40																
Ash	~52																
Component	Percentage																
Organic	12%																
Inorganic	88%																